ABSTRACT

The effect of free stream turbulence intensity of the entering fluid on transition in flow from laminar to turbulent and on the hydrodynamic entry length of a circular tube are experimentally studied. Further, the hydrodynamic and thermal entrance lengths,and friction factor and Nusselt number distributions are analytically predicted.

For the laminar flow heat transfer, the integral method has been used instead of the numerical methods usually available in literature for simplicity. The method yields simple closed form expressions for predicting the boundary layer thickness and Nusselt number distribution in a circular duct. For the turbulent flow region, modified Reichardt's expression for the eddy diffusivity of momentum was used. The results of turbulent flow heat transfer are mostly based upon the turbulent Prandtl number of unity.

In the experimental work, damping screens were placed in the settling chamber to vary the turbulence intensity of the entering fluid. The screen mesh size and number used varied over a wide range.

Results show that the phenomenon of turbulent flow and heat transfer in a duct is, in general, affected very much by the free stream turbulence intensity of the entering fluid. It also shows that the assumption of turbulent boundary layer from the beginning of the entrance could sometimes lead to totally inaccurate results,specially when the turbulence intensity and the Reynold's number are low.

ACKNOWLEDGEMENT

The author wishes to express his sincere gratitude to Dr. Y. Lee who initiated and supervised the present project. His valuable suggestions, critical discussions and the innumerable hours he so willingly spent with me are particularly appreciated.

Sincere thanks are also due to the technical staff, Mechanical Engineering Department, and to the staff of the Computing Centre, University of Ottawa, for their generous assistance.

TABLE OF CONTENTS

Page

LIST OF TABLES

LIST OF FIGURES

NOMENCLATURE

A, B	=constants defined by Eqn.(3.18)
I_1, I_2	=integrals defined by Eqn.(3.21a)
C	=constant
c_p	=specific heat at constant pressure
D	=diameter
F, G, G_1	=functions defined by Eqn.(3.19)
f	=friction factor; $\tau_0/(\rho u_b^2/2)$
g	=acceleration due to gravity
h	=convective heat transfer coefficient
k	=thermal conductivity
M	=distance between wire centers
n	=constant, exponent
Nu	=Nusselt number; hD/k
P	=parameter defined by Eqn.(3.12)
p	=pressure
p^*	=non-dimensional static pressure parameter; $(p_0-p)/\rho u_b^2/2)$
Pr	=Prandtl number; $\mu c_p/k$
q	=heat flux
r	=radial distance
r^+	=dimensionless distance parameter; ru_τ/ν
r_0	=radius
R	$=r/r_0$, universal gas constant
Re_d	=Reynold's number based on D; $\rho u_b D/\mu$
Re_x	=Reynold's number based on x; $\rho u_b x/\mu$
t	=temperature, parameter defined by Eqn.(3.12)
t^+	=dimensionless temperature parameter; $(t_0-t)c_p\rho u_\tau/q_0$

T =dimensionless temperature; $(t_0-t)/(t_0-t_e)$

Tu =turbulence intensity; $\sqrt{\overline{u_e'^2}}/u_e \times 100$

u =velocity

u_τ =shear velocity; $\sqrt{\tau_0/\rho}$

u^+ =dimensionless velocity; u/u_τ

V =voltage, non-dimensionalised axial velocity; u/u_b

x =distance from entrance in the flow direction

x^* =non-dimensionalised axial distance parameter; $x/(DRe_d)$

y =distance from wall

y^+ =dimensionless distance parameter; yu_τ/ν

Y =non-dimensionalised radial distance from wall; y/r_0

Greak Symbols

α =molecular thermal diffusivity; $k/(\rho c_p)$

δ =thickness of hydrodynamic boundary layer, wire diameter

δ^+ =dimensionless hydrodynamic boundary layer thickness parameter; $\delta u_\tau/\nu$

δ_t =thickness of thermal boundary layer

δ_t^+ =dimensionless thermal boundary layer thickness parameter; $\delta_t u_\tau/\nu$

Δ =non-dimensionalised hydrodynamic boundary layer thickness; δ/r_0

Δ_t =non-dimensionalised thermal boundary layer thickness; δ_t/r_0

ϵ =eddy diffusivity

μ =viscosity

ν =kinematic viscosity ; μ/ρ

σ =eddy diffusivity ratio; ϵ_H/ϵ_M

τ =shear stress

Superscripts

$'$ =fluctuating component

$\bar{\ }$ =mean

Subscripts

1 =lower value, at the point of transition from laminar to turbulent, at station 1

2 =upper value, at station 2

b =bulk

c =core

cr =critical

d =fully developed, based on diameter

e =at the entrance

H =heat

m =mean

M =momentum

max =maximum

0 =at the wall, at the entrance

T, t =thermal

δ =at the edge of hydrodynamic boundary layer

δ_t =at the edge of thermal boundary layer

τ =shear

CHAPTER I

INTRODUCTION

It is well-known that heat transfer in the entrance region of a duct is considerably higher than that in the fully established flow away from the entrance. On the other hand, friction drag is also comparatively more in the entrance region. Apart from this, both the friction drag and heat transfer rate are more when the fluid is in turbulent motion as compared to when it is in laminar motion. It is, therefore, necessary for an accurate prediction of heat transfer coefficient and friction factor in a duct to know the entrance length and the effect of some of the factors which affect the onset of transition from laminar to turbulent flow in a straight duct. This information is required in the design of many heat transfer systems using short and compact heat exchangers.

A circular tube geometry has been the subject of many investigators in fluid flow and heat transfer problems because of its wide engineering applications. A number of studies, both experimental and analytical, have been made on a fluid flowing through a circular tube. But very little information is available in the open literature for the effect of free stream turbulence on the entrance lengths in a circular tube.

When a fluid flows through a duct or a channel, its velocity profile undergoes a change from its initial entrance form to a fully developed form at an axial location downstream of the entrance due to the viscosity of the fluid. Similar effects are also observed for a fluid entering a region having wall temperature different from that of the fluid in which case the temperature profile takes on different forms depending upon the heat flux boundary conditions and past history of the fluid. In general, the distance required for the velocity distribution to attain its fully developed form is called the hydrodynamic entrance length and that required by the temperature profile to attain its fully developed form, the thermal entrance length. In this context, a profile is said to be fully developed when its shape becomes invariant in the flow direction.

Results on both hydrodynamic and thermal entrance lengths of a circular duct have been obtained previously by many investigators both experimentally and analytically. There is a great deal of discrepency among the results of some of the investigators for the hydrodynamic entrance length of a circular duct. For example, Schlichting(1)* reports data by Kirsten showing that this entry length is about 50 to 100 diameters depending on Reynold's number, Re_d, whereas according to Nikuradse, the fully developed turbulent velocity profile exists after an inlet length of 25 to 40 diameters. The anomaly between the two typical results on the entry length must be closely associated with the entrance conditions of the fluid.

For an undisturbed flow at the entrance of a straight

---

* Numbers in parentheses designate the References at the end of the thesis.

duct, the boundary layer near the inlet length is usually laminar becoming turbulent further down. The transition in a flow from laminar to turbulent in the boundary layer on a solid wall is primarily affected by the nature of the disturbances in the initial free stream, other parameters such as the pressure distribution in the flow, the wall roughness, etc. being equal. Therefore, the numerical values of the critical Reynold's number, $Re_{x,cr}$, should depend very strongly on the conditions which prevail in the entry. It can be shown that if $Re_{x,cr}$ is fixed, $(x/D)_{cr} = (Re_{x,cr})/Re_d$. Therefore, with large Re_d, the length required for flow transition from laminar to turbulent becomes shorter and this trend has been observed in the case of flow in a concentric annulus(2).

Since the boundary layer developes faster in a turbulent flow than in a laminar flow because of vigorous momentum transport, it is expected that the shorter the laminar inlet length, the less will be the distance required by the boundary layer to develope fully for a given Re_d. In other words, the entrance length will be shorter for a disturbed flow at the entrance. Because when the flow is disturbed at the inlet of a duct, the transition would occur at a shorter distance from the entrance. In the extreme case, when the flow is made turbulent right at the beginning of the entrance by some suitable means such as a trip wire at the entrance, previous works(2,3) showed both experimentally and analytically that the entrance lengths for circular ducts are much shorter.

We can also expect that behaviour of the thermal boundary layer in a turbulent flow will be different from its behaviour in a laminar flow.Therefore, the heat transfer in a duct would depend on the relative lengths of the laminar and turbulent regions;that is, the Nusselt number distribution and thermal entrance length will be affected by transitional phenomenon which in turn depends on the free stream turbulence at the entrance.

In the present thesis, turbulent flow in the entrance region of a circular duct is studied in detail. The effect of free stream turbulence on the boundary layer transition is studied experimentally. Further, the hydrodynamic and thermal entrance lengths, friction factor and Nusselt number distributions are predicted.

The disagreement among the experimental results on the entry length for flow in a circular duct by many investigators can be partially explainable by the present study.

CHAPTER II

LITERATURE SURVEY

2.1. EFFECT OF FREE STREAM TURBULENCE ON TRANSITIONAL FLUID FLOW

The phenomenon of boundary layer transition has attracted widespread interest in the past. A number of investigators attempted to solve the the theoretical problem of the stability of laminar flow by determining under what conditions small disturbances in the form of velocity variations would increase or reduce with time. According to Tollmien[4] theory, small disturbances in velocity of any wavelength lying within a certain region would be amplified, whereas disturbances of shorter or longer wavelength would be damped. The amplified disturbances were assumed to grow until they caused a breakdown of laminar flow. The theory is now generally discredited because no evidence of disturbances with these characteristics has ever been found in boundary layers.

So far as the author is aware of, no work seems to be available for the effect of free stream turbulence intensity of the entering fluid on transitional boundary layer fluid flow in a duct at high Reynold's number. However, some results are available in literature for the case of flow over a flat plate. Hinze[5] suggested that transition can occur if the value of Re_x excedes a critical value. Schubaur and Skramstad[6] determined this critical value, $Re_{x,cr}$, for the onset of turbulence in the laminar boundary layer over a flat plate. Their results show that the magnitude of $Re_{x,cr}$ is not affected by the relative intensity of turbulence of the free stream, if this intensity decreased below roughly 0.1%.

But for turbulence intensity higher than about 0.2%, the value of $Re_{x,cr}$ is greatly affected by free stream turbulence. For example, at a turbulence intensity of 0.5%, the value of $Re_{x,cr,1}$ decreased to about 10^6 from its value of $3x10^6$ at free stream turbulence intensity below 0.1%. According to Dryden[7], this value decreased further to about 10^5 when the relative intensity of turbulence was increased to 3%.

Shapiro and smith[8] obtained experimentally the value of $Re_{x,cr}$ for a circular tube and its magnitude is $5x10^5$. They also made a qualitative remark based upon their experimental results, that inducing turbulence artificially acts either to move forward the point of transition from laminar to turbulent or to eliminate the laminar boundary layer altogether. But a detailed study for the effect of free stream turbulence on transitional phenomenon in a circular tube seems to be lacking.

2.2. ADIABATIC FLOW IN THE ENTRANCE REGION OF A CIRCULAR TUBE

Flow in the entrance region of a circular tube has drawn the attention of many investigators in the past because of its many engineering applications. The literature on laminar flow in the entrance region of a circular tube is very elaborate. An excellent compilation of the prominent works in this field is made by, for example, Campbell and Slattery[9]. They also applied a macroscopic momentum balance using Schiller's[10] velocity profile to give pressure distribution in the entrance region of a circular duct. Their results are the best overall description of laminar velocity within the tube entrance currently available.

An approximate analysis of flow within a turbulent boundary layer was first made by Latzko[11] using one seventh power velocity law. A similar analysis for closed jet wind tunnels was later given by Glauert[12]. The one seventh power law is valid over a limited Reynold's number range and away from the the wall region, so that Latzko's and Glauert's analyses are not reliable for flows at high Reynolds numbers. Ross and Whippany[13] also made an approximate analysis of developing turbulent pipe flow by combining the continuity, momentum, and energy equations for a pipe.

One of the most extensive studies of turbulent flow in a circular duct was made by Deissler[3]. He used the momentum integral method with the Von Kármán eddy diffusivity relation in the turbulent core region. The Von Kármán eddy diffusivity model as it is should be used for fully developed flow only and it may yield inaccurate velocity profiles when used in the developing region. Reichardt[14] proposed an eddy diffusivity model, based upon experimental data for the turbulent core region in a smooth pipe. His relation is also applicable in the fully developed region only, but its modified form has been used by Lee and Park[2] and Levy[15] for the developing and the developed flows through concentric annulus, respectively.

Deissler's[3] analysis assumed a turbulent boundary layer right from the beginning of the entrance which is not always true. In some of the practical cases, the turbulent boundary layer in the entrance of a duct is preceded by a laminar boundary layer at the beginning of the entrance. For the turbulent boundary layer preceded by a laminar boundary layer, the assumption of Prandtl[16] may be used in the sense that in the presence of a laminar boundary layer at the beginning of the entrance of a duct, the turbulent portion of the boundary layer behaves as if the boundary layer were turbulent all way from the entrance. But a complete solution of the turbulent flow through a circular duct with laminar entry is not available in the literature.

2.3. EFFECT OF TURBULENCE ON HEAT TRANSFER

The various factors which influence heat transfer in a duct are numerous; i.e. Reynold's number, Prandtl number, initial velocity distribution, wall boundary and heat flux condition, duct geometry, variable fluid properties, initial tripping of the boundary layer, shape of the inlet section, free stream turbulence intensity of the entering fluid, etc.

Deissler[3] studied analytically the effect of Reynold's number, Prandtl number and variable fluid properties on heat transfer in a circular duct. He also outlined in brief the effect of initial velocity distribution, wall boundary condition and duct geometry. The effect of heat flux on boundary layer transition in a circular duct has been studied experimentally by Siegel and Shapiro[17]. It has been shown that moderate heating does not have any appreciable effect on boundary layer transition. Tripping of the boundary layer at the entrance of a tube causes an earlier transition in flow from laminar to turbulent[8].

Boelter, Young and Iversen[18] experimentally studied the heat transfer distribution in a circular tube for different shapes of the inlet section. Their results indicate that heat transfer in duct depends very much on the entering fluid conditions. The numerical value of heat transfer coefficient for fully developed flow however, does not vary with the entering fluid conditions. They also made a qualitative analysis of the effect of various entering fluid conditions on heat transfer in a circular duct, but a detailed study of the effect of free stream turbulence on heat transfer in a circular duct could not be found in the published works.

2.4. DIABATIC FLOW IN THE ENTRANCE REGION OF A SMOOTH CIRCULAR TUBE

The problem of laminar flow heat transfer in a circular duct with simultaneously developing velocity and temperature profiles has been studied by many investigators(19-21). All of them used various numerical methods to solve the differential energy equation which are lengthy and require a large computational time. On the other hand, the integral method is very simple to use. The validity of the integral method for heat transfer problems in ducts has been demonstrated for turbulent flows by many investigators; e.g. Deissler[3], Park[22], etc. However, within the knowledge of the author, no one has used the integral method for solving the laminar flow heat transfer problem in a circular duct.

Iversen[23] made a simplified analysis for the turbulent flow heat transfer in the simultaneously developing region of a circular duct and presented closed form expressions for entrance length and Nusselt number. But the work of Deissler[3] is most extensive in this field. He used the momentum and energy integral equations with appropriate eddy diffusivity models of heat and momentum. Deissler used an eddy diffusivity ratio ($\frac{\epsilon_H}{\epsilon_M}$) of unity based upon Reynold's analogy. It is now well established from the experimental results of many workers that this ratio does not seem to be unity, but it is greater than unity for air and less than unity for liquid metals.

Mizushina et al[24] measured the eddy diffusivity of heat in a rectangular duct for Reynold's number range of 10,000 to 24,000. They showed that the eddy diffusivity of heat is independent of Prandtl number over their experimental range of Prandtl number between 6-40. Recently, Park[22] presented an empirical relation based upon his experimental results for flow of air through concentric annulus which, he reported to be valid for $Pr > 0.5$.

Deissler[3] also assumed that the flow is turbulent right from the beginning of the entrance. As mentioned earlier in Sec.(2.2), this assumption is incorrect for some of the practical problems in engineering. A thorough study of the problem of heat transfer in a circular duct is, therefore, required for better designs of many heat transfer systems.

CHAPTER III

ANALYTICAL STUDIES

3.1. FLUID FLOW

Strictly speaking, flow in the entrance region of a pipe is not a problem in boundary layer theory, but it has been solved with the aid of the methods used in the theory[1].

For the present analysis, the turbulent flow in the entrance region of a circular duct was divided into two regions (Fig. 3.1):

(a) developing laminar boundary layer flow upto the critical length, x_{cr} and

(b) turbulent boundary layer flow downstream from x_{cr}.

The relative lengths of the two regions depend mainly upon Reynold's Number and the conditions existing at the inlet and other factors such as wall roughness. If a suitable trip wire is used at the entrance, the flow can be made turbulent right from the beginning of the entrance[3] and a solution for this case has been obtained for a circular tube by Deissler[3]. But in actual practice, when there is no trip wire, the flow in the entrance region of a duct always progresses from laminar to turbulent and the length of the laminar inlet region could be very significant, especially at low values of Re_d.

3.1.1. Laminar Boundary Layer

Many investigators have obtained solutions for the laminar inlet region of a circular tube. The final results are similar in each case. Campbell and Slattery[9] solved the problem utilising the macroscopic momentum balance to Schiller's velocity profile. Their results are simple to use and give a best overall description of velocity within the tube entrance currently available. Therefore, their results were used for the present study.

3.1.1(a) <u>Velocity Profile and Friction Factor</u>

Following Schiller, the velocity distribution is assumed to be:

$$\frac{u}{u_{max}} = -\left(\frac{r_0 - r}{\delta}\right)^2 + 2\left(\frac{r_0 - r}{\delta}\right) \quad \text{for } y \leq \delta;$$

$$\text{and } \frac{u}{u_{max}} = 1 \quad \text{for } y \geq \delta \text{ ; for all } x \geq 0 \qquad (3.1)$$

From continuity, momentum and energy relations in the entrance region, the following relations for bulk velocity and static pressure distribution are obtained[9];

$$u_b = u_c \frac{\Delta^2 - 4\Delta + 6}{6} \qquad (3.2)$$

where u_c is the core velocity and $\Delta = \frac{\delta}{r_0}$

$$p^* = \frac{p_0 - p}{\rho u_b^2} = \frac{1}{420}\Bigg[3816 \ln(2-\Delta) - 416 \ln(1-\Delta) - 1700 \ln(\Delta^2 - 4\Delta + 6) - \frac{3(521\Delta + 582)}{\Delta^2 - 4\Delta + 6} + \frac{324(108-\Delta)}{(\Delta^2 - 4\Delta + 6)^2} + \frac{1979}{\sqrt{2}} \tan^{-1}\left(\frac{2-\Delta}{\sqrt{2}}\right)\Bigg]_0^{\Delta} + \frac{24(15 - 14\Delta + 4\Delta^2)}{5(\Delta^2 - 4\Delta + 6)^2} \qquad (3.3)$$

Eqns.(3.1) and (3.2) can be combined together to give velocity distribution in the laminar boundary layer as:

$$V = \frac{u}{u_b} = \frac{6}{\Delta(\Delta^2 - 4\Delta + 6)}\left[2\left(\frac{r_o - r}{r_o}\right) - \frac{1}{\Delta}\left(\frac{r_o - r}{r_o}\right)^2\right] \quad (3.4)$$

3.1.1(b) Momentum Equation

Campbell and Slattery[9] obtained a relation for the boundary layer thickness, δ, at any axial length using macroscopic mechanical energy balance. The final equation is:

$$1680\, x^* = \Big[336\,\Delta - 26 \ln(1-\Delta) + 318 \ln(2-\Delta) + 148 \ln(\Delta^2 - 4\Delta + 6) + \frac{27(52\Delta + 3)}{\Delta^2 - 4\Delta + 6} - \frac{2084}{\sqrt{2}} \tan^{-1}\left(\frac{\Delta - 2}{\sqrt{2}}\right)\Big]_0^{\Delta} \quad (3.5)$$

where $x^* = \dfrac{x}{D\, Re_d}$.

Eqn.(3.5) is a transcendental equation in Δ and can be solved by using any one of the iterative schemes available in the literature[25]. Interval halving technique was used in the present study to solve Eqn.(3.5) for Δ .

3 .1.2. Turbulent Boundary Layer

3.1.2(a) Velocity Profile and Friction Factor

The basic governing equation for adiabatic turbulent flow through a straight duct is:

$$\frac{\tau}{\rho} = (\nu + \epsilon_M)\frac{du}{dy}$$

or nondimensionalising in terms of the nondimensional parameters defined in the nomenclature, one obtains:

$$\frac{\tau}{\tau_0} = \left(1 + \frac{\epsilon_M}{\nu}\right)\frac{du^+}{dy^+} \tag{3.6}$$

In order to obtain the velocity distribution within the boundary layer, two things must be known:

(a) shear stress distribution $(\frac{\tau}{\tau_0})$ and

(b) eddy diffusivity of momentum $(\frac{\epsilon_M}{\nu})$.

For this purpose, the boundary layer region is divided into two parts:

(i) laminar sublayer region near the wall and

(ii) turbulent core region away from the wall.

For the laminar sublayer region, Deissler's eddy diffusivity model is used; i.e.

$$\frac{\epsilon_M}{\nu} = n^2 u^+ y^+ \left[1 - \exp(-n^2 u^+ y^+)\right] \tag{3.7}$$

where 'n' is an experimentally determined constant and its value is given by $n^2 = 0.0154$.

Substituting Eqn.(3.7) in Eqn.(3.6) and neglecting the shear stress variation near the wall, the velocity profile in the laminar sublayer region is given by:

$$u^+ = \int_0^{y^+} \frac{dy^+}{1 + n^2 u^+ y^+ \left[1 - \exp(-n^2 u^+ y^+)\right]} \tag{3.8}$$

For the turbulent core region, Reichardt[14] proposed an eddy diffusivity model which he obtained for fully developed flow only.

$$\frac{\epsilon_M}{\nu} = \frac{k r_0^+}{6}\left[1 - \left(\frac{r}{r_0}\right)^2\right]\left[1 + 2\left(\frac{r}{r_0}\right)^2\right]$$

where k =0.4.

The equation has been modified by Lee and Park[2] for developing turbulent flow through a concetric annulus. In the same way, it was also modified for the entrance region of a circular duct in the present study. The modified expression for the eddy diffusivity away from the wall is:

$$\frac{\epsilon_M}{\nu} = \frac{k\delta^+}{6}\left[1-\left(\frac{y-\delta}{\delta}\right)^2\right]\left[1+2\left(\frac{y-\delta}{\delta}\right)^2\right] \qquad (3.9)$$

The shear stress distribution away from the wall can be obtained by making a force balance in the developing region (see Fig. 3.1). Neglecting the effect due to change in momentum flux[26], the shear stress distribution is obtained by:

$$\frac{\tau}{\tau_0} = \frac{r_0}{r_0-y}\left(\frac{y^2-2r_0y-\delta^2+2r_0\delta}{2r_0\delta-\delta^2}\right) \qquad (3.10)$$

Eqn.(3.10) gives the actual shear stress distribution in the turbulent core region of a circular tube. But according to Deissler's study[3], the variations across the flow boundary layer of the shear stress, τ, have a negligible effect on the velocity distributions. So, as long as the choice of the shear stress distribution is consistent with one that agrees well with experimental results for the pipe flow case, a function of shear stress distribution which would lead to a much simpler and more convenient velocity profiles than those given by using Eqn.(3.10) would seem to be more practical. Therefore, as an alternative to Eqn.(3.10) the local shear stress distribution within the boundary layer is assumed to vary linearly with the distance as:

$$\frac{\tau}{\tau_0} = \frac{\delta-y}{\delta} \qquad (3.11)$$

Eqn.(3.11) has been used for flow through a concetric annulus by Lee and Park[2]. Substituting Eqn.(3.9) and Eqn.(3.11) in Eqn.(3.6), one obtains for the turbulent core region:

$$u^+ = \int \frac{(\delta^+ - y^+)/\delta^+}{1 + \frac{k\delta^+}{6}\left[1 - \left(\frac{\delta^+ - y^+}{\delta^+}\right)^2\right]\left[1 + 2\left(\frac{\delta^+ - y^+}{\delta^+}\right)^2\right]} dy^+$$

Or integrating, one obtains:

$$u^+ = \frac{1}{2P} \ln\left[\frac{6P + k - 4kt}{6P - k + 4kt}\right] + C \qquad (3.12)$$

where $P = \sqrt{\frac{k^2}{4} + \frac{4k}{3\delta^+}}$

and $t = \left(\frac{\delta^+ - y^+}{\delta^+}\right)^2$

The constant 'c' in Eqn.(3.12) can be determined by joining the velocity profiles in the laminar and in the turbulent core region at a suitable point. Both Lee and Park[2] and Deissler[3] suggested from their experimental results that the most suitable point at which the two velocity profiles can be joined together is at $y^+ = 26$.

The velocity profiles computed from Eqns.(3.12) and (3.8) are compared with the velocity profile of Deissler in Fig. 3.2.

The local friction factor ignoring the effect due to changes in momentum flux* due to a developing velocity profile is defined here as:

$$f_x = \frac{\tau_{o,x}}{\frac{1}{2}\rho u_{b,x}^2}$$

----

* The effect due to change in momentum flux on friction factor has been studied by Barbin and Jones[26] and has been shown to be negligible.

Converting into nondimensional form, this can be written as:

$$f_x = \frac{2}{u_{b,x}^{+2}} \tag{3.13}$$

where $u^+_{b,x}$ is defined as:

$$u^+_{b,x} = \left(\frac{\int_0^{r_0^+} u^+ y^+ dy^+}{\int_0^{r_0^+} y^+ dy^+} \right)_x = \left(\frac{2}{r_0^{+2}} \int_0^{r_0^+} u^+ y^+ dy^+ \right)_x \tag{3.14}$$

3.1.2(b) Momentum Integral Equation

Application of the momentum principle to the differential annulus shown in Fig. 3.1 gives:

$$2\pi \tau_0 r_0 dx + \pi [r_0^2 - (r_0 - \delta)^2] dP = 2\pi u_\delta d\left[\int_0^\delta \rho u r dy\right] - 2\pi \cdot d\left[\int_0^\delta \rho u^2 r dy\right] \tag{3.15}$$

If the flow outside the boundary layer is assumed to be frictionless, we can write:

$$dP = -\rho u_\delta du_\delta \tag{3.16}$$

Substituting Eqn.(3.16) in Eqn.(3.15), one gets after some re-arrangement,

$$\tau_0 r_0 dx = \frac{1}{2} \rho u_\delta du_\delta (2 r_0 \delta - \delta^2) + u_\delta \rho d\left[\int_0^\delta u r dy\right] - \rho d\left[\int_0^\delta u^2 r dy\right] \tag{3.17}$$

We now assume that the flow is laminar upto some distance (say $x = x_1$) where the boundary layer thickness is δ_1 and core velocity is u_{δ_1} and that the flow is turbulent everywhere for $x > x_1$. We also assume that at $x \gg x_1$, the boundary layer will behave as if it were turbulent all way from the entrance, and for the turbulent boundary layer, $\delta x = x_1 = \delta_1$.

Thus, integrating Eqn.(3.17) from $x=x_1$ to any $x > x_1$, one obtains:

$$x - x_1 = \int_{u_{\delta_1}}^{u_\delta} \frac{\delta(2r_o - \delta)}{2\tau_o r_o} \rho u_\delta \, du_\delta - \int_{A_1}^{A} \frac{dA}{\tau_o r_o} + \int_{B_1}^{B} \frac{u_\delta \, dB}{\tau_o r_o} \tag{3.18}$$

where
$$A = \int_0^\delta \rho u^2 (r_o - y)\, dy$$
$$B = \int_0^\delta \rho u (r_o - y)\, dy$$

A_1 and B_1 are the values of A and B respectively at $x=x_1$.

Converting into nondimensional form and after making some manipulations, Eqn.(3.18) becomes:

$$\frac{x - x_1}{D} = \int_{u^+_{\delta_1}}^{u^+_\delta} F \, du^+_\delta + \int_{G_1}^{G} dG \tag{3.19}$$

where
$$F = \left[\frac{\delta^+}{2r_o^+} - \left(\frac{\delta^+}{2r_o^+}\right)^2 \right] u^+_\delta - \int_0^{\delta^+} u^+ \left[\frac{1}{2r_o^+} - \frac{y^+}{2r_o^{+2}} \right] dy^+$$
$$G = \int_0^{\delta^+} (u^+_\delta - u^+)\, u^+ \left(\frac{1}{2r_o^+} - \frac{y^+}{2r_o^{+2}} \right) dy^+$$

$u^+_{\delta_1}$ and G_1 are respectively the values of the nondimensional core velocity, u^+_δ, and G (as defined above) at $x=x_1$ and have to be calculated from laminar flow theory.

In order to solve Eqn.(3.19), r_0^+ must be known in terms of δ^+ and Re_d. This relation can be obtained from the law of conservation of mass. From the definition of the mean bulk velocity, we have:

$$u_b \pi r_o^2 = \int_0^{r_o - \delta} 2\pi r u_r \, dr + \int_{r_o - \delta}^{r_o} 2\pi r u \, dr$$

Substituting $r=r_0-y$ and converting into nondimentional form, we obtain,

$$(u_b^+)_x = \frac{2}{(r_0^+)_x}\left[\int_0^{\delta^+}(r_0^+ - y^+)\,u^+ dy^+ + \int_{\delta^+}^{r_0^+}(r_0^+ - y^+)\,u^+ dy^+\right]_x \quad (3.20)$$

Substituting $(Re_d) = 2(u_b^+)_x(r_0^+)_x$ and $u^+ = u_\delta^+$ for $\delta^+ \leq y^+ \leq r_0^+$, Eqn.(3.20) can be re-arranged to give after a few steps:

$$r_0^{+2}(2u_\delta^+) + r_0^+(4I_1 - 4\delta^+ u_\delta^+ - Re_d) + (2u_\delta^+ \delta^{+2} - 4I_2) = 0 \quad (3.21)$$

$$\text{where} \quad \left.\begin{aligned} I_1 &= \left(\int_0^{\delta^+} u^+ dy^+\right)_x \\ I_2 &= \left(\int_0^{\delta^+} u^+ y^+ dy^+\right)_x \end{aligned}\right\} \quad (3.21a)$$

Eqn.(3.21) is a quadratic in $(r_0^+)_x$ and can be solved for $(r_0^+)_x$ in terms of Re_d and $(\delta^+)_x$ to give:

$$(r_0^+)_x = \frac{1}{u_\delta^+}\left[-I_1 + \delta^+ u_\delta^+ + \frac{Re_d}{4} \pm\sqrt{\left(I_1 - \frac{Re_d}{4}\right)^2 + u_\delta^+\left(2I_2 + \frac{Re_d\,\delta^+}{2}\right) - 2I_1\delta^+}\,\right] \quad (3.22)$$

The ambiguous sign in Eqn.(3.22) is chosen according to the physical significance of the final results. Thus,

$$(r_0^+)_x = \frac{1}{u_\delta^+}\left[-I_1 + \delta^+ u_\delta^+ + \frac{Re_d}{4} + \sqrt{\left(I_1 - \frac{Re_d}{4}\right)^2 + u_\delta^+\left(2I_2 + \frac{Re_d\,\delta^+}{2}\right) - 2I_1\delta^+}\,\right] \quad (3.23)$$

3.1.3. Entrance Length

The entrance lengths for turbulent flow preceded with laminar flow were calculated by combining together the analysis of Sec. 3.1.1 and Sec. 3.1.2. The method of computation and the results are described in Sec. 3.1.4. In the present analytical studies, the entrance length was defined as the axial distance at which the ratio of the core velocity to the bulk velocity equals unity ($u_s^+/u_b^+ = 1.00$).

Entrance lengths were also calculated for the case when the boundary layer is assumed to be turbulent from the beginning of the entrance in which case only the analysis of Sec. 3.1.2 was used and Eqn.(3.19) reduced to:

$$\frac{x}{D} = \int_0^{u_s^+} F \, du_s^+ + G \tag{3.24}$$

3.1.4. Method of Computation and Results

In this section, the method of computation of the problem of turbulent flow through a pipe using the analyses of Secs. 3.1.1 and 3.1.2 will be described. The following relations are useful in converting into each other the two different forms of nondimensional parameters used in the laminar and turbulent flows.

$$\left.\begin{aligned} Re_d &= 2\,(u_b^+)_x\,(r_o^+)\,x \\ f_x &= 2\,/\,(u_b^{+2})_x \\ u^+ &= (u/u_\tau) = \frac{u}{u_b}\,u_b^+ \\ y^+ &= \frac{y\,u_\tau}{\nu} = \frac{y\,r_o^+}{r_o} \end{aligned}\right\} \tag{3.25}$$

Using these and Eqn.(3.1), the expression for G_1 to be used in Eqn.(3.19) was calculated to be:

$$G_1 = \frac{3\Delta}{10}\left(\frac{8-3\Delta}{\Delta^2-4\Delta+6}\right) \tag{3.26}$$

and the expression for F at $x=x_1$ is:

$$F_1 = \frac{\Delta}{4} u_b^+ \left(\frac{4 - \Delta}{\Delta^2 - 4\Delta + 6} \right) \tag{3.27}$$

and

$$u_{\delta_1}^+ = \frac{6\, u_b^+}{\Delta^2 - 4\Delta + 6} \tag{3.28}$$

where Δ was taken to be the boundary layer thickness at the critical point $x=x_1$.

The following are the steps for calculation:

(1) The values of initial free stream turbulence (Tu) and Reynold's number (Re_d) are prescribed.

(2) For given Tu and Re_d, the values of $(x/D)_{i,i=1,2}$ at which transition from laminar to turbulent flow takes place are taken from the experimental results (Fig. 4.15, Sec. 4.5). Experiment gives two values of $(x/D)_{cr}$— one at which boundary layer changes from laminar to transition region and the other at which it changes from transition to turbulent region. In the present analysis, entrance lengths were computed from both the values of $(x/D)_{cr}$ and compared with the experimental results.

(3) Knowing $x_1/D=(x/D)_i$, the analysis of Sec. 3.1.1 was applied upto this value of (x_1/D). Also the values of G_1, F_1, $u_{\delta_1}^+$, and δ_1^+ were calculated from Eqns.(3.25) to (3.28) at $x/D=x_1/D$.

(4) For the turbulent boundary layer, a value of $\delta^+ > \delta_1^+$ is assumed. At this value of δ^+, velocity profiles are obtained from Eqns.(3.8) and (3.12).

(5) The values of the integrals I_1 and I_2 in Eqn.(3.23) defined by Eqn.(3.21a) are computed. Then r_0^+ can be calculated from Eqn.(3.23).

(6) Eqn.(3.19) will then give the values of x/D for the assumed value of δ^+ and the friction factor can be calculated

from Eqns.(3.13) and(3.14).

(7) Value of δ^+ in step (4) is increased by a certain prescribed amount and steps (4) to (6) are repeated till $\delta^+/r_0^+=1.00$. i.e. the fully developed conditions are obtained. The value of (x/D) at this point is then the entrance length for the given conditions.

The computed velocity profiles in the turbulent boundary layer are compared with that obtained by Deissler[3] in Fig. 3.2 whereas the velocity profiles in the developing are presented in Fig. 3.3.

The fully developed friction factors obtained from the present analysis are compared with the experimental results of Blausius[27] in Fig. 3.4.

The results of hydrodynamic entrance lengths are presented in Figs. 4.16 and 4.17.

The boundary layer developement for a typical case of turbulent flow preceded by a laminar flow through a circular tube is shown in Fig. 3.5.

Predicted friction factors for turbulent flow preceded with a laminar boundary layer for various values of $Re_{x,cr}$. are presented in Fig. 3.6. Predicted hydrodynamic entrance lengths are tabulated in Table 1.

3.2. HEAT TRANSFER

In Sec. 3.1, the problem of adiabatic flow through a circular tube was considered and the effect of free stream turbulence or that of transitional phenomenon from laminar to turbulent on the hydrodynamic entrance length was studied. In this section, we shall consider the effect of free stream turbulence intensity on heat transfer in a circular duct. Both the velocity and the temperature profiles are assumed to be uniform at the entrance. As before, the flow will be considered laminar upto the critical length, $x_{i,i=1,2}$ and turbulent downstream of x_i. For the laminar inlet region, the usefulness of the simple integral method will be demonstrated which has been ignored for laminar flow heat transfer problems in internal flows. Local Nusselt number and entrance length will be obtained for the various combinations of Reynold's numbers, Prandtl numbers and entrance conditions.

In the present study, the analysis was limited only to the case of constant heat flux at the boundary wall.

3.2.1. Laminar Flow Heat Transfer

A large number of solutions for the simultaneous developement of thermal and hydrodynamic boundary layers in laminar flow through a circular tube are available in the literature (19-21). All of them solved the differential energy equation using various numerical methods. In the present study, however, to keep consistency, it was thought better to make use of the integral energy equation, which has been used extensively for turbulent flows, as well as for the laminar flow. Temperature profile was obtained by modifying the fully developed temperature profile in laminar flow through circular tube. With this, closed form expressions were obtained for the thermal boundary layer thickness and Nusselt number which are very simple to use compared to the various complex numerical methods available in the literature.

3.2.1(a) Temperature Profile and Nusselt Number

The fully developed temperature profile obtained by integrating the energy differential equation for laminar flow through a circular tube and using a parabolic velocity profile is[28].

$$t = t_o - \frac{2u_b}{\alpha}\frac{dt_m}{dx}\left(\frac{3}{16}r_o^2 + \frac{r^4}{16r_o^2} - \frac{r^2}{4}\right) \quad (3.29)$$

Also from an energy balance in the differential element, we have:

$$\frac{dt_m}{dx} = \frac{2q_o}{r_o V \rho C_p} \quad (3.30)$$

Combining Eqns.(3.29) and (3.30) and converting the resulting equation into nondimensional form and re-arranging, we obtain:

$$t^+ = Pr\frac{r_o^+}{4}\left[\left(\frac{y^+}{r_o^+}\right)^4 - 4\left(\frac{y^+}{r_o^+}\right)^3 + 2\left(\frac{y^+}{r_o^+}\right)^2 + 4\left(\frac{y^+}{r_o^+}\right)\right] \quad (3.31)$$

Eqn.(3.31) is applicable in the fully developed region only and implies the assumptions of constant fluid properties and negligible axial conduction.

In the present analysis, we further postulate that Eqn.(3.31) is also applicable for the developing region with suitable modifications as:

$$t^+ = Pr\frac{\delta_t^+}{4}\left[\left(\frac{y^+}{\delta_t^+}\right)^4 - 4\left(\frac{y^+}{\delta_t^+}\right)^3 + 2\left(\frac{y^+}{\delta_t^+}\right)^2 + \left(\frac{y^+}{\delta_t^+}\right)\right] \quad (3.32)$$

which satisfies the boundary conditions.

From Eqn.(3.32), we obtain:

$$t^+_{\delta_t} = \frac{3}{4} P_r \, \delta^+_t \tag{3.33}$$

Dividing Eqn.(3.32) by Eqn.(3.33), we obtain the temperature profile in the laminar inlet region of a circular tube:

$$T = \frac{t^+}{t^+_{\delta_t}} = \frac{1}{3}\left[\left(\frac{y^+}{\delta_t^+}\right)^4 - 4\left(\frac{y^+}{\delta_t^+}\right)^3 + 2\left(\frac{y^+}{\delta_t^+}\right)^2 + 4\left(\frac{y^+}{\delta_t^+}\right)\right]$$

or in a different form:

$$T = \frac{1}{3}\left[\left(\frac{Y}{\Delta_t}\right)^4 - 4\left(\frac{Y}{\Delta_t}\right)^3 + 2\left(\frac{Y}{\Delta_t}\right)^2 + 4\left(\frac{Y}{\Delta_t}\right)\right] \tag{3.34}$$

Knowing the temperature profile, Nusselt number can be calculated easily from the following relations:

$$Nu_x = \frac{h_x D}{k} = \frac{2\left(\frac{\partial T}{\partial Y}\right)_{Y=0}}{T_b} \tag{3.35}$$

$$\text{where} \quad T_b = 2\int_0^1 V T (1-Y)\, dY \tag{3.36}$$

It is to be noted in using Eqn.(3.36) that $V=V_\Delta$ for $Y \geqslant \Delta$ and $T=T_{\Delta_t}$ for $Y \geqslant \Delta_t$. For this purpose, the integral in Eqn.(3.36) is broken into three parts as shown below:

$$T_b = 2\left[\int_0^{\Delta_t} V T (1-Y)\, dY + \int_{\Delta_t}^{\Delta} V\, T_{\Delta_t}(1-Y)\, dY + \int_{\Delta}^{1} V_\Delta T_{\Delta_t}(1-Y)\, dY\right] \tag{3.37a}$$

for $\Delta_t \leq \Delta$

and

$$T_b = 2\left[\int_0^{\Delta} V T (1-Y)\, dY + \int_{\Delta}^{\Delta_t} V_\Delta T (1-Y)\, dY + \int_{\Delta_t}^{1} V_\Delta T_{\Delta_t}(1-Y)\, dY\right] \tag{3.37b}$$

for $\Delta_t \geqslant \Delta$

Using Eqns.(3.37),(3.34) and (3.4), T_b is obtained as:

$$T_b = \frac{12}{\Delta^2 - 4\Delta + 6}\left[\frac{1}{2} - \frac{\Delta}{3} + \frac{\Delta^2}{12} - \frac{\Delta_t^2}{5\Delta} + \frac{13}{315}\frac{\Delta_t^3}{\Delta^2} + \frac{26}{315}\frac{\Delta_t^3}{\Delta} + \frac{577}{2520}\frac{\Delta_t^4}{\Delta} - \frac{\Delta_t^4}{4\Delta^2}\right]$$

for $\Delta_t \leq \Delta$ (3.38a)

and

$$T_b = \frac{4}{\Delta^2 - 4\Delta + 6}\left[\frac{3}{2} - \frac{17}{15}\Delta_t + \frac{3}{10}\Delta_t^2 - \frac{\Delta^5}{105\Delta_t^4} + \frac{\Delta^4}{15\Delta_t^3} - \frac{\Delta^3}{15\Delta_t^2} - \frac{\Delta^2}{3\Delta_t} + \frac{\Delta^6}{168\Delta_t^4} - \frac{4\Delta^5}{105\Delta_t^3} + \frac{\Delta^4}{30\Delta_t^2} + \frac{2\Delta^3}{15\Delta_t}\right]$$

for $\Delta_t \geq \Delta$ (3.38b)

Substituting the values of $\left(\frac{\partial T}{\partial Y}\right)_{Y=0}$ from Eqn.(3.34) into Eqn.(3.35), we also obtain:

$$Nu_x = \frac{8}{3\Delta_t T_b} \tag{3.39}$$

Eqn.(3.38) and (3.39) can be used together to calculate Nusselt number provided that the hydrodynamic and thermal boundary layer thicknesses are known. The hydrodynamic and thermal boundary layer thicknesses are calculated from the momentum and energy integral equations respectively. The latter equation will be developed in the following section.

3.2.1(b) Energy Integral Equation

The energy integral equation for flow through a circular tube can be written from Fig. 3.7. Neglecting axial conduction;

$$2\pi r_o q_o \, dx = d\left[\int_0^{\delta_t} c_p t \rho u \, 2\pi (r_o - y)\, dy\right] - c_p t_{\delta_t} d\left[\int_0^{\delta_t} \rho u \, 2\pi (r_o - y)\, dy\right] \quad (3.40)$$

Since t_{δ_t} is invariant in axial direction, Eqn.(3.40) can be written as:

$$dx = \frac{c_p \rho}{r_o q_o} d\left[\int_0^{\delta_t} (t - t_{\delta_t})\, u\,(r_o - y)\, dy\right]$$

For constant heat rate problem, q_0 is also independent of x. Therefore, this equation can be integrated, simplified and re-arranged into the following form:

$$\frac{x}{D Re_d Pr} = \frac{3}{16} \Delta_t \left[\int_0^{\Delta_t} (1-T)\, V\,(1-Y)\, dY\right] \quad (3.41)$$

Eqn.(3.41) is valid for $\Delta_t \leqslant \Delta$ or $\Delta_t \geqslant \Delta$, provided that $V = V_\Delta$ for $Y \geq \Delta$.

Substituting the expressions for T and V from Eqns.(3.34) and (3.4) respectively, into Eqn.(3.41) and integrating, we obtain with some algebraic manipulations:

$$\frac{x}{D Re_d Pr} = \frac{9}{40\Delta(\Delta^2 - 4\Delta + 6)} \left[\Delta_t^3 - \frac{13\Delta_t^4}{63}\left(\frac{1}{\Delta} + 2\right) + \frac{53}{104}\frac{\Delta_t^5}{\Delta}\right] \quad (3.42a)$$

for $\Delta_t \leqslant \Delta$

and

$$\frac{x}{DRe_d Pr} = \frac{3\Delta^2}{8(\Delta^2-4\Delta+6)}\Big[\left(\frac{\Delta}{\Delta_t}\right)^3\left(\frac{8-5\Delta}{840}\right)+\left(\frac{\Delta}{\Delta_t}\right)^2\left(\frac{4\Delta-7}{105}\right)$$
$$+\frac{\Delta}{\Delta_t}\left(\frac{2-\Delta}{30}\right)+\frac{5-2\Delta}{15}+\frac{\Delta_t}{\Delta}\left(\frac{\Delta-4}{\Delta}\right)$$
$$+\frac{17}{15}\left(\frac{\Delta_t}{\Delta}\right)^2-\frac{3\Delta}{10}\left(\frac{\Delta_t}{\Delta}\right)^3\Big]$$

for $\Delta_t \geq \Delta$ (3.42b)

Eqns.(3.42) are the energy integral equations which can be used to calculate Δ_t, with the known Δ from the momentum integral equation, Eqn.(3.5).

3.2.2. Turbulent Flow Heat Transfer

3.2.2(a) Temperature Profile and Nusselt Number

The basic governing equation forthe turbulent flow heat transfer in dimensionless form is:

$$\frac{q}{q_0} = \left(\frac{1}{Pr}+\frac{\epsilon_H}{\nu}\right)\frac{dt^+}{dy^+} \tag{3.43}$$

In order to obtain the temperature profile, two things must be known:

(i) heat flux variation across the boundary layer (q/q_0) and

(ii) eddy diffusivity of heat (ϵ_H/ν).

Heat flux distribution can be obtained in a simplified form from an energy balance in the developing region of a circular tube and assuming $\frac{dt}{dx} = \frac{dt_b}{dx}$ and $u=u_b$(29). This relation is applicable only for the fully developed flow. However, since the heat fluxes are already small away from the wall, the assumption concerning the velocity field on the heat flux distribution is not critical in the region of greatest importance. This matter has been critically studied by Barrow[29].

The final expression for the heat flux distribution away from the wall with the assumptions stated above is:

$$\frac{q}{q_0} = \frac{r_0}{r} \; \frac{r^2 - r_{\delta_t}^2}{r_0^2 - r_{\delta_t}^2} \tag{3.44}$$

For the laminar sublayer region very close to the wall, it is assumed that $q/q_0 = 1.0$.

The eddy diffusivity of heat has a major effect on the prediction of temperature profiles and Nusselt numbers in the entrance region of a duct. Most of the workers in the past have used the ratio (ϵ_H/ϵ_M) of unity following the Reynold's analogy. Strictly speaking, the ratio (ϵ_H/ϵ_M) is unity only for a fluid of Pr=1 and deviates very much from unity for other fluids[30]. For this reason, a great deal of research has been done to establish a relation for the eddy diffusivity of heat for different fluids.

Mizushina et al[24] proposed the following expressions for the eddy diffusivity of heat in the turbulent boundary layer based upon experimental results using Mach-Zehnder interferometer for Pr=6~40:

$$\left.\begin{aligned} \frac{\epsilon_H}{\nu} &= 1.31 \times 10^{-5} (y^+)^4 && \text{for } 0.4 < y^+ \leq 14 \\ \frac{\epsilon_H}{\nu} &= 1.93 \times 10^{-4} (y^+)^3 && \text{for } 14 < y^+ \leq 42 \\ \frac{\epsilon_H}{\nu} &= 0.36\, y^+ - 1 && \text{for } y^+ > 42 \end{aligned}\right\} \tag{3.45}$$

Park[22] used his own empirical relation obtained from experimental results for flow of air through a concetric annulus. His correlation

$$\sigma(y^+) = \frac{\epsilon_H}{\epsilon_M}(y^+) = 0.968\,\alpha^{0.045}\,y^{+\,0.031} \qquad (3.46)$$

is valid for a concetric annulus where 'α' is the ratio of the outer to inner radius. For the present study, Eqn.(3.46) was modified slightly for a circular pipe as:

$$\sigma(y^+) = y^{+\,0.031} \qquad (3.47)$$

Eqn.(3.46) is valid for $Pr > 0.5$. For $Pr < 0.5$, a correlation for the ratio proposed by Dwyer[31] is given by:

$$\sigma(y^+) = 1.0 - \frac{0.2/Pr - 2.0}{(\epsilon_M/\nu)^{0.9}} \qquad (3.48)$$

In the present study, most of the calculations were performed by using the ratio $\epsilon_H/\epsilon_M = 1.0$. However, in some cases, the final results are also compared by using Eqns.(3.45), (3.47) and (3.48).

Eqns.(3.43) and (3.44) can now be used along with one of the above mentioned expressions for eddy diffusivity of heat to give the temperature profile as:

$$t^+ = \int \frac{q/q_0}{\left(\frac{1}{Pr} + \frac{\epsilon_H}{\nu}\right)}\,dy^+ \qquad (3.49)$$

Once the temperature profile is known, Nusselt number can be obtained from:

$$Nu_x = \frac{2\,r_0^+\,Pr}{t_b^+} \qquad (3.50)$$

where t_b^+ is the mean bulk temperature defined in dimensionless parameters as:

$$t_b^+ = \frac{\int_0^{r_o^+} t^+ u^+ (r_o^+ - y^+)\, dy^+}{\int_0^{r_o^+} u^+ (r_o^+ - y^+)\, dy^+}$$

$$= \frac{2}{u_b^+ r_o^{+2}} \int_0^{r_o^+} t^+ u^+ (r_o^+ - y^+)\, dy^+ \qquad (3.51)$$

Again it is apparent in using Eqn.(3.51) that $t^+ = t^+_{\delta_t}$ for $y^+ \geq \delta_t^+$ and $u^+ = u^+_\delta$ for $y^+ \geq \delta^+$.

3.2.2(b) Energy Integral Equation

Eqn.(3.40) which is derived for laminar flow through a circular duct is also applicable for turbulent flow. In this case, however, it is re-arranged in a different form for simplicity as:

$$\frac{x}{D} = \frac{1}{2 r_o^{+2}} \int_0^{\delta_t^+} (t^+_{\delta_t} - t^+)\, u^+ (r_o^+ - y^+)\, dy^+ \qquad (3.52)$$

Again Eqn.(3.52) is valid for $\delta_t^+ < \delta^+$ or $\delta_t^+ > \delta^+$, provided that $u^+ = u^+_\delta$ for $y^+ \geq \delta^+$.

For the case when the turbulent boundary layer is preceded by a laminar one, Eqn.(3.52) becomes:

$$\frac{x - x_1}{D} = \left[\frac{1}{2 r_o^{+2}} \int_0^{\delta_t^+} (t^+_{\delta_t} - t^+)\, u^+ (r_o^+ - y^+)\, dy^+\right]_{x=x}$$

$$- \left[\frac{1}{2 r_o^{+2}} \int_0^{\delta_{t_1}^+} (t^+_{\delta_t} - t^+)\, u^+ (r_o^+ - y^+)\, dy^+\right]_{x=x_1} \qquad (3.53)$$

where x_1 is the distance at which transition from laminar to turbulent takes place and $\delta_{t_1}^+$ is the dimensionless boundary layer thickness at $x=x_1$ calculated from Eqn.(3.42).

3.2.3. Entrance Length

The thermal entrance length for simultaneously developing turbulent flow were calculated by combining the analyses of Secs. 3.1.1, 3.1.2, 3.2.1, and 3.2.2. The method of computation and the results are described in the following section.

The thermal entrance length in a simultaneously developing flow is defined as the length of duct needed from the entrance to a crossection in the flow direction where both the generalised velocity and temperature profiles are invariant in the flow direction, when the fluid properties are assumed to be constant. This definition can be stated as:

$$\frac{\partial}{\partial x}\left(\frac{t_o - t}{t_o - t_b}\right) = 0 \qquad (3.54)$$

For the case of constant heat flux, as in the present study, the differentiation of Eqn.(3.54) with the definition of heat transfer coefficient,

$$h_x = \frac{q_x}{(t_o - t_b)_x} \qquad (3.55)$$

leads to the following expression:

$$\frac{\partial t}{\partial x} = \frac{dt_o}{dx} = \frac{dt_b}{dx} \qquad (3.56)$$

Therefore, the linear temperature gradient indicates that the fully developed region has been reached.

Entrance lengths were also calculated for the case when the boundary layer is assumed to be turbulent from the beginning of the entrance in which case only the analyses of Secs. 3.1.2 and 3.2.2 were used along with Eqn.(3.24) instead of Eqn.(3.19) and Eqn.(3.52) instead of Eqn.(3.53).

3.2.4. Method of Computation and Results

The following steps were performed in order to obtain $t^+(y,x/D,Re_d,Pr,Tu)$, $Nu(x/D,Re_d,Pr,Tu)$ and $(x/D)_{d,T}(Re_d,Pr,Tu)$ for the simultaneously developing turbulent boundary layer.

(1) The values of Tu, Re_d, and Pr are prescribed.

(2) The value of $(x/D)_{i,i=1,2}$ for a given value of Re_d and Tu are taken from the empirical results described in Sec. 5.3.

(3) For $(x/D) \leq (x/D)_i$, Δ is calculated from Eqn.(3.5). Knowing Δ, Δ_t can be calculated from Eqns.(3.42). Eqns.(3.42) are simple polynomials in Δ_t and can be solved by any iterative method. Newton-Raphson method was used in the present study. Knowing Δ and Δ_t, the Nusselt number can be calculated by using Eqns.(3.38) and (3.39). The value of $\delta^+_{t_1}$ at $x=x_i$ to be used later for the solution of turbulent part is also computed from this step.

(4) For $(x/D) > (x/D)_i$, subsections (4,5,6) of Sec. 3.1.4 are performed to calculate δ^+ and r_0^+ at a particular value of (x/D). Velocity profile is also calculated from subsection (4) of Sec. 3.1.4.

(5) Knowing δ^+, r_0^+ and velocity profile from step (4) above, a value of $\delta_t^+ > \delta^+_{t_1}$ and $\delta_t^+ < r_0^+$ is assumed. Then temperature profile is computed from Eqn.(3.49) and (3.44) with one of the eddy diffusivity models described in Sec. 3.2.2a. Then a new value

of (x/D) is calculated from the energy equation, i.e. Eqn.(3.53) and is compared with the actual value of (x/D) used in subsection (4) above. The assumed value of δ_t^+ is then changed according to a definite iterative scheme* until the value of (x/D) computed from Eqn.(3.53) coincides with the value of (x/D) used in subsection (4) above. This value of δ_t^+, then gives the thermal boundary layer thickness at the value of (x/D) assumed in subsection (4).

(6) Knowing δ^+, δ_t^+, r_0^+, and temperature profile at a particular value of (x/D) from the previous subsections, Nusselt number is easily calculated from Eqns.(3.50) and (3.51). Simpson's rule with suitable interval size was used in all the numerical integrations performed during the course of the computation.

(7) The value of (x/D) in subsection (4) is increased and subsections (5) and (6) are repeated until fully developed conditions are obtained both for the thermal and for the hydrodynamic boundary layers.

The final computer program is very lengthy and only a simple flow diagram is presented in Fig. 3.8 to clarify the sequence of operations. All computations were performed on an IBM 360/65 digital computer using Fortran IV.

The results of Nusselt numbers in the laminar inlet region of present study using the integral method are compared with the available numerical solutions in Fig. 3.9 whereas Nusselt numbers over a range of Prandtl number predicted from present study are shown in Fig. 3.10.

---

* Here also the Interval Halving Technique was used to give quick convergence.

The analytical results of heat transfer for turbulent flow preceded by a laminar flow are presented in Figs. 3.11 to 3.18. Fig. 3.11 gives the temperature profile in the simultaneously developing region. Fig. 3.12 shows a probable trend of Nusselt number distribution for turbulent flow preceded by a laminar boundary layer. Figs. 3.13 to 3.16 show respectively the effects of Pr, Re_d, Tu, and choice of σ on Nusselt number distribution in the simultaneously developing region. In these figures, the values of Nusselt numbers for fully developed conditions are compared with those given by Kays[28], pp. 173. Figs. 3.17 and 3.18 give effects of Tu and Pr respectively on the entrance lengths under simultaneous developement of boundary layers. The results of entrance lengths are also presented in tabulated forms in Tables 2 (a) and (b).

CHAPTER IV

EXPERIMENTAL STUDIES

4.1. APPARATUS

The experimental apparatus used in the present investigation was essentially the same as used by Park[22] except for a few modifications. The test tube was made of copper with an internal diameter of 3.814 inches. Air was drawn through a flow measuring orifice; 3.15 inches B. S. orifice into a settling chamber and through a bell mouthed contraction into the test section by a centrifugal blower with a rating of 300 cfm at 20 in. of water located at the downstream end as shown in Fig. 4.1.

The settling chamber, 42"x30"x30", consists of filters and settling screens to remove the dust and the initial disturbance caused by the orifice, respectively. An additional provision for measuring turbulence intensity just upstream of the entrance was also made for the present investigation. The turbulence intensity at the inlet was varied by changing the damping screen placed upstream of the entrance. Five different screens of varying mesh sizes and wire diameters were used. The essential dimensions of the screens are given in Table 3.

The bell mouthed section was machined from a 12"x12"x8" plexiglas block. The trip wire used in the previous work was removed. Extreme care was taken in making a smooth connection between the test tube and the bell-mouth to ensure that there will be no tripping of the boundary layer at the entrance.

Along the test section, provitions were made for the measurement of static pressure distribution and detailed exploration of flow field at various crossections in the developing region.

The traversing mechanism carries the measuring instrument such as a hot-wire probe or pitot tube to make the measurement of local turbulence intensity and flow fields possible. The radial displacement of a probe is measured within 0.001 inch by means of a dial gage mounted on the traversing mechanism. The starting position (y=0) of the probe was known accurately by means of an electrical contact, i.e. by measuring the resistance between the probe and the test tube by an AVOmeter. The resistance was very high when the probe did not touch the bottom of the pipe and it dropped to a very low value as soon as a slight contact was achieved between the probe and the pipe.

The assembled test section is mounted horizontally on several supports. The horizontal alignment of the whole assembly could be easily accomplished by adjusting the heights of these supports with the help of levelling screws provided at the bottom of each support. The horizontal alignment was checked by a surveying level. The maximum mis-alignment was about 0.12 inch for 18 feet of length. The axial alignment was taken care of during the manufacturing stage by drilling and reaming all the flanges simultaneously after clamping them together.

To minimise pressure loss and to isolate the vibration from the blower, a conical diffuser and a flexible tube were used (see Fig. 4.1).

4.2. INSTRUMENTATION

4.2.1. Hot-wire Anemometry

A DISA 55D00 series constant temperature hot-wire anemometer system in conjuction with miniature hot-wire probes (DISA 55F31) was used to detect the longitudenal turbulence level. The probe wire was platinum-plated tungsten, 5 microns in diameter and 1.25 mm. long with an electrical resistance of 3.5 ohms*.

The signal from the probe was fed to the anemometer, DISA 55D01, which was in turn connected to the auxiliary unit, DISA 55D25, and the output signal was fed to the linearizer, DISA 55D10. The linearized signal was then integrated by RMS voltmeter, DISA 55D35, and finally, root mean squared values were either read on the dial of RMS meter, DISA 55D35, or on DVM, DISA 55D30. The typical combination of the turbulence measurement system is shown in Fig. 4.2.

4.2.2. Pitot Tube, Pressure Measuring System and Orifice Plate

Velocity distribution was measured by a pitot tube having an I. D. of 0.027 inch and an outer diameter of 0.032 inch. Static pressure tappings, 1/16 inch in diameter and 3/8 inch long, were made of brass tubing of about 1/4 inch O. D. and these were provided along the tube. Pressure drop was measured by a micro-manometer used in conjuction with DISA 55D41/42

---

* Detailed technical data of hot-wire probes are given in DISA Probe Catalog No. 603.

hot-wire probe calibration unit. To measure mean velocity in each run, a B. S. -3.15 inches orifice was used. Further details for these instruments can be found in Ref.(22).

4.3. CALIBRATION OF INSTRUMENTS

All the instruments used in the present investigation were described in the previous section and their functions were also explained. To check all these instruments against known standards is obviosly important to reduce error involved in any measurement.

Calibration can be accomplished by a comparison of the particular instrument with either (a) preliminary standard (b) secondary standard with a higher accuracy than the instrument to be calibrated (c) a known input source.

In this section, the methods of calibration used in the present study are described.

4.3.1. Calibration of Orifice Plate

The mean flow velocities measured from the pitot tube traversing were used to calibrate the orifice. The velocity distribution measurements were taken for five to ten cross-sectins along the entire tube for the whole of the available range of Reynold's number, The results of calibration are shown in Fig. 4.3. The accuracy of the orifice was, therefore, estimated at abut ±1% for the range of Reynold's number studied.

4.3.2. Calibration of Hot-wire Probe

It is well-known that the output voltage of a constant temperature anemometer is a non-linear function of the flow velocity under measurement. This nonlinearity is not very importent in measurements of small degrees of turbulence, in which case a small section of the calibration curve may be considered sufficiently linear. At a higher degree of turbulence, on the other hand, the distortion caused by the curvature of the calibration curve becomes noticeable and measurements at a wide range of mean flow velocity are difficult because the subsequent treatment of results obtained in both cases is not a very satisfactory solution and an electronic circuit is usually adopted to take care of the linearization problem[32].

The relation between flow velocity, U, and output voltage, V, can be represented by the equation:

$$V^2 = A + BU^n \tag{4.1}$$

A, B, and n are constants whose values depend on the probe connected to the anemometer. Assuming a proper choice of constants, the formula will fit the calibration curve within a wide velocity range.

During the calibration, the probe was placed in an air flow of known velocity. DISA 55D41/42 calibration unit was used for this purpose along with a vertical adapter, DISA 55A67, to keep the probe in an identical position during calibration and measurement. Details of operation of this equipment are given in the DISA service manual[33]. The output voltage of the anemometer was linearised by making proper compensation for the exponent, n, in Eqn.(4.1) and temperature changes. For this purpose, DISA 55D10 Linearizer was used. Fig. 4.4 shows a typical calibration curve using a linearizer.

4.4. EXPERIMENTAL PROCEDURE AND DATA REDUCTION

Before taking any reading, the apparatus was run for a certain period of time to achieve steady state conditions in all experimental runs. The apparatus was considered to have reached a steady state when the readings on the various instruments such as the manometer were not changed for a reasonable period of time. Then the ambient temperature and atmospheric pressure were recorded. For each size of screen, Reynold's number was varied approximately from 30,000 to 100,000 in steps of about 10,000. Local flow velocities were measured at different axial locations and at many radial locations at a particular axial position for some of the screens to calibrate the orifice plate.

The mean velocity at the bell-mouth entrance and the root-mean- square (RMS) value of the axial component of velocity was measured by the anemometer unit to calculate the turbulence intensity at the entrance. At the beginning of each experiment, the hot-wire probes were calibrated as described in Sec. 4.3.2. The hot-wire anemometer was allowed one to two hours warming up time before measurements were made as prescribed by the manufacturer.

Static pressure measurements were made at 16 different locations along the entire length of the pipe with the help of a differential micro-manometer (Sec. 4.2.2).

The procedure was repeated with five different types of screens mentioned in Table 1 and with no screen at all.

Data Reduction

(a) Local mean velocity was calculated from the relation:

$$u = \left[2\left(\frac{\rho_{water} - \rho_{air}}{\rho_{air}}\right) \times g \times \text{constant} \times \text{manometer reading} \right]^{1/2}$$

(b) Bulk velocity was calculated by

$$u_b = \frac{2}{r_o^2} \sum_{i=1}^{40} u_i r_i \, dr_i$$

(c) Reynold's number was calculated from the definition

$$Re_d = \frac{u_b D}{\nu}$$

(d) Friction Factor:

The local apparent friction factor is defined by:

$$f = \frac{p_1 - p_2}{x_2 - x_1} \cdot \frac{D}{2 \rho u_b^2}$$

where p_1 and p_2 are the static pressures (measured at the wall of the duct) at the axial locations x_1 and x_2 respectively. The value of 'f' calculated from this relation was taken to be the value midway between stations 1 and 2, or, in other words, at the axial location $(x_1+x_2)/2$. This type of friction coefficient includes the effects of changes in momentum flux associated with changes in velocity profile. When the velocity profile is fully developed, the local apparent friction factor is the same as the true drag coefficient $(2\tau_o/\rho u_b^2)$. But even in the entrance region, except very near the inlet ($x/D \gtrsim 1$), Barbin and Jones[26] have shown that the effect of change in momentum flux on the static pressure distribution is negligible compared to the effect due to skin friction.

During all these calculations, the dynamic viscosity (μ) of air corresponding to the measured ambient temperature was calculated from the following equation based on the data of Sigwart[34] for the temperature range of 70 to 400^0F.

$$\mu = 0.11005 \times 10^{-4} + 0.18071 t \times 10^{-7} - 0.5158 t^2 \times 10^{-11}$$

where μ is in lb/sec ft and t is in degrees Fahrenheit.

The density of air was calculated from the Ideal Gas Law $p = \rho RT$ corresponding to the ambient conditions.

4.5. EXPERIMENTAL RESULTS

In the present study, experiments were performed to study the effect of turbulence intensity on the boundary layer transition in a circular tube. Turbulence intensity was varied over a wide range by varying the mesh size and number of the damping screen used in the settling chamber. For each screen size, Reynold's number was varied from about 30,000 to 100,000 and for each value of Reynold's number, friction factor and velocity profiles were measured at various axial locations along the entire length of the pipe.

Fig. 4.5 shows the turbulence intensity, Tu, at the bell mouth entrance (x=-6") as a function of Re_d for various kinds of screens used.

Results on friction measurement are presented in Figs. 4.6 to 4.11 where the local friction factor, f_x, is plotted against ratio of the distance from the inlet to the tube diameter, (x/D). Figs. 4.6 to 4.9 are drawn at fixed Reynold's number, Re_d, and show the effect of turbulence intensity, Tu, on f_x whereas Figs. 4.10and 4.11 are drawn keeping the turbulence intensity constant and show the effect of Reynold's number on f_x.

Velocity profiles are plotted in Figs. 4.12 and 4.13 where a comparison with the theoretically predicted velocity profiles is also made.

Figs. 4.14 (a) and (b) show the effect of Re_d on critical Reynold's number, $Re_{x,cr}$. Transition in flow from laminar to turbulent was perceived by the changes in friction factor along the flow direction as described in Sec. 5.2. Fig. 4.15 shows the effect of free stream turbulence on the critical Reynold's number.

In Fig. 4.16, the effects of Tu on the entry length, $(x/D)_{d,M}$ is shown. The experimental entrance lengths in Fig. 4.16 are based upon fully developed friction factor.

CHAPTER V

DISCUSSION

From the results of both the analytical and experimental studies described in the previous chapters, we can study the effect of free stream turbulence on the phenomenon of turbulent flow and heat transfer in a circular duct. Basically, the method employed is to study experimentally the effect of turbulence intensity (Tu) on the transitional phenomenon in a circular duct, i.e. to obtain the values of $Re_{x,cr,1}$ and $Re_{x,cr,2}$ as functions of Tu as shown in Fig. 4.15. Then the effect of $Re_{x,cr}$ on various aspects of fluid flow and heat transfer in a circular duct has been predicted. An advantage of the approach used is that if the effect of some other parameter on $Re_{x,cr}$ is known, then its effect on fluid flow and heat transfer in a circular duct can be studied from the present analytical studies.

5.1. TURBULENCE INTENSITY

Fig. 4.15 shows the results of turbulence measurements at the bell-mouth entrance, x=-6". The turbulence intensity is plotted against Re_d for different kinds of screens used. Since the turbulence at a distance from the screens in the settling chamber in general can be assumed to become isotropic, it is decided to use the relation $Tu=100x\sqrt{\overline{u_e'^2}}/U_e$ as the turbulence level in place of the usual more rigorous definition, $Tu=100x \sqrt{\frac{1}{3}(\overline{u'^2}+\overline{v'^2}+\overline{w'^2})}/U$.

Fig. 4.5 shows that the turbulence intensity is independent of Reynold's number which means that by increasing or decreasing the Reynold's number, the RMS value of the fluctuating component ($\sqrt{\overline{u_e'^2}}$) increases or decreases in the same proportion as the local mean velocity (u_e). Therefore, the ratio Tu$(=\sqrt{\overline{u_e'^2}}/u_e)$ remains independent of Reynold's number.

5.2. FRICTION FACTOR AND VELOCITY PROFILE

The experimental results on friction factor are presented in Figs. 4.6 to 4.11 in the form of curves in which the local friction factor, f_x, is plotted against the ratio of the distance from the inlet to the tube diameter. The figures cover a range of turbulence intensity from 1.2 to 6.3 and a Reynold's number range of about 30,000 to 100,000.

Superimposed on the experimental data are the theoretical curves of Campbell and Slattery[9] for the laminar flow and present analysis for the turbulent boundary layer.

The experimental points show that the friction factor at first decreases with distance, x, more or less along the theoretical curve for laminar region. Then at a certain distance $x=x_{cr,1}$ the experimental results start to deviate from this theoretical curve and instead of decreasing, start to increase. This is the point at which it is assumed that trasition from laminar to turbulent is taken place.

After the friction factor starts increasing from $x=x_{cr,1}$, one of the following two phenomena were observed as seen in Figs. 4.6 to 4.11.

(i) If the Reynold's number and the turbulence intensity are relatively high, the friction factor increases above the theoretical curve for turbulent boundary layer. Then after reaching a peak value at $x=x_{cr,2}$, it again starts to decrease to its fully developed value. Therefore, the point at which friction factor starts decreasing from its peak value is taken to be the point at which turbulent region begins.

(ii) If the Reynold's number and the turbulence intensity are relatively low, the friction factor seems to increase gradually to its fully developed value and become constant after that. In this case, the point at which it reaches the fully developed value characterises the beginning of the turbulent region.

Now, Fig. 3.6 has been drawn purely on a theoretical basis assuming that the transition from laminar to turbulent takes place instantaneously at one particular point, i.e. there is no transition region in between laminar and turbulent regions. This figure indicates that when transition takes place at a smaller distance (which is true at high Tu and high Re_d), the friction factor does rise to a peak value above its fully developed value, but when transition takes place at a comparatively longer distance (which is true at low Tu and low Re_d), the friction factor suddenly rises from its minimum value to the fully developed value and remains constant from that point on. The curves shown in Fig. 3.6 are based on an entirely hypothetical case in which there is no transition region. In actual practice, the transition takes place through a finite distance as is obvious from the experimental data shown in such as Figs. 4.6 to 4.11 and consequently the friction factor, instead of rising sharply as shown in Fig. 3.6, increases gradually from its minimum value.

Having distinguished the two critical points, i.e., one at which boundary layer changes from laminar to transition and the other at which it changes from transition to turbulent, the process was repeated for Tu=1.2~6.3 and Re_d= 10,000~ 100,000. A discussion on the results of these critical transition lengths is given in the following section. Figs. 4.10 and 4.11 show the effect of Reynold's number on friction factor distribution for fixed values of Tu equal to 2.0 and 6.3 (which have been chosen arbitrarily) where the critical transition points can be clearly observed.

Figs. 4.12 and 4.13 show a comparison between the theoretically predicted and the experimentally determined velocity profiles. The figures show a fair agreement between the two velocity profiles for $(x/D) < (x/D)_{cr,1}$ and for $(x/D) > (x/D)_{cr,2}$. But for $(x/D)_{cr,1} < (x/D) < (x/D)_{cr,2}$, the predicted velocity profiles do not agree with the experimental ones, as expected.

5.3. CRITICAL REYNOLD'S NUMBER

A few of the typical results of the two transition lengths (lower and upper) are presented in Figs. 4.14 (a) and (b) which show the effect of Reynold's number, Re_d, on the transition lengths for various different values of Tu. Here, Reynold's number based upon axial length is defined as:

$$Re_x = \frac{\rho u_b x}{\mu} = Re_d \left(\frac{x}{D}\right) \qquad (5.1)$$

in a similar way as for external flows.

Fig. 4.14 is then the plot of $Re_{x,cr}$ based upon critical transition length against Re_d. It shows that the critical Reynold's number based upon critical length is independent of Re_d for a given value of Tu. This result is similar to the one for a flat plate(5). It implies that if the Reynold's number based on diameter is high, transition from laminar to turbulent occurs closer to the entrance and if it is low, transition occurs far from the entrance. The figure also shows that the axial distance at which transition occurs is inversely proportional to Re_d. Consequently, $Re_{x,cr}$ as defined by Eqn.(5.1) is independent of Re_d.

Fig. 4.15 shows the effect of turbulence intensity on the transitional phenomenon in a circular tube very clearly. It is observed that, as a general rule, transition occurs earlier when the turbulence intensity is high and vice-versa. This is explainable by noticing that a high turbulence intensity of the entering fluid tends to disturb the stability of the laminar boundary layer to cause it to change to turbulent earlier. It is also seen that in the beginning, at low values, turbulence intensity has a comparatively larger effect in moving the point of transition upstream than at high turbulence intensity.

5.4. HYDRODYNAMIC ENTRANCE LENGTHS

Fig. 4.16 shows the effect of turbulence intensity on the entry length in a circular duct. It shows that the turbulence intensity has a significant effect on the entry length.. At low turbulence intensity, the entrance length is larger at a given Re_d. The opposite is also true. The reason is that at low turbulence intensity, transition occurs far from the entrance as seen in Fig. 4.15 which implies that the boundary layer is laminar for a longer distance. Since a laminar boundary layer developes much slower than a turbulent boundary layer, it is obvious that the total distance required for the boundary layer to develope fully will be long for low turbulence intensity and short for high Tu.

As is obvious from Fig. 4.15, at higher Tu, $Re_{x,cr}$ is very small and if Re_d is also sufficiently high, then the value $(x/D)_{cr}=Re_{x,cr}/Re_d$ will be very small. For such a case, the laminar inlet region at the beginning of the entrance can be neglected or it may be assumed that the boundary layer is turbulent from the beginning of the entrance. This is the basic assumption of a majority of the analytical works available so far in literature; e.g. the work of Deissler[3].

As the values of Tu and Re_d increase, the results are closer to those obtained by using the assumption that the turbulent boundary layer starts at x=0. But Fig. 4.16 indicates that the error caused by neglecting the laminar entry region increases considerably at lower values of Tu and Re_d.

There is a great deal of discrepency among the experimental results on the entry length for the flow in a circular duct by many investigators; e.g. Schlichting[1] reports data by Kirsten showing that the entrance length for a circular tube is about 50 to 100 tube diameters depending on Re_d, whereas according to Nikuradse, the fully formed turbulent velocity profiles exist after an inlet length of 25 to 40 diameters. The simplified analyses of Deissler[3] andothers could not explain the cause of the disagreement between these two typical results. Instead, Deissler[3] obtained analytically that the fully developed friction factors in a circular duct are attained within less than 10 tube diameters which is very small than the experimental results of Kirsten and Nikuradse. The disagreement, however, may be explained by means of the present study which shows that the entrance lengths in a circular tube could vary as much as from about 10 to 250 tube diameters within the range of Tu studied (or possibly even higher, depending on the ranges of Tu and Re_d)

In Fig. 4.16, the predicted entrance lengths are given for three different cases. One of them is the idealised hypothetical case when $(x/D)_{cr}=0$. But the other two values of entrance lengths are obtained by using the two values of transition lengths, e.g. $(x/D)_{cr,1}$ and $(x/D)_{cr,2}$. The experimental points superimposed in Fig. 4.16 suggest that usually $(x/D)_{cr,2}$ should be used for predicting the entrance lengths analytically, using the momentum integral method.

Fig. 4.16 also shows the effect of Reynold's number on the entrance length. It shows that for low values of Re_d, the entrance length decreases with increasing Reynold's number whereas for high Re_d, the entrance length increases with increasing Reynold's number. The reason is that Re_d affects the entrance length in two ways. First an increase in Re_d by virtue of Eqn.(5.1) decreases the laminar inlet length near the entrance which tries to decrease the total entry length. Secondaly, an increase in Re_d causes the turbulent boundary layer after the laminar boundary layer to require a longer distance to develope fully which in other words means that it tries to increase the entrance length. At low Re_d, the effect of decrease in entrance length with increasing Reynolds number is predominating whereas at high Re_d, the effect of increase in entrance length with decreasing Reynold's number is predominating. Therefore, the entrance length, at first, decreases with Re_d upto a certain point and then it starts increasing with Re_d.

Fig. 4.17 shows that the lower the Reynold's number the more significant is the effect of turbulence intensity on the entrance length and at high Reynold's numbers the effect of turbulence intensity becomes negligible.

5.5. HEAT TRANSFER

In the present study, heat transfer for trubulent flow through a circular pipe is analysed by using the integral method to study the effects of free stream turbulence, Prandtl number, Reynold's number, and choice of eddy diffusivity ratio on heat transfer coefficients and thermal entrance lengths under simultaneous developement of the boundary layers. First, solutions for a completely laminar flow and for a completely turbulent flow are obtained and then the two solutions are joined at a suitable point depending upon turbulence intensity to study the heat transfer in turbulent flow preceded by a laminar flow boundary layer.

Most of the results of heat transfer could not be compared with experiment or other works because of non-availability of information in the published literature.

In Fig. 3.9 the results for laminar flow heat transfer for the case of air, Pr=0.7 obtained from present study are compared with the exact solutions of other investigators. The figure shows that all the methods give more or less the same results farther down from the entrance. But very close to the entrance, the integral method predicts Nusselt numbers which are lower than those predicted by the exact methods of Manohar (19) and Ulrechson and Schmitz (20). The difference may be due to the difference in either the velocity profiles or the methods used. Manohar[19] and Ulrichson and Schmitz[20] used Langhaar's velocity profiles whereas in the present study, the parabolic velocity profiles of Campbell and Slattery[9] were used.

Fig. 3.10 shows the effects of Prandtl number on laminar flow heat transfer in the entrance region. It is seen that as the Prandtl number increases, its effect becomes less in the developing region of the duct. The reason is that at higher Prandtl number, the hydrodynamic boundary layer developes much faster than the thermal boundary layer. In this case, therefore, the distance required by the hydrodynamic boundary layer to develop fully may be neglected in comparison to that required by the thermal boundary layer to do so.

The predicted temperature prefiles in the developing region are shown in Fig. 3.11 for different Prandtl number fluids and at various values of δ/r_0. Fig. 3.12 shows the effect of the laminar boundary layer preceding the turbulent boundary layer on Nusselt number distribution. When the flow is assumed to be turbulent from the beginning of the entrance, the Nusselt number decreases gradually with distance x. However, for a turbulent flow preceded by a laminar boundary layer, the Nusselt number first decreases with distance x till it reaches the first critical transition point. Then there should be a gradual rise in Nusselt number followed by a gradual dropping down to the fully developed value as in the case of friction factor. Fig. 3.12 is drawn at a fixed value of turbulence intensity. But for a comparison there are two different curves in this figure for two different values of $Re_{x,cr}$, i.e. $Re_{x,cr,1}$ and $Re_{x,cr,2}$ obtained from experimental studies. In actual practice, the Nusselt number is expected to follow the smooth trend shown by broken line in Fig. 3.12.

Fig. 3.13 to 3.16 show the effect of various parameters on the Nusselt number distribution in turbulent flow preceded by a laminar boundary layer. These figures are based on the smooth trend in the region between $(x/D)_{cr,1}$ and $(x/D)_{cr,2}$. In Figs. 3.13 to 3.15, the ratio of eddy diffusivities was assumed to be unity. The reason was that the choice of σ does not have a major effect on Nusselt number as shown in Fig. 3.16.

The effect of turbulence intensity on the predicted thermal entrance lengths is shown in Fig. 3.17 which shows that the thermal entrance length is a strong function of the turbulence intensity, specially at low Reynold's number as was the case for hydrodynamic entrance length (Fig. 4.17). For high Reynold's number flows, the transition length is so small that the assumption of turbulent boundary layer from the beginning of the entrance does not lead to an appreciable error. Fig. 3.18 shows the effect of Prandtl number. Prandtl number seems to have little influence on the thermal entry length within the range of Prandtl number studied. Moreover, the effect of Prandtl number becomes less significant as the Reynold's number increases.

Reynold's number influences the entry length in a different way. Like the hydrodynamic entry length, the thermal entrance length also decreases with Reynold's number upto a certain point, after which it increases with Reynold's number. The reason is the same as discussed in Sec. 5.4 in connection with the hydrodynamic entrance length.

CHAPTER VI

CONCLUSIONS

The following conclusions were drawn from both the analytical and experimental studies of the turbulent flow and heat transfer in a circular duct under simultaneous developement of boundary layers.

(1) Turbulence intensity of the entering fluid measured just upstream of the entrance (x=-6") of the duct and defined as $Tu=\sqrt{\overline{u_e'^2}}/u_e x100$ is not a function of the flow Reynold's number.

(2) Free stream turbulence intensity varies with the mesh size and number of damping screen. No correlation of these effects was fruitful.

(3) Transition Reynold's numbers, $Re_{x,cr,1}$ and $Re_{x,cr,2}$ are independent of the Reynold's number, Re_d, for a given value of Tu. But they are strongly dependent on the free stream turbulence intensity of the entering fluid.

(4) The overall phenomena of turbulent flow and heat transfer in a duct are, in general, affected very much by the free stream turbulence intensity. From this, it can also be concluded that the simple analyses of Deissler(3) and other investigators which used the assumption of turbulent boundary layer from the beginning of the entrance could sometimes lead to altogether inaccurate results, especially when the turbulence intensity and the Reynold's number are low where these effects are more pronounced

(5) The usefulness of the integral method for fluid flow and heat transfer in a circular duct is demonstrated.

(6) Finally, from this study, some anomaly in the published results in the entrance region of a pipe can be partially explained.

Table 1 Predicted Hydrodynamic Entrance Lengths for Flow Through a Straight Circular Duct

$Re_{x,cr,2}$	2.5×10^6	1.4×10^6	8.4×10^5	4.2×10^5	3.1×10^5	2.7×10^5	0
Tu / Re_d	0.5	1.2	2.0	3.0	4.8	6.3	
10^4	250	143	84.0	41.9	30.7	26.5	10.0
2×10^4	125	76.5	42.0	20.9	15.3	14.4	10.8
3×10^4	83.3	47.7	28.0	14.9	14.3	14.0	11.2
4×10^4	63.0	35.7	21.0	14.6	14.0	13.9	11.6
5×10^4	50.0	28.6	16.8	14.4	14.0	13.8	11.8
6×10^4	42.0	23.8	15.4	14.3	13.9	13.7	12.1
7×10^4	36.0	20.4	15.3	14.3	14.0	13.8	12.3
8×10^4	31.3	17.9	15.3	14.3	14.0	13.8	12.5
9×10^4	28.0	15.9	15.3	14.3	14.0	13.8	12.6
10^5	25.0	15.8	15.2	14.3	14.1	13.9	12.7
2×10^5	16.2	15.6	15.1	14.6	14.4	14.3	13.7
3×10^5	16.1	15.6	15.3	14.9	14.8	14.7	14.3
4×10^5	16.2	15.8	15.5	15.2	15.1	14.9	14.7
5×10^5	16.3	15.9	15.7	15.5	15.4	15.1	15.0
6×10^5	16.3	16.0	15.8	15.7	15.5	15.3	15.3
7×10^5	16.4	16.2	16.0	15.8	15.7	15.5	15.5
8×10^5	16.5	16.3	16.2	16.0	15.8	15.7	15.7
9×10^5	16.6	16.5	16.4	16.2	16.0	15.9	15.9
10^6	16.7	16.6	16.5	16.3	16.2	16.1	16.1

Table 2(a) Entrance Lengths Under Simultaneous Developement in a Circular Duct

Pr =0.7

$Re_{x,cr,2}$	1.43×10^6	4.19×10^5	2.65×10^5	0
Re_d \ Tu	1.2	3.0	6.3	
10,000	143	49.1	34.9	12.2
30,000	59.3	27.3	22.5	14.9
50,000	42.8	23.6	20.8	16.3
80,000	34.0	22.0	20.2	17.6
100,000	31.2	21.6	20.2	18.2
200,000	26.5	21.4	20.7	19.7
300,000	25.3	21.7	21.0	20.4
500,000	24.2	22.8	22.0	21.6
1,000,000	25.3	24.9	24.7	23.8

Table 2(b) Entrance Lengths Under Simultaneous Developement in a Circular Duct

Tu =3.0

Re_d \ Pr	0.1	0.7	5.0
10,000	41.9	49.1	52.1
30,000	22.3	27.3	27.8
50,000	20.3	23.6	23.6
80,000	20.0	22.0	21.6
100,000	20.1	21.6	21.1
200,000	20.7	21.4	20.6
300,000	21.2	21.7	20.8
500,000	22.3	22.8	21.3
1,000,000	24.8	24.9	24.0

Table 3 Dimensions of Screens

Mesh/in.	M (inch)	δ (inch)	M/δ
100x90	0.0100 along 100 mesh, 0.0111 along 90 mesh	0.005 along 100 mesh, 0.006 along 90 mesh	2.00 along 100 mesh, 1.85 along 90 mesh
16x16	0.0625	0.023	2.72
4x4	0.2500	0.063	3.97
2x2	0.5000	0.120	4.17
8x8	0.1250	0.025	5.00

M =distance between wire centres

δ =wire diameter

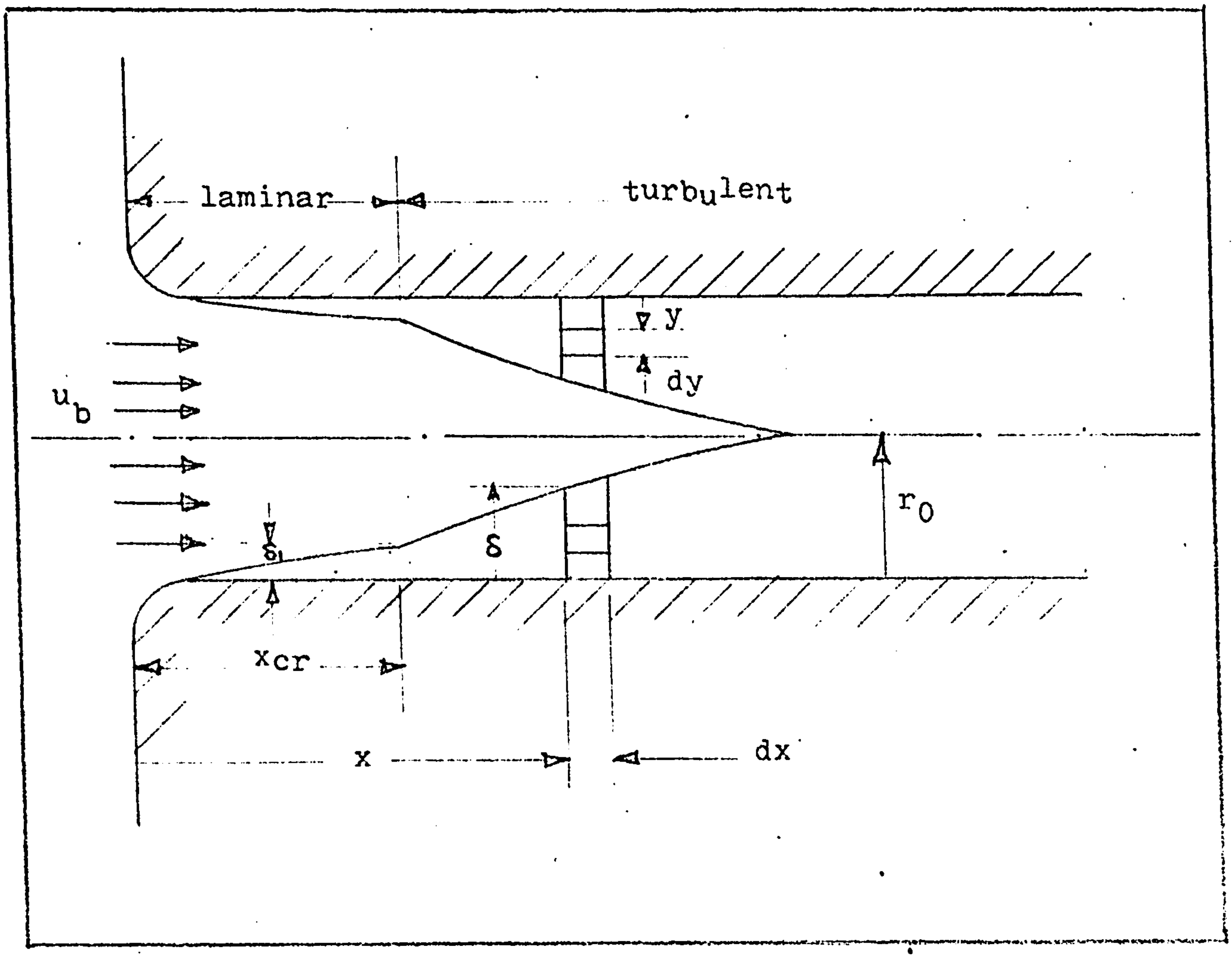

Fig. 3.1 Idealised Model, Hydrodynamic Boundary Layer

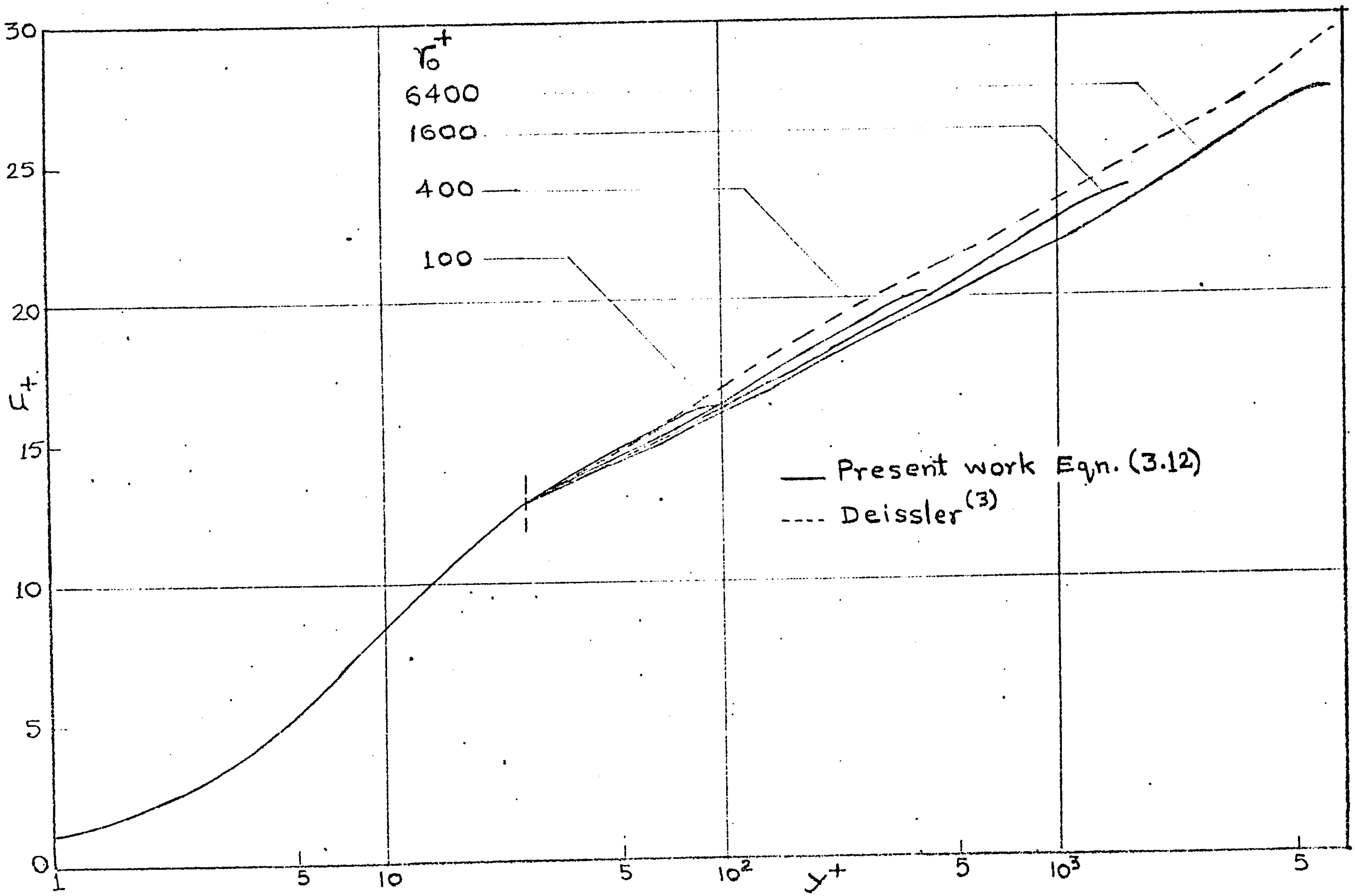

Fig. 3.2 Predicted Velocity Profiles in the Fully Developed Turbulent Boundary Layer

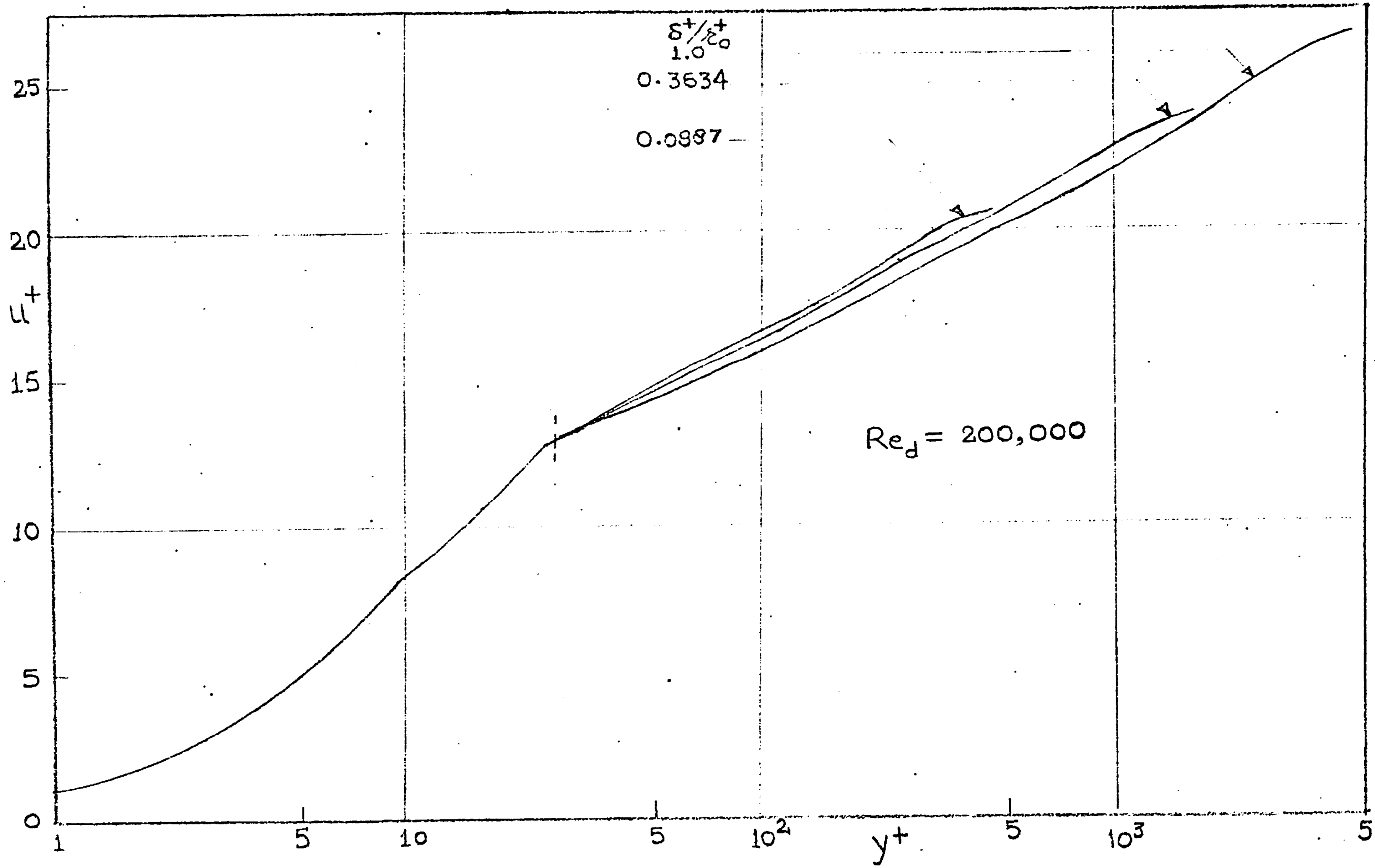

Fig. 3.3 Predicted Velocity Profiles in Developing Turbulent Boundary Layer

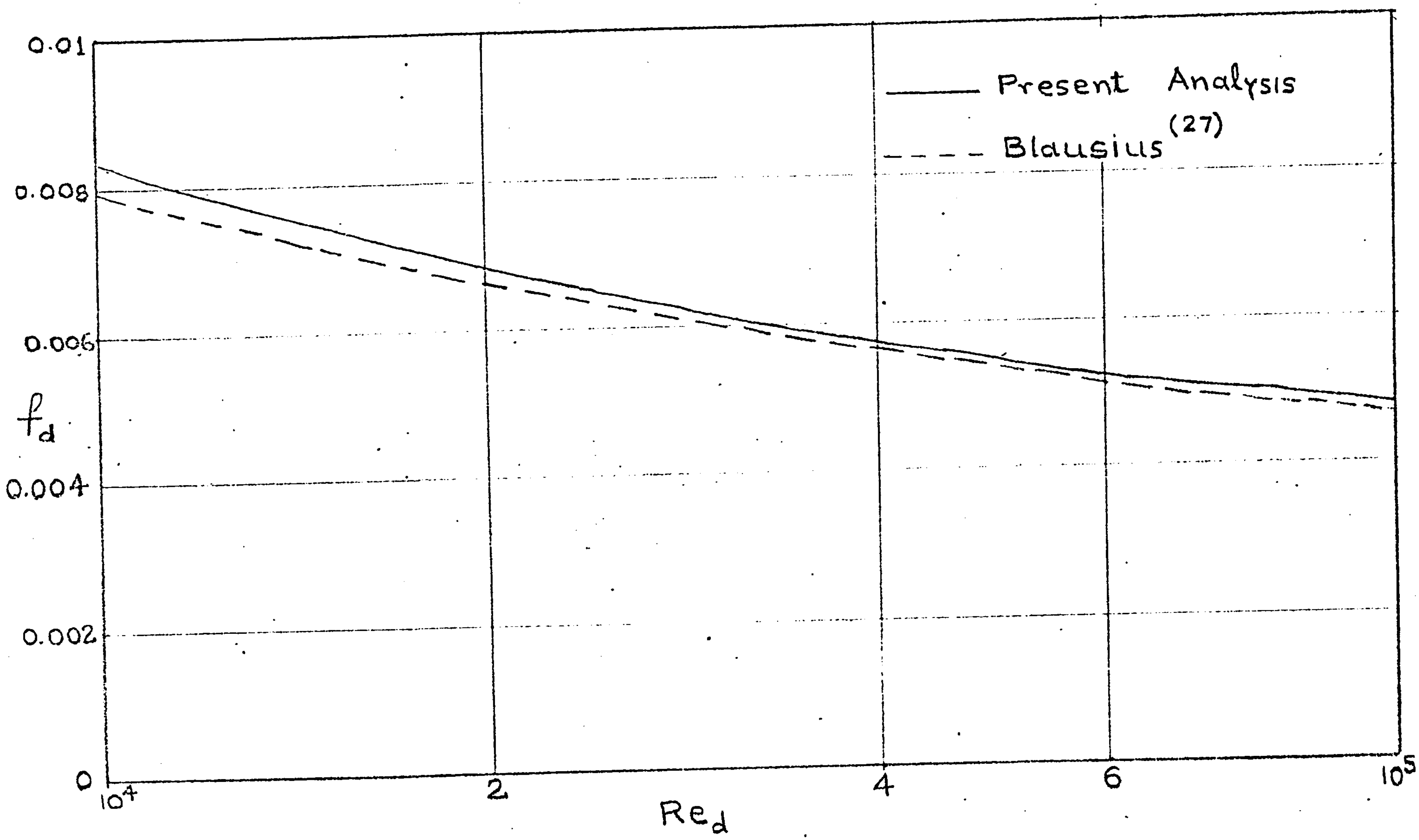

Fig. 3.4 Predicted Friction Factors, Fully Developed Flow

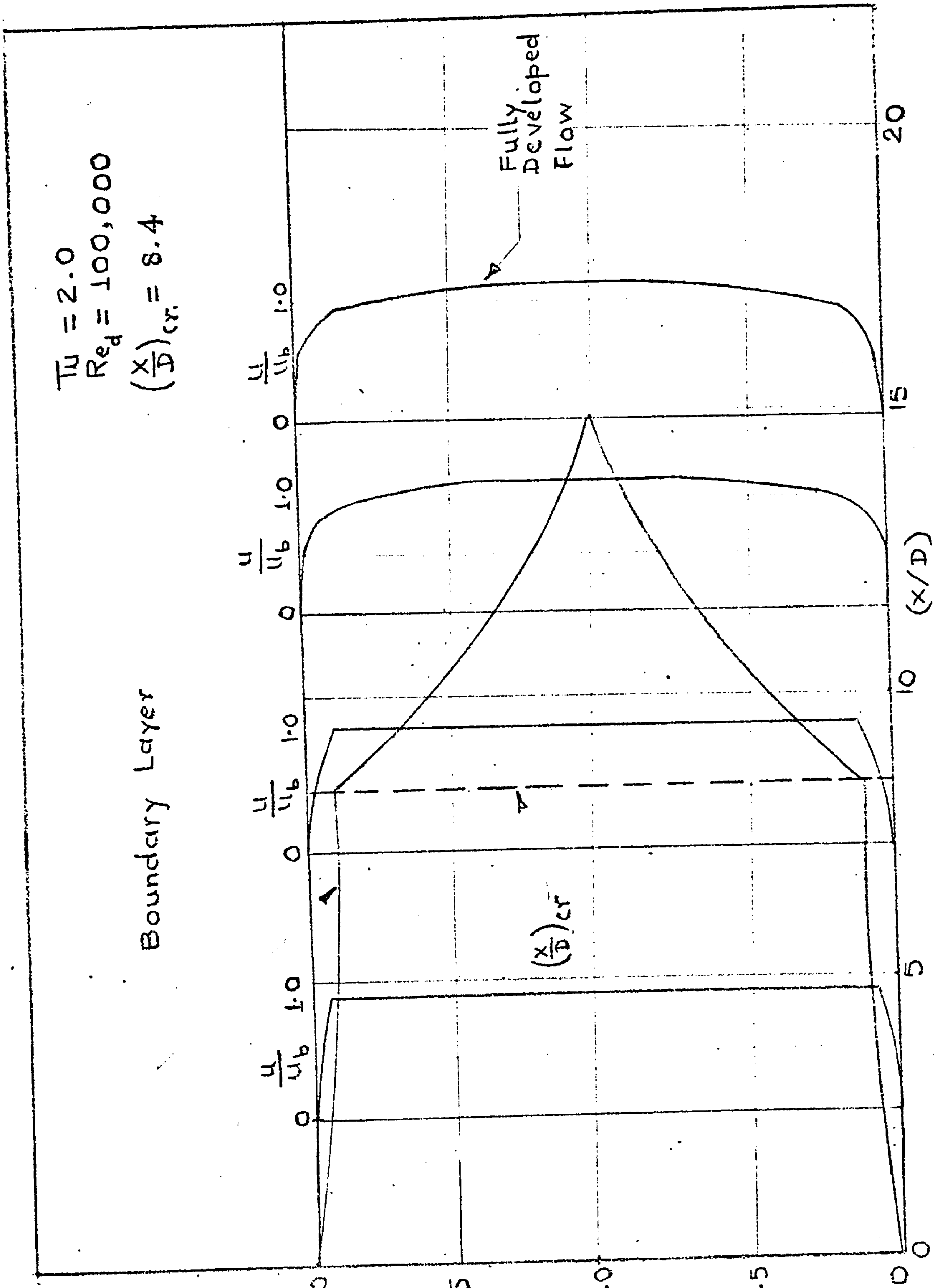

Fig. 3.5 Boundary Layer Development for Turbulent Flow Preceded by a Laminar Flow Through a Circular Tube

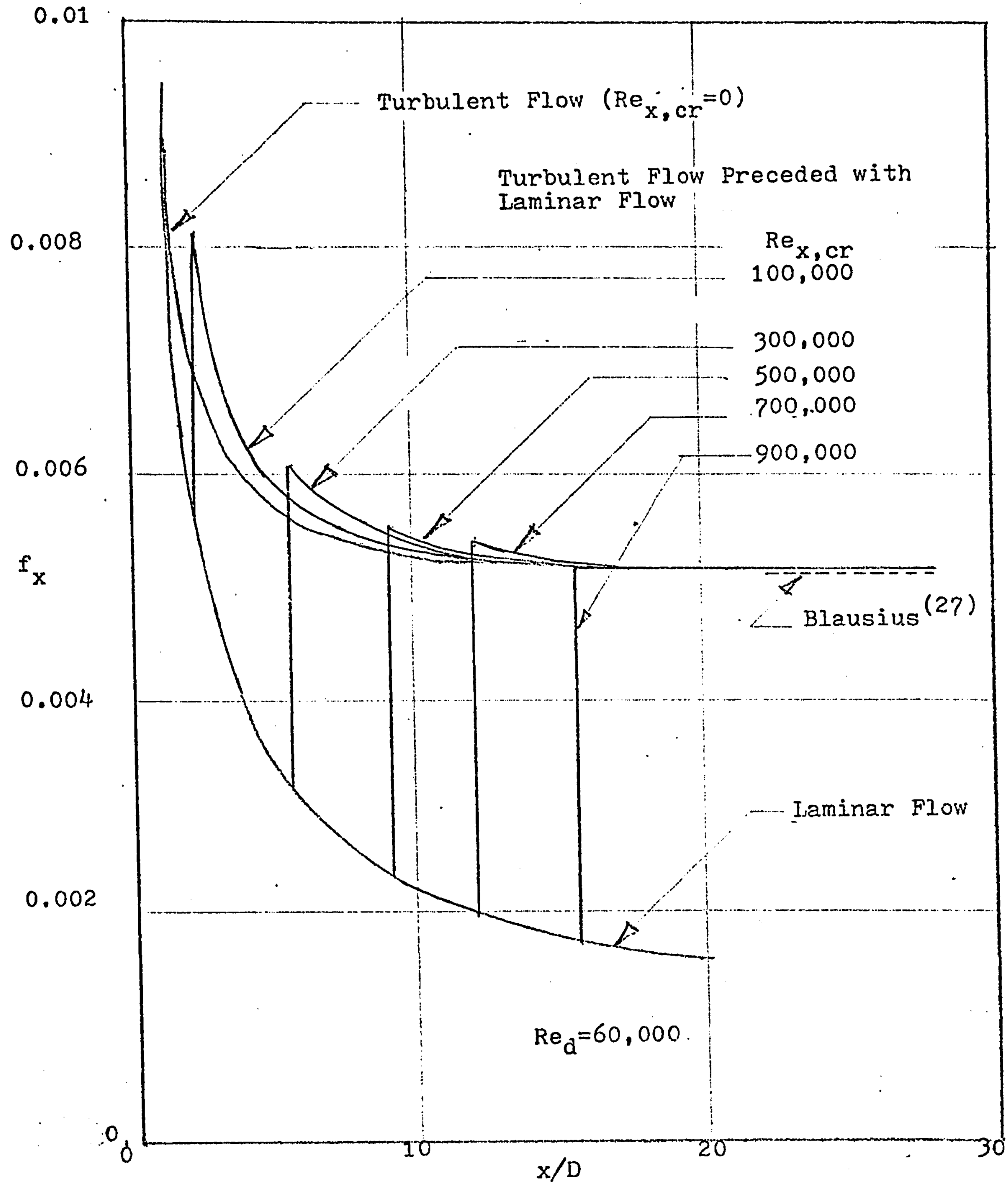

Fig. 3.6 Predicted Friction Factor for Turbulent Flow Preceded by Laminar Boundary Layer

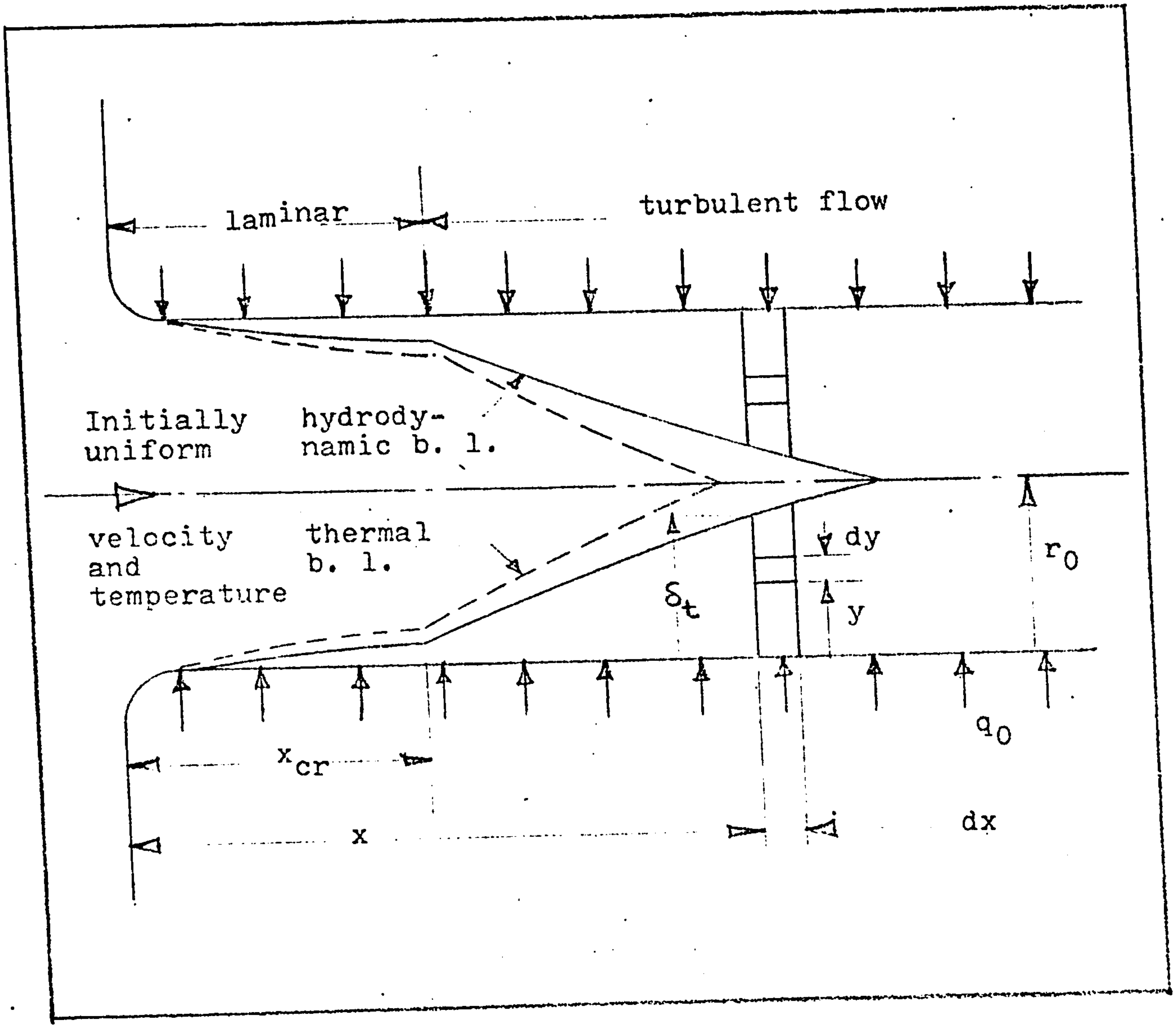

Fig. 3.7. Idealised Model, Thermal Boundary Layer

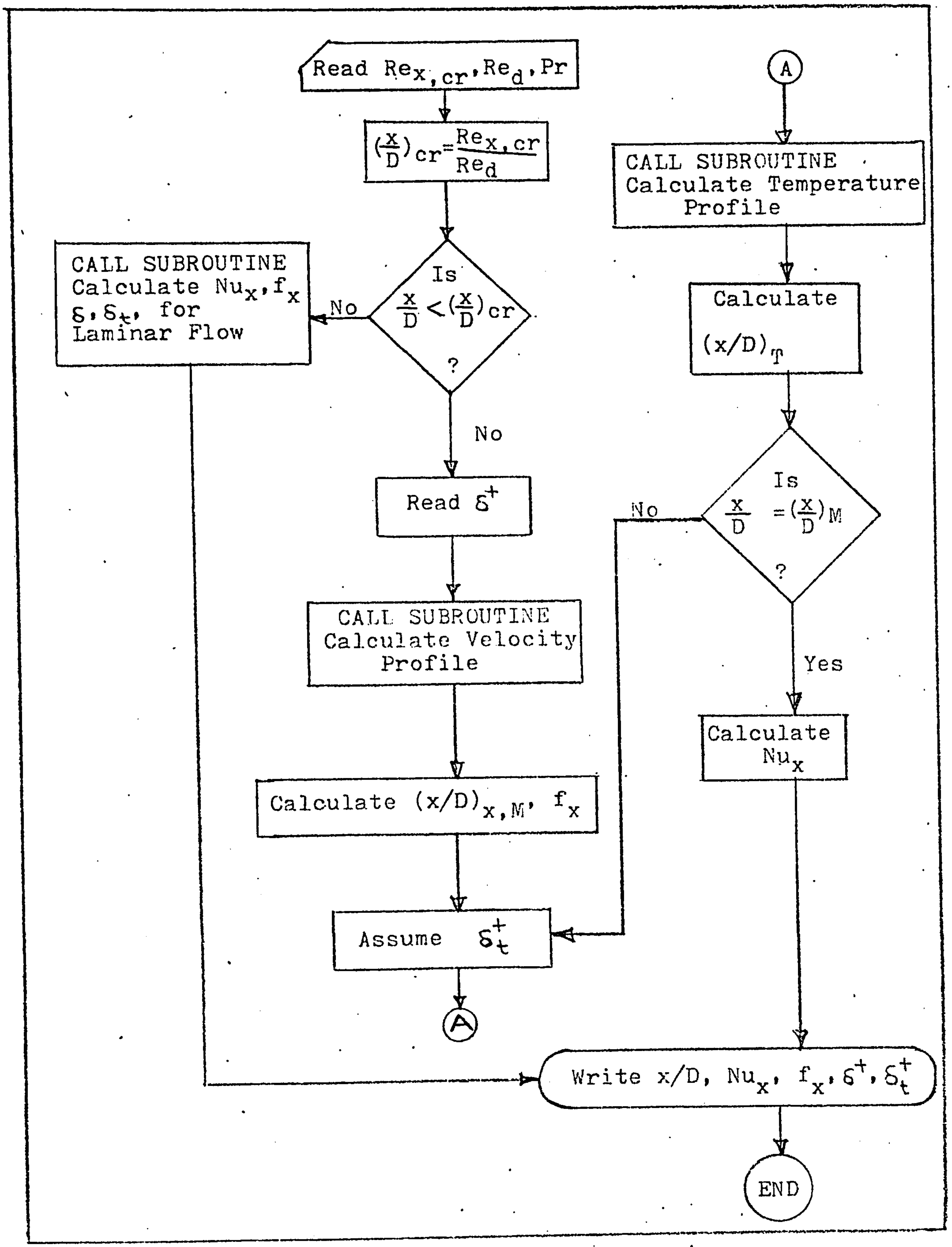

Fig. 3.8 Simplified Flow Diagram of Computational Procedure

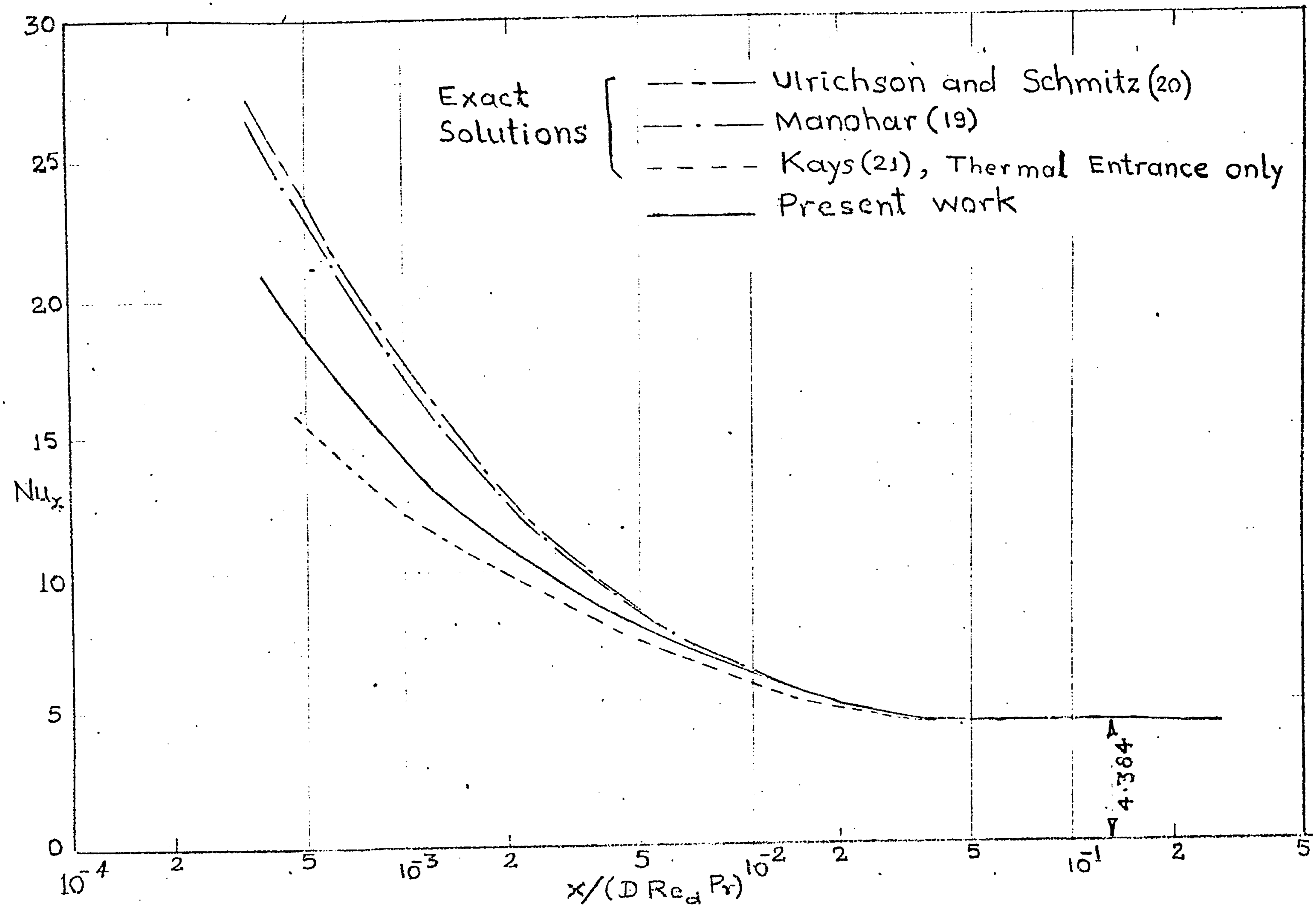

Fig. 3.9 Comparison Between Present Prediction and Other Correlations for Nusselt Number in the Laminar Inlet Region

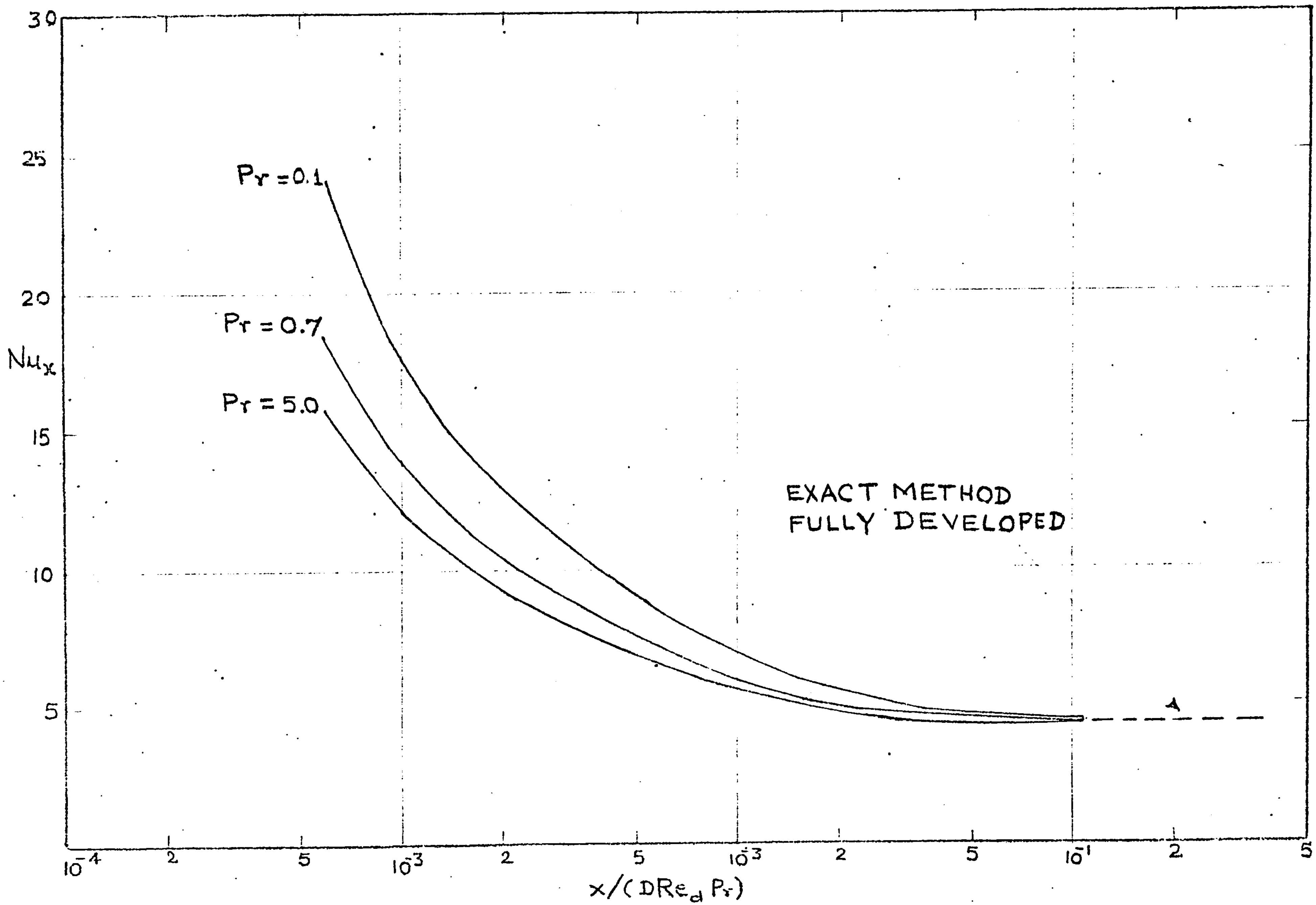

Fig. 3.10 Predicted Nusselt number in the Laminar Inlet Region Using Integral Method

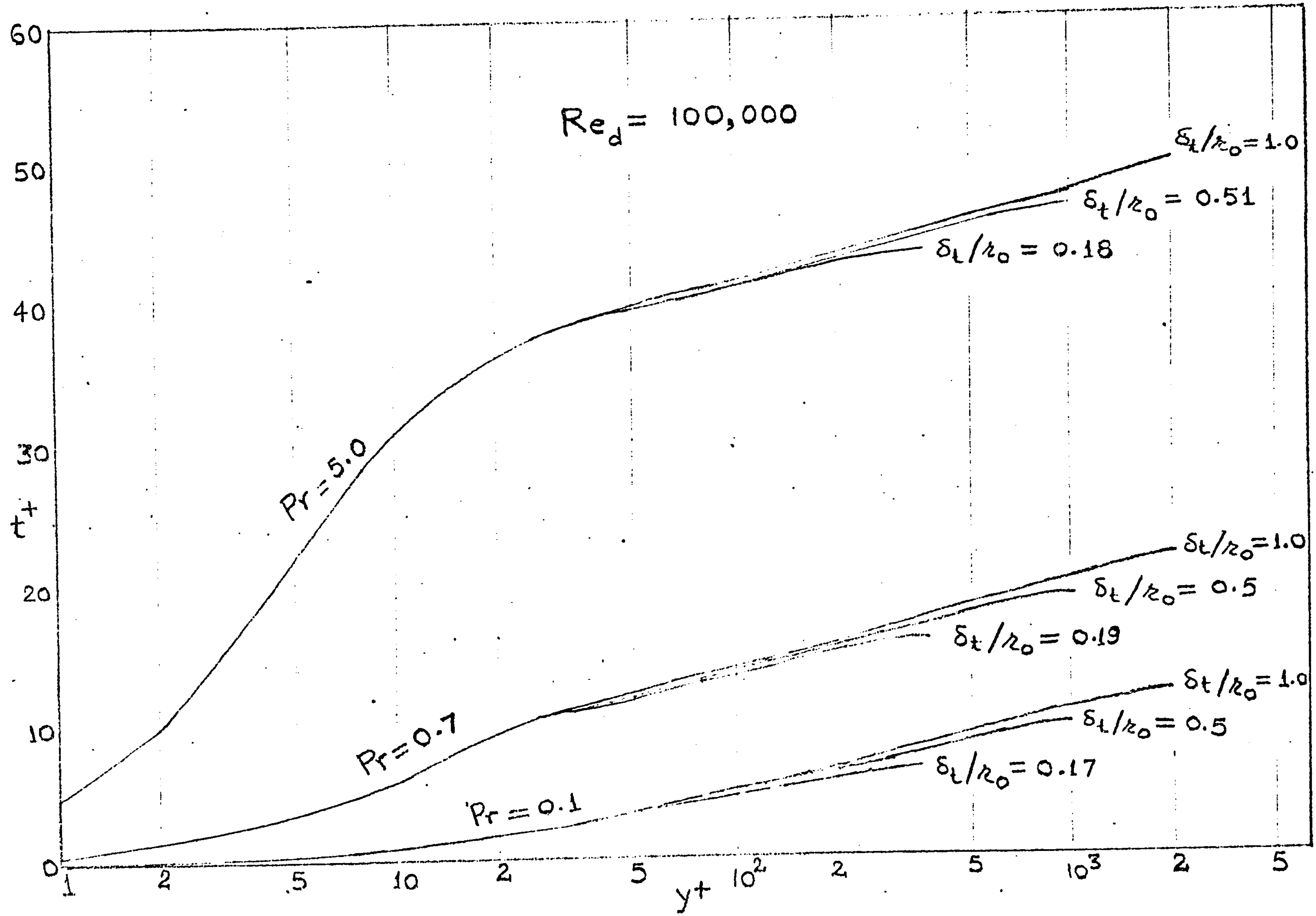

Fig. 3.11 Predicted Temperature Profiles in the Simultaneously Developing Region

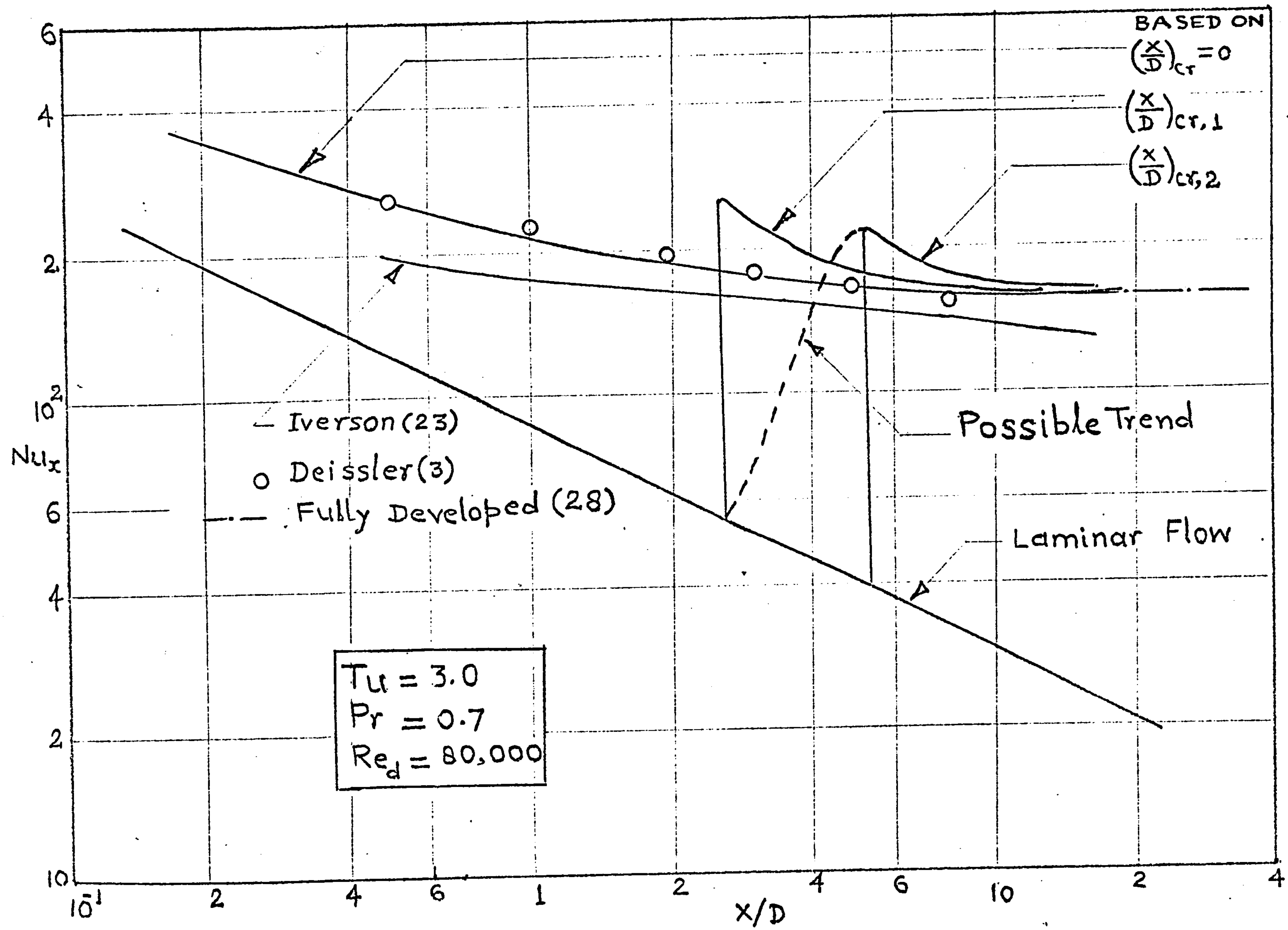

Fig. 3.12 Nusselt Number in the Entrance Region of a Duct

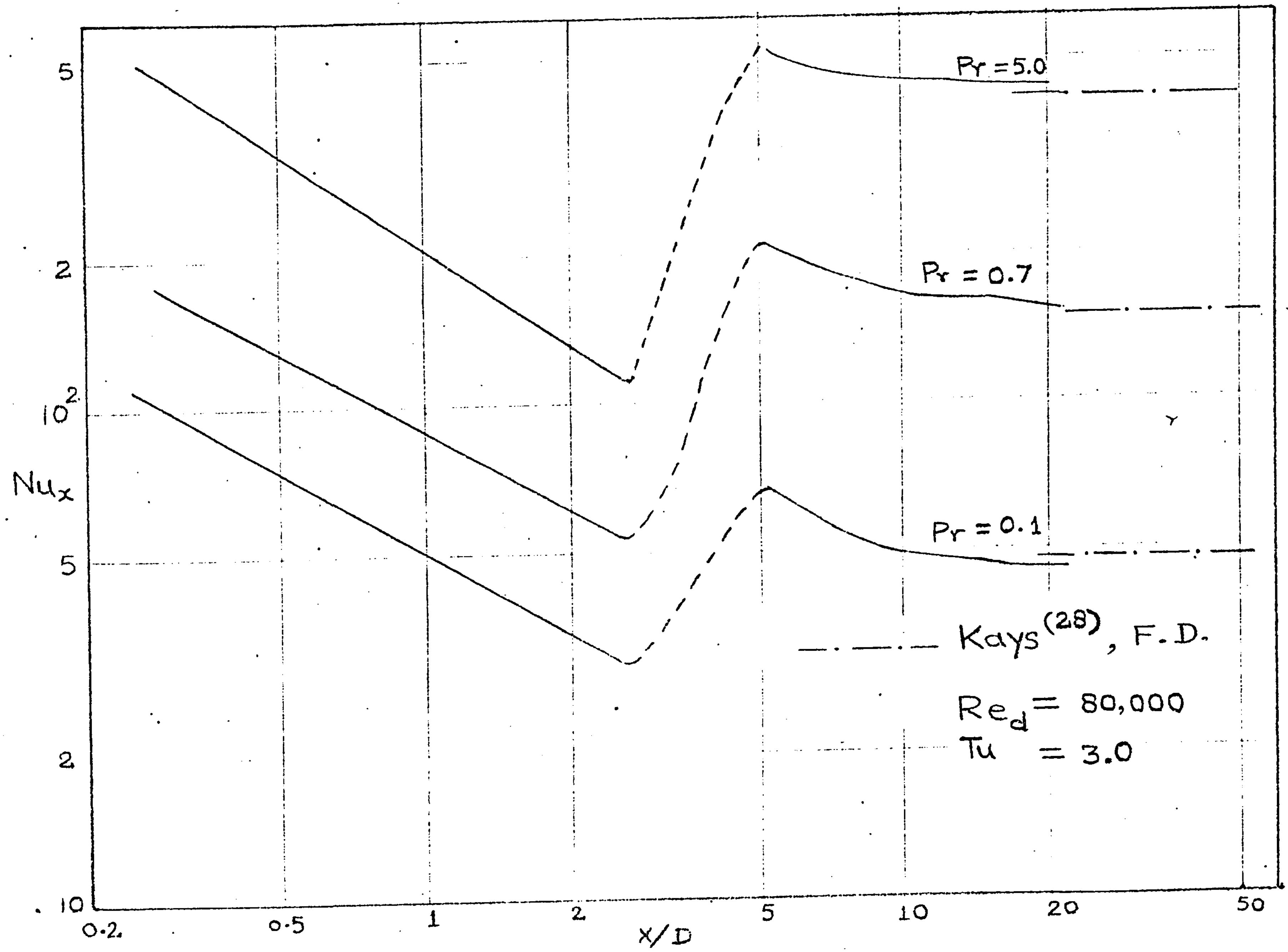

Fig. 3.13 Predicted Nusselt Number in the Simultaneously Developing Region (Effect of Pr)

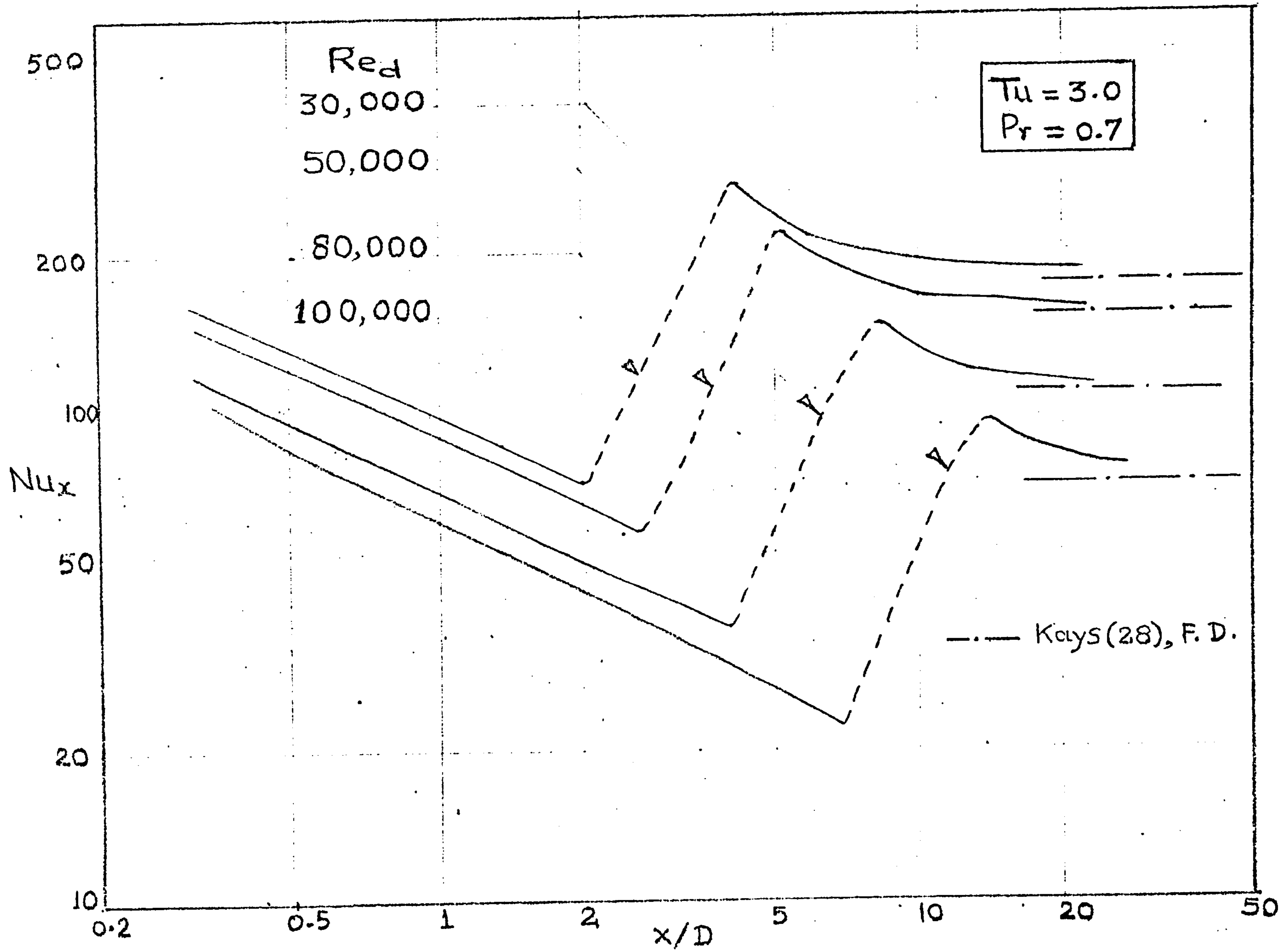

Fig. 3.14 Predicted Nusselt Number in the Simultaneously Developing Region
(Effect of Reynold's Number)

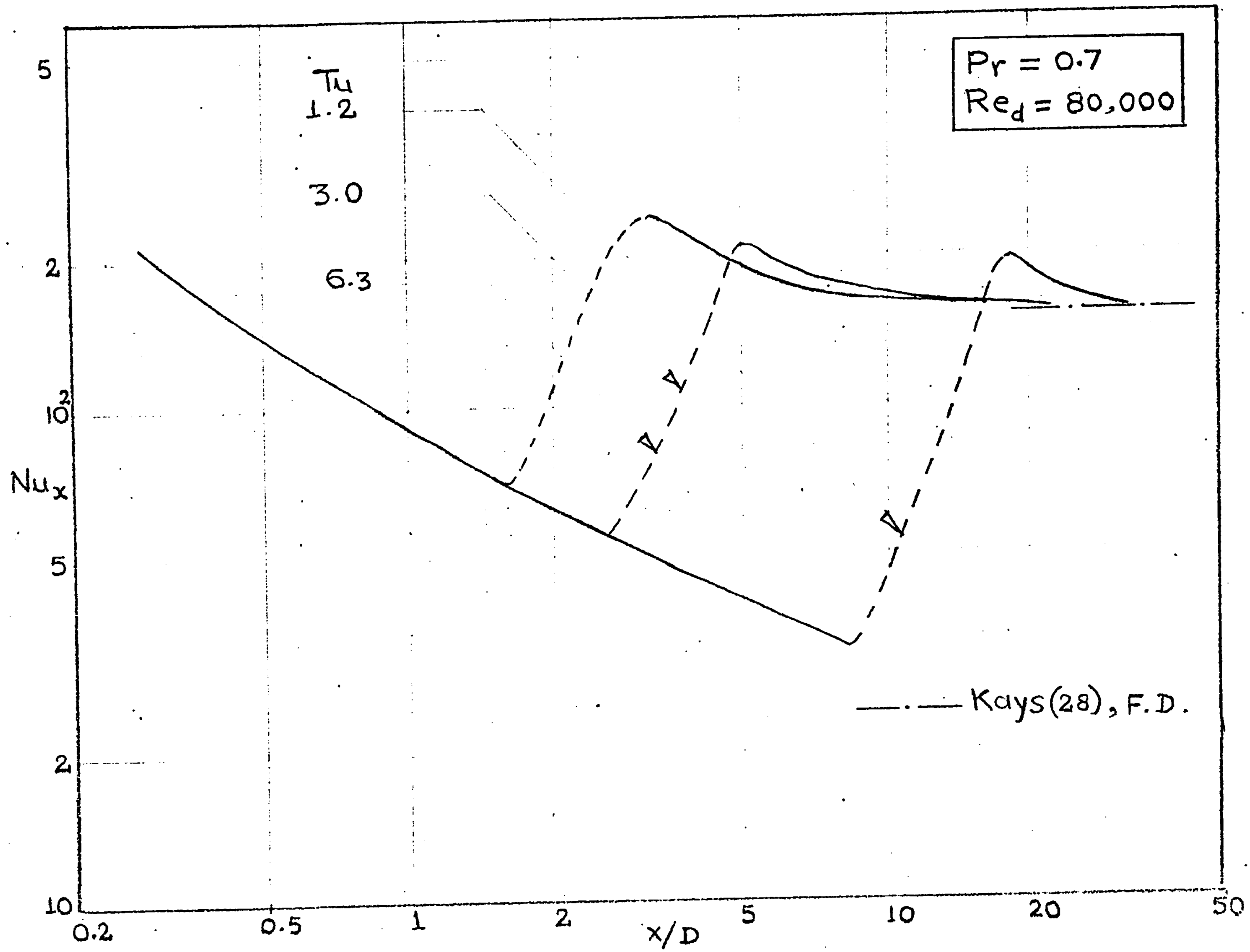

Fig. 3.15 Predicted Nusselt Number in the Simultaneously Developing Region
(Effect of Turbulence Intensity)

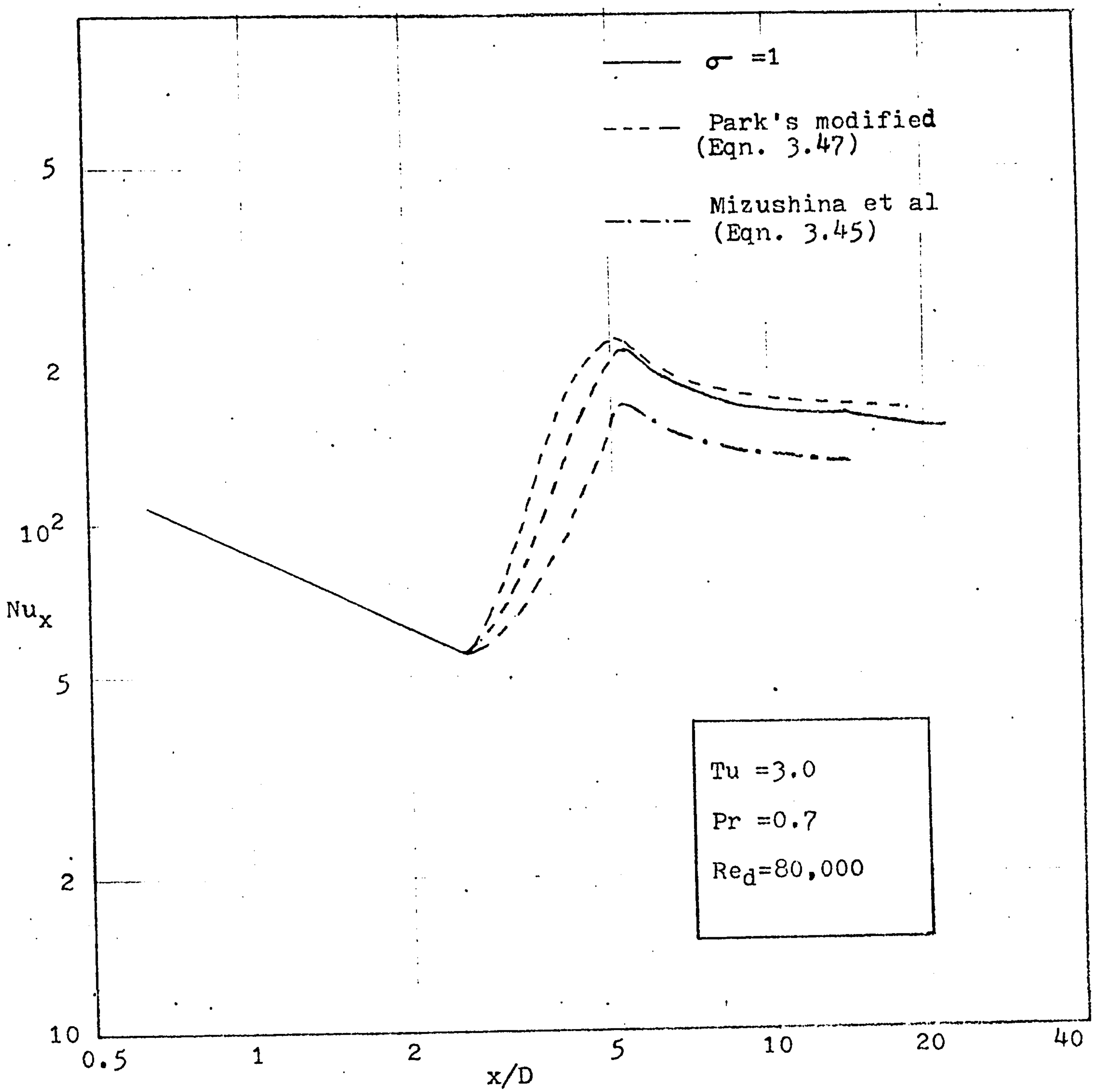

Fig. 3.16 Nusselt Number in the Entrance Region of a Duct
(Effect of Ratio of Eddy Diffusivities)

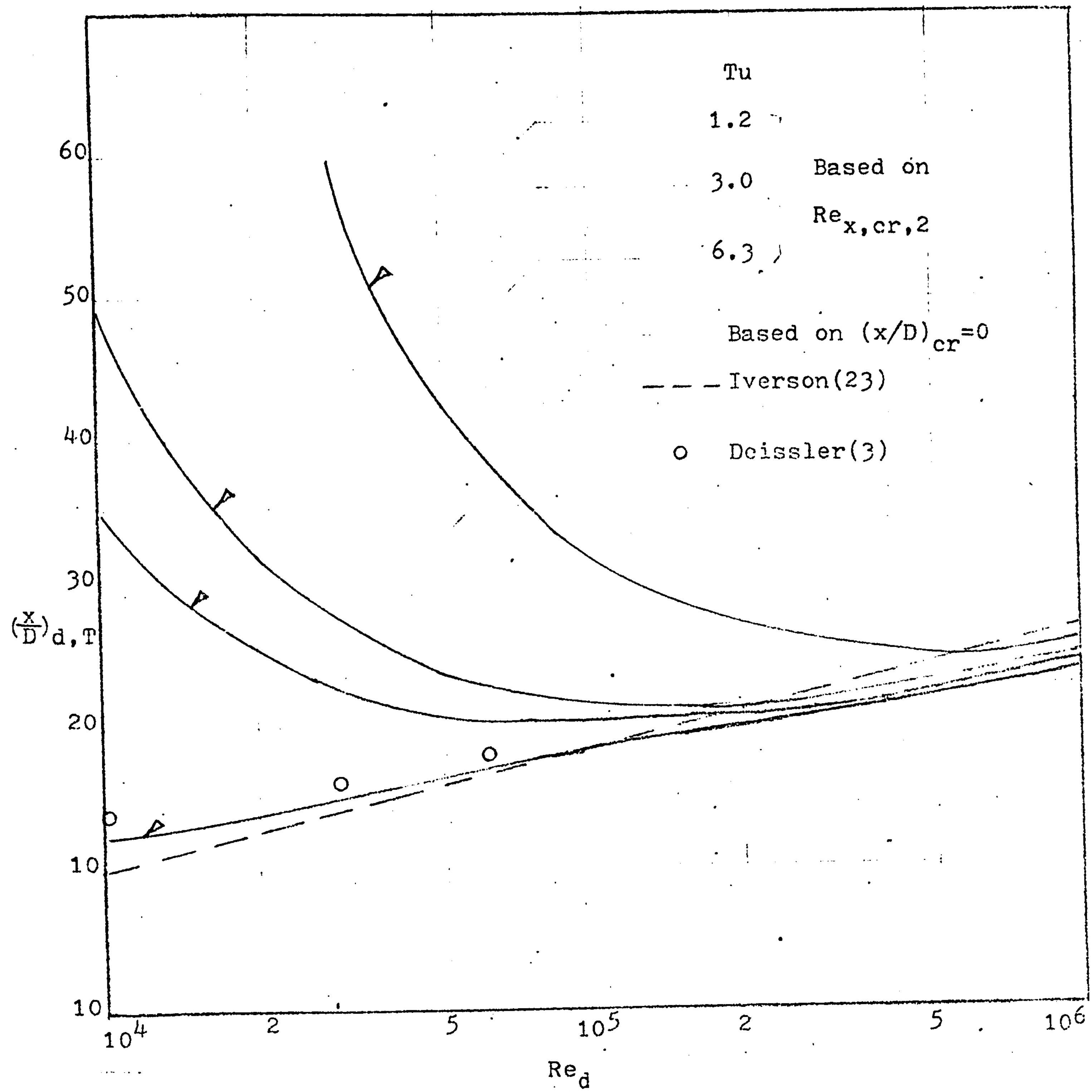

Fig. 3.17 Entrance Lengths Under Simultaneous Developement (Effect of Tu)

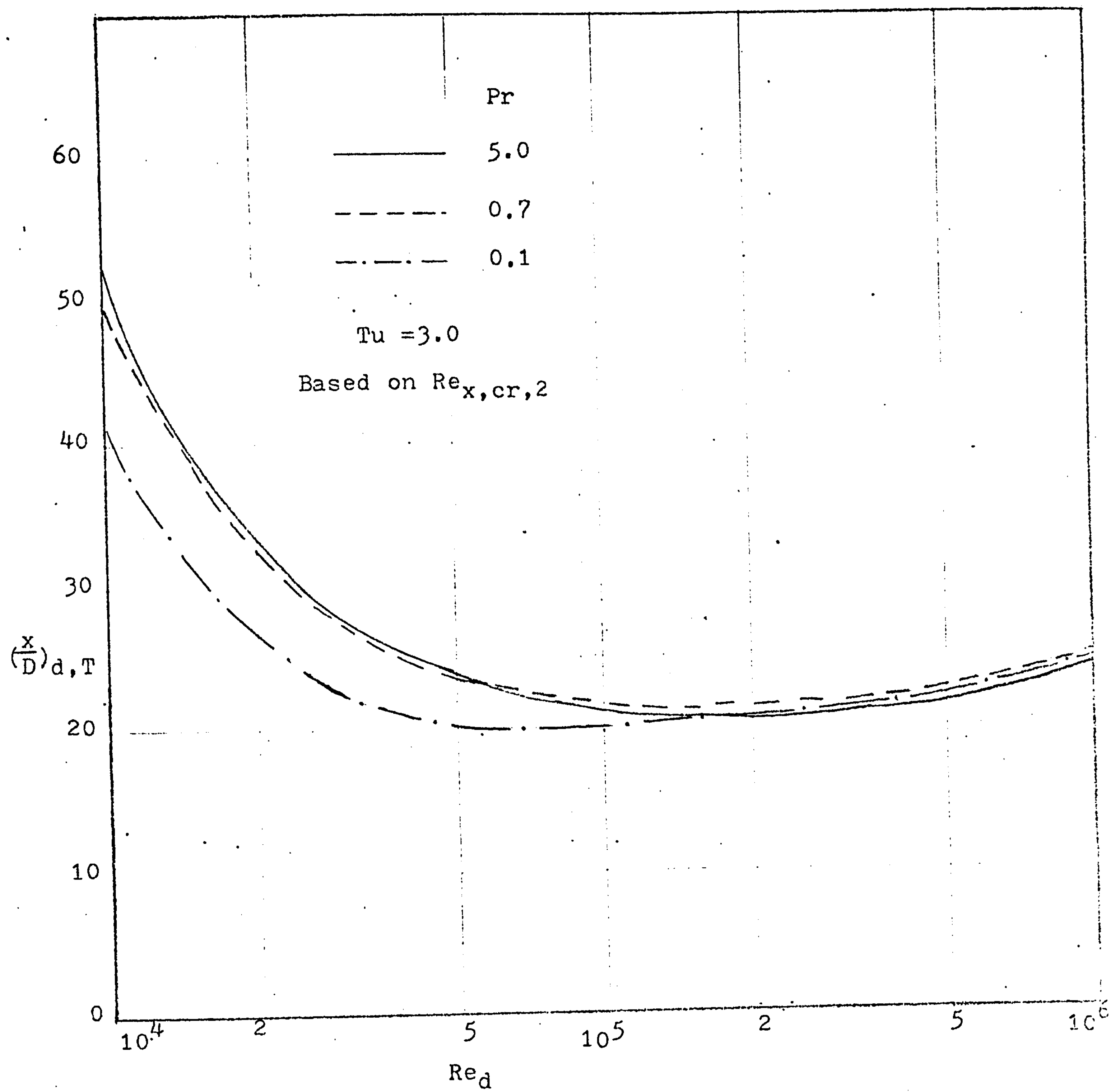

Fig. 3.18 Entrance Lengths Under Simultaneous Developement
(Effect of Pr)

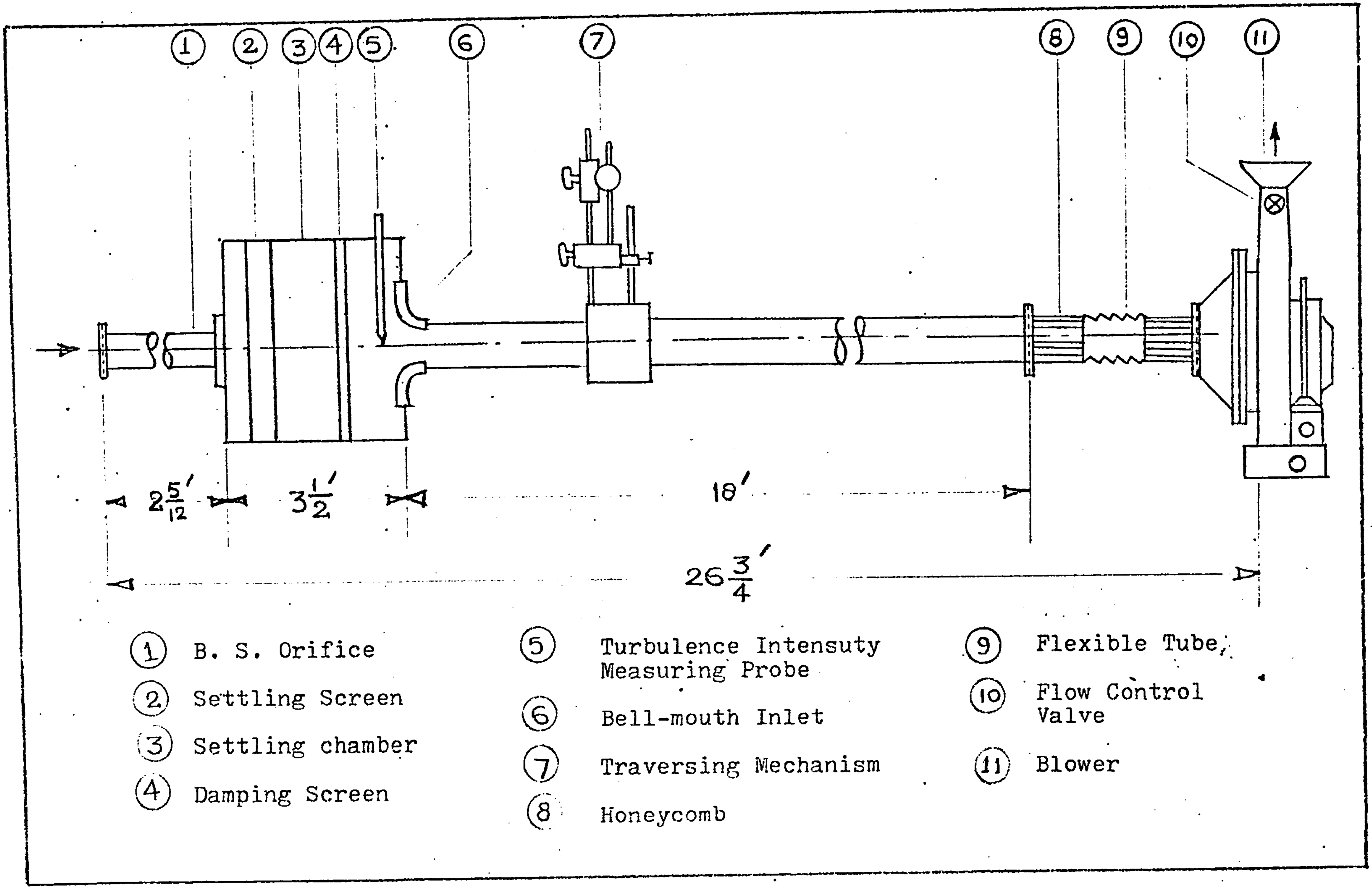

Fig. 4.1 Schematic Diagram of Experimental Apparatus

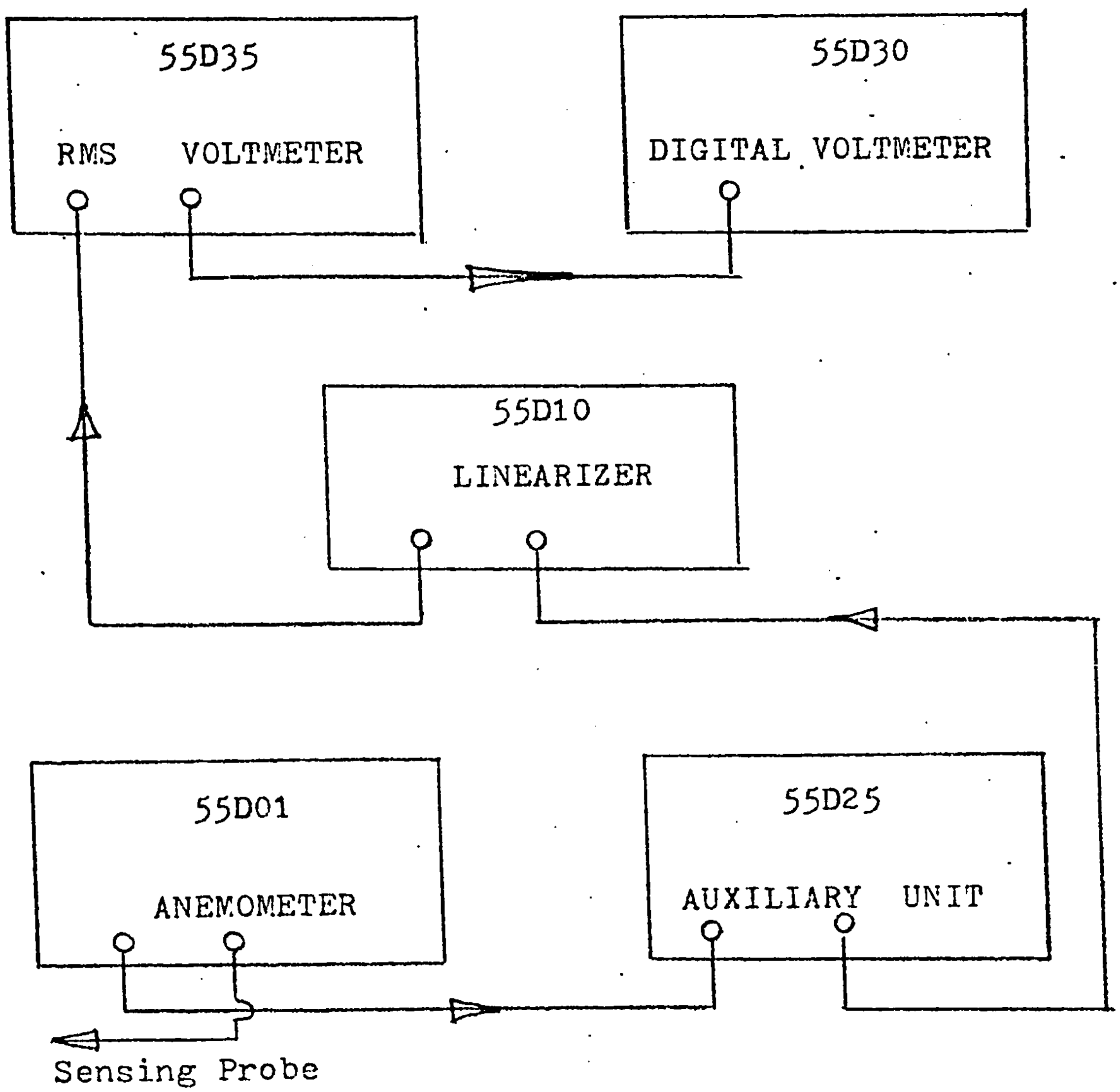

Fig. 4.2 Hot-wire Anemometry System

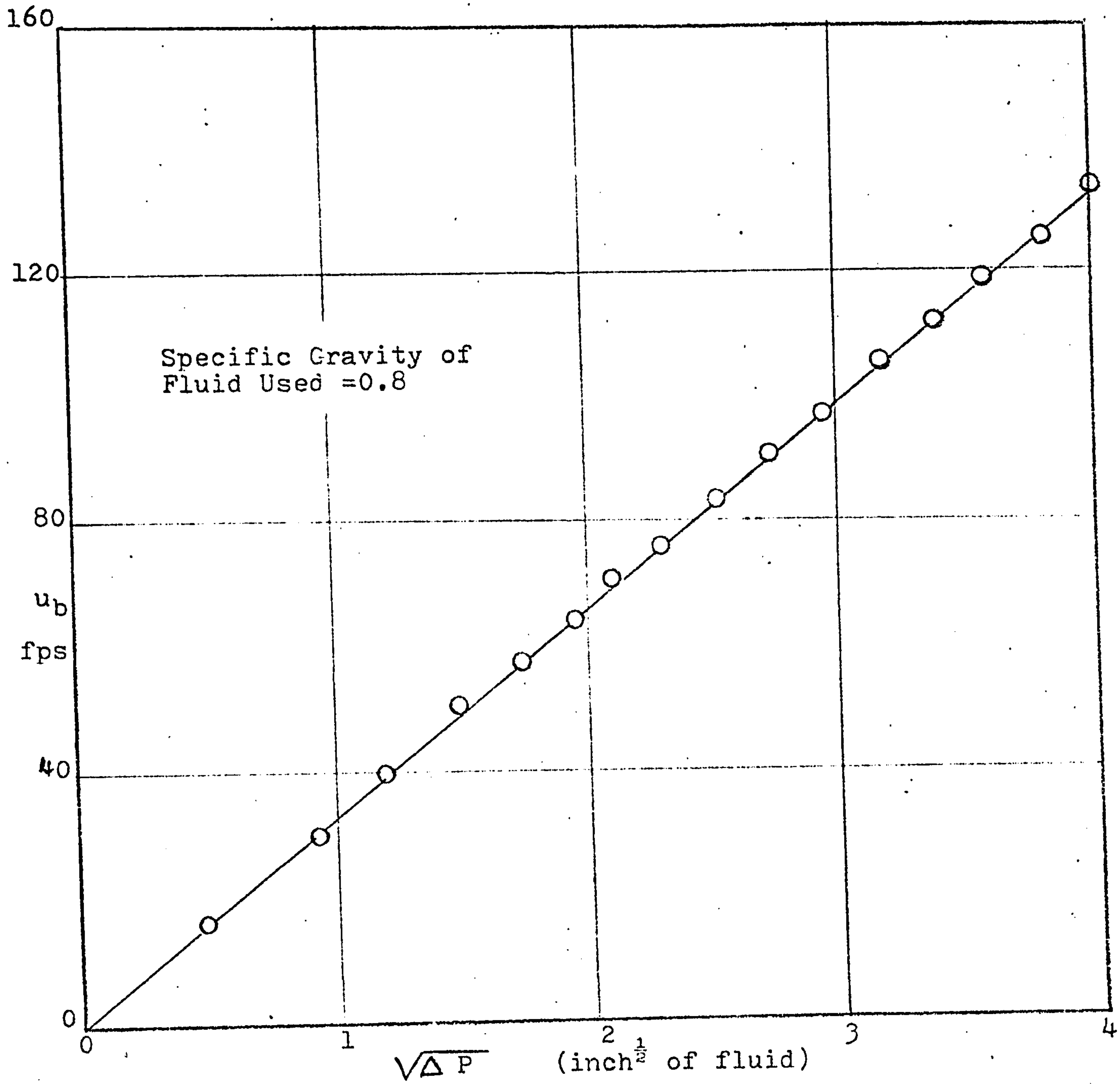

Fig. 4.3 Calibration Curve for Orifice.

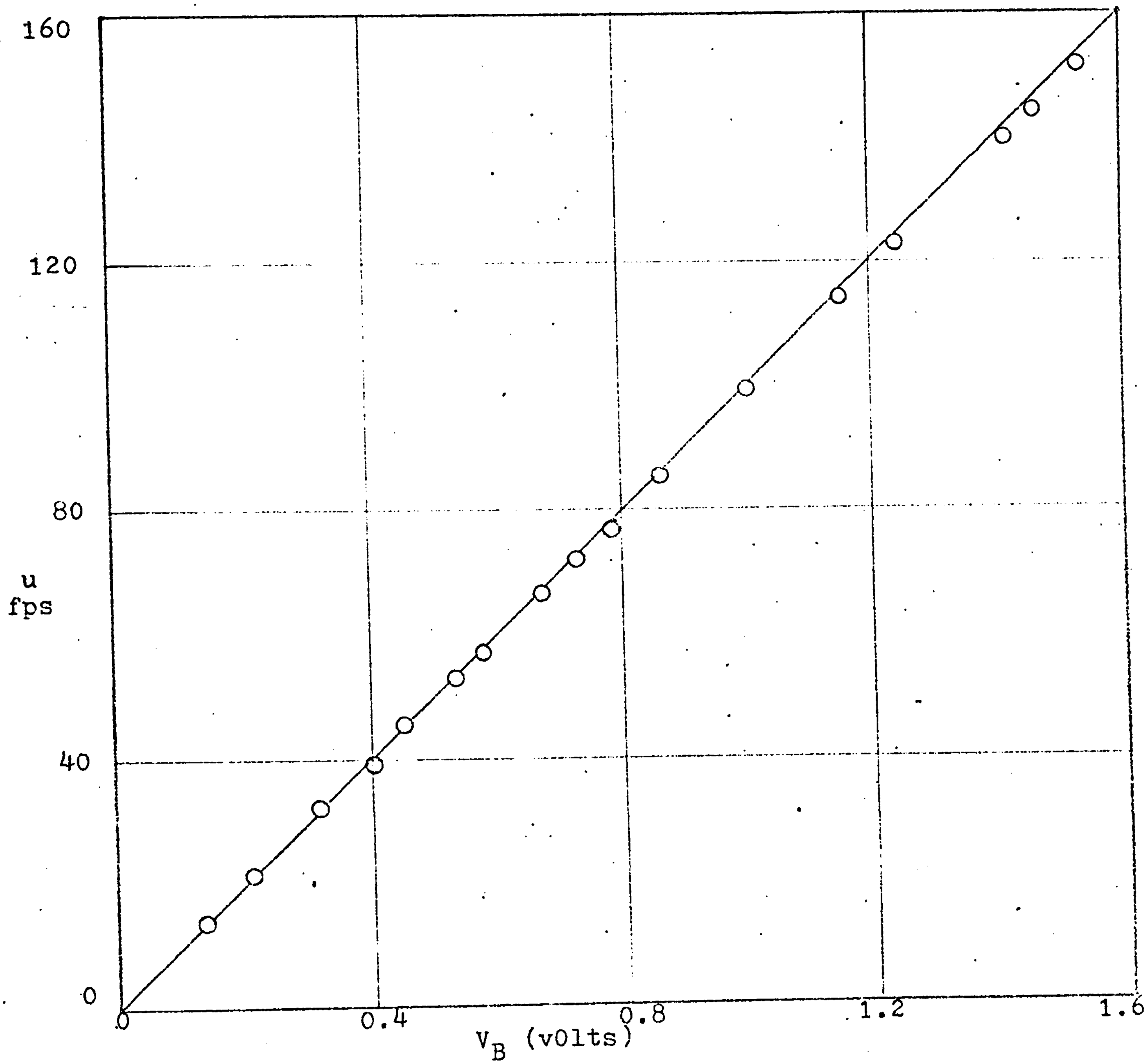

Fig. 4.4 Linearised Calibration Curve of a Hot-wire Probe

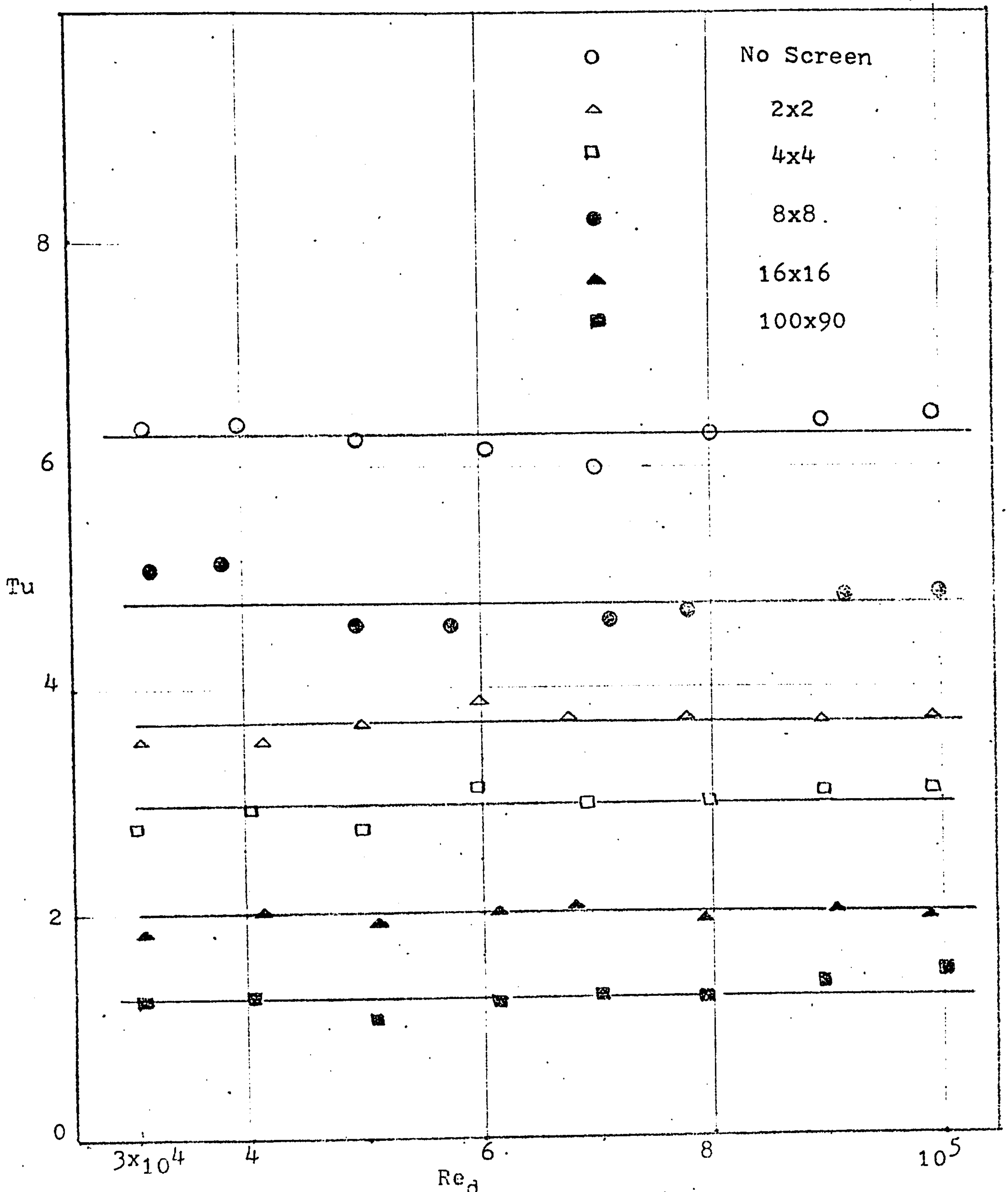

Fig.4. 5 Effect of Reynold's number on Turbulence Intensity at the Bell-mouth Entrance (x=-6")

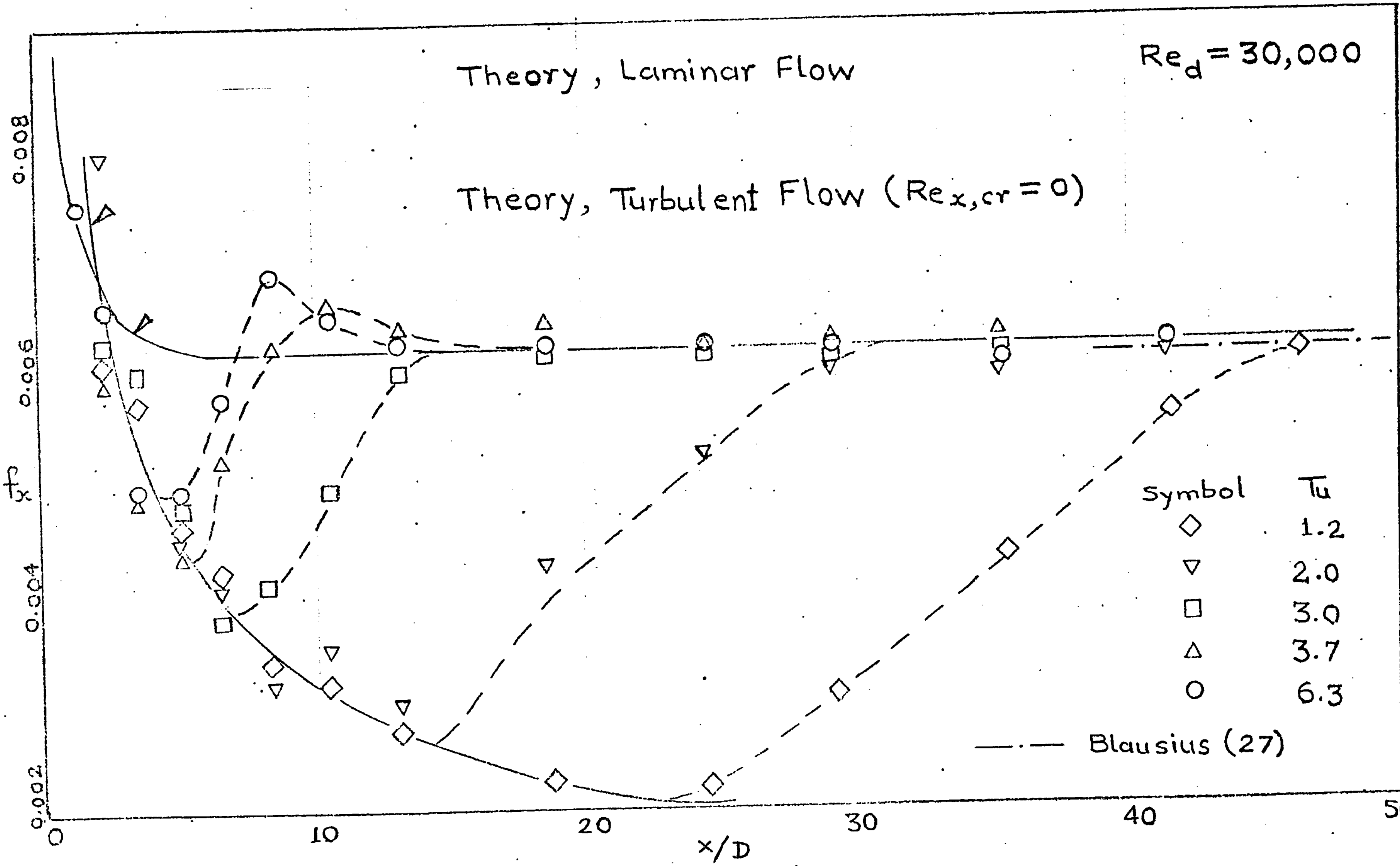

Fig. 4.6 Effect of Free Stream Turbulence on Friction Factor in the Entrance Region (Re_d 30,000)

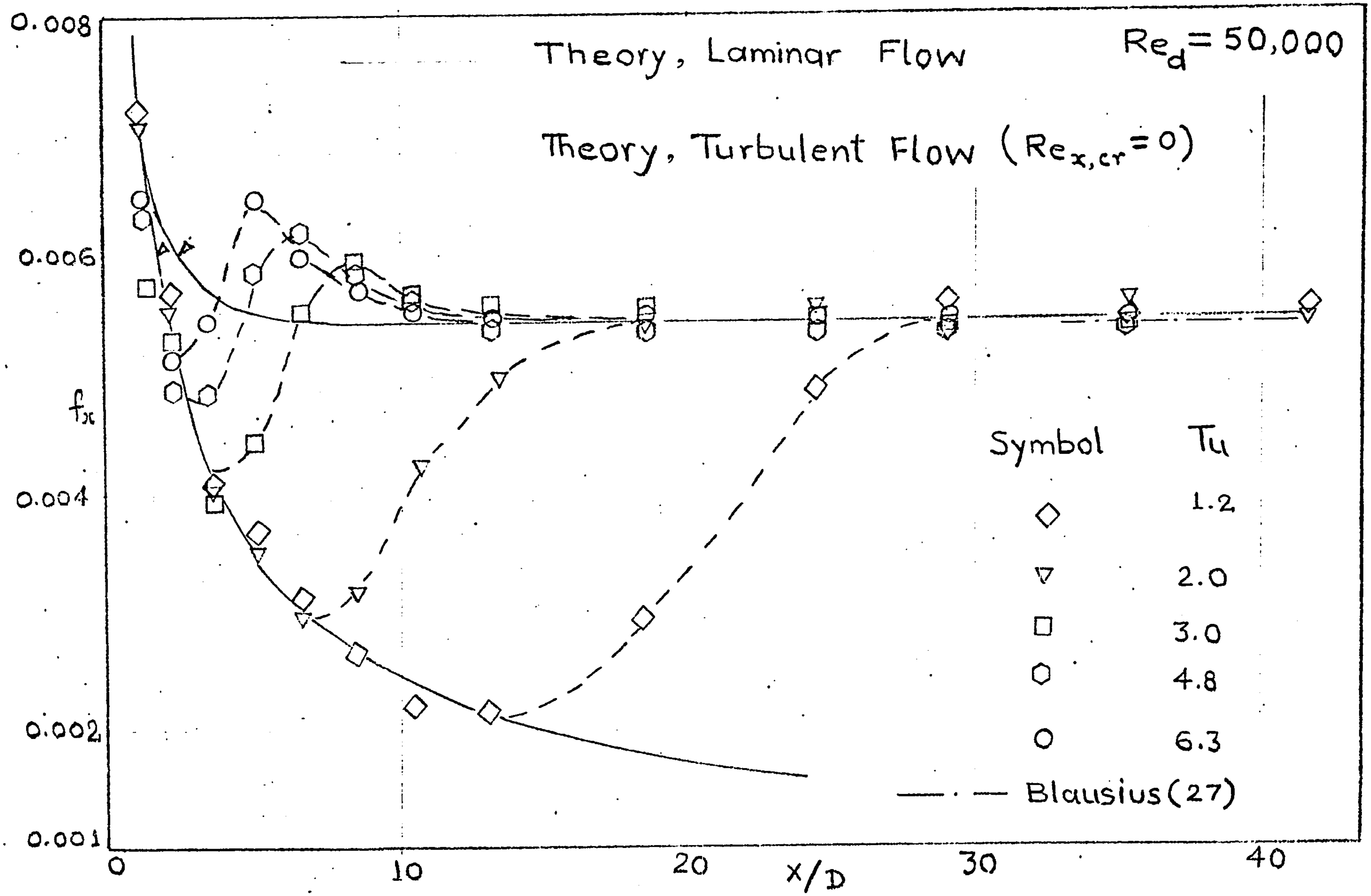

Fig. 4.7 Effect of Free Stream Turbulence on Friction Factor in the Entrance Region (Re_d 50,000)

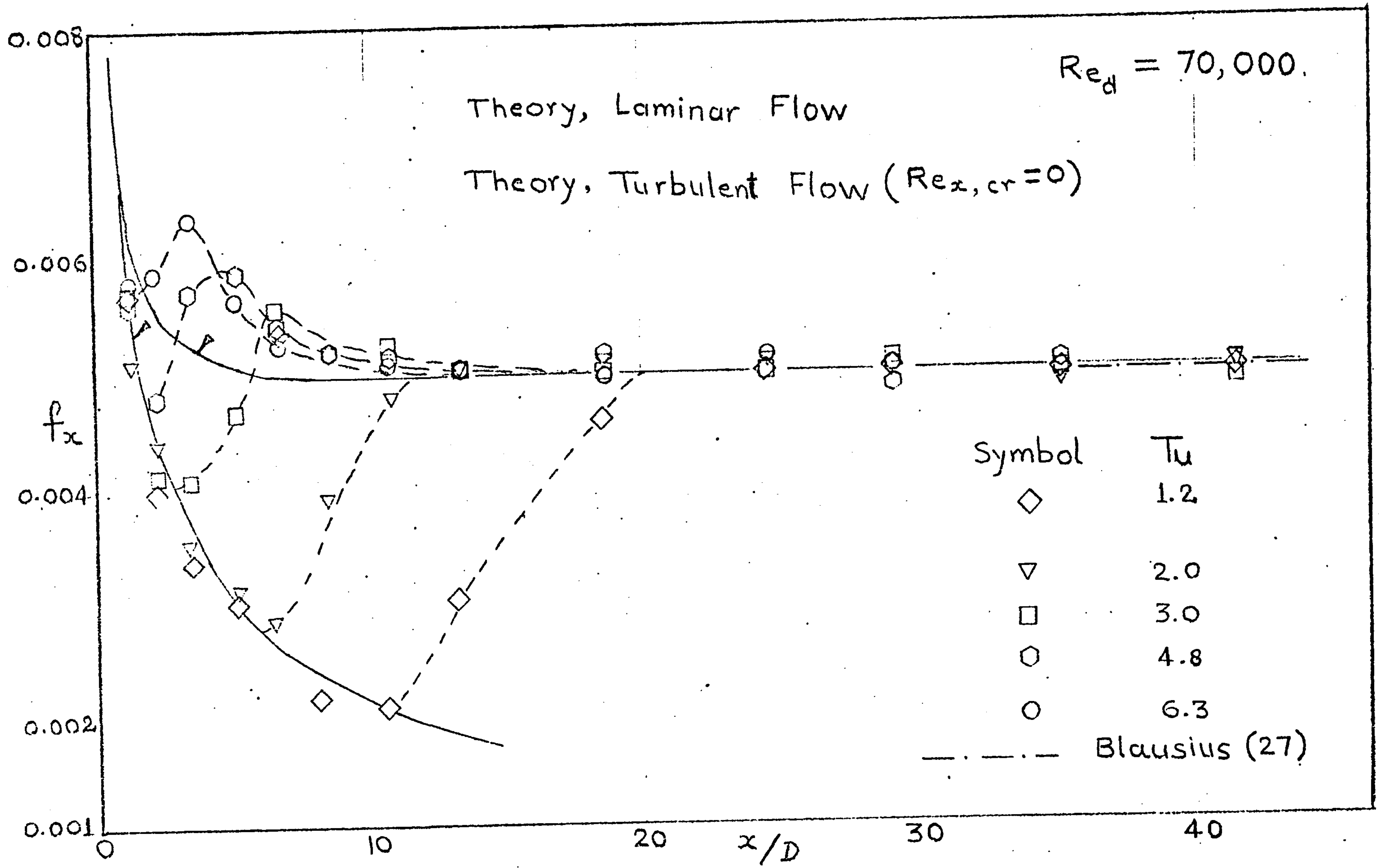

Fig. 4.8 Effect of Free Stream Turbulence on Friction Factor in the Entrance Region (Re_d 70.000)

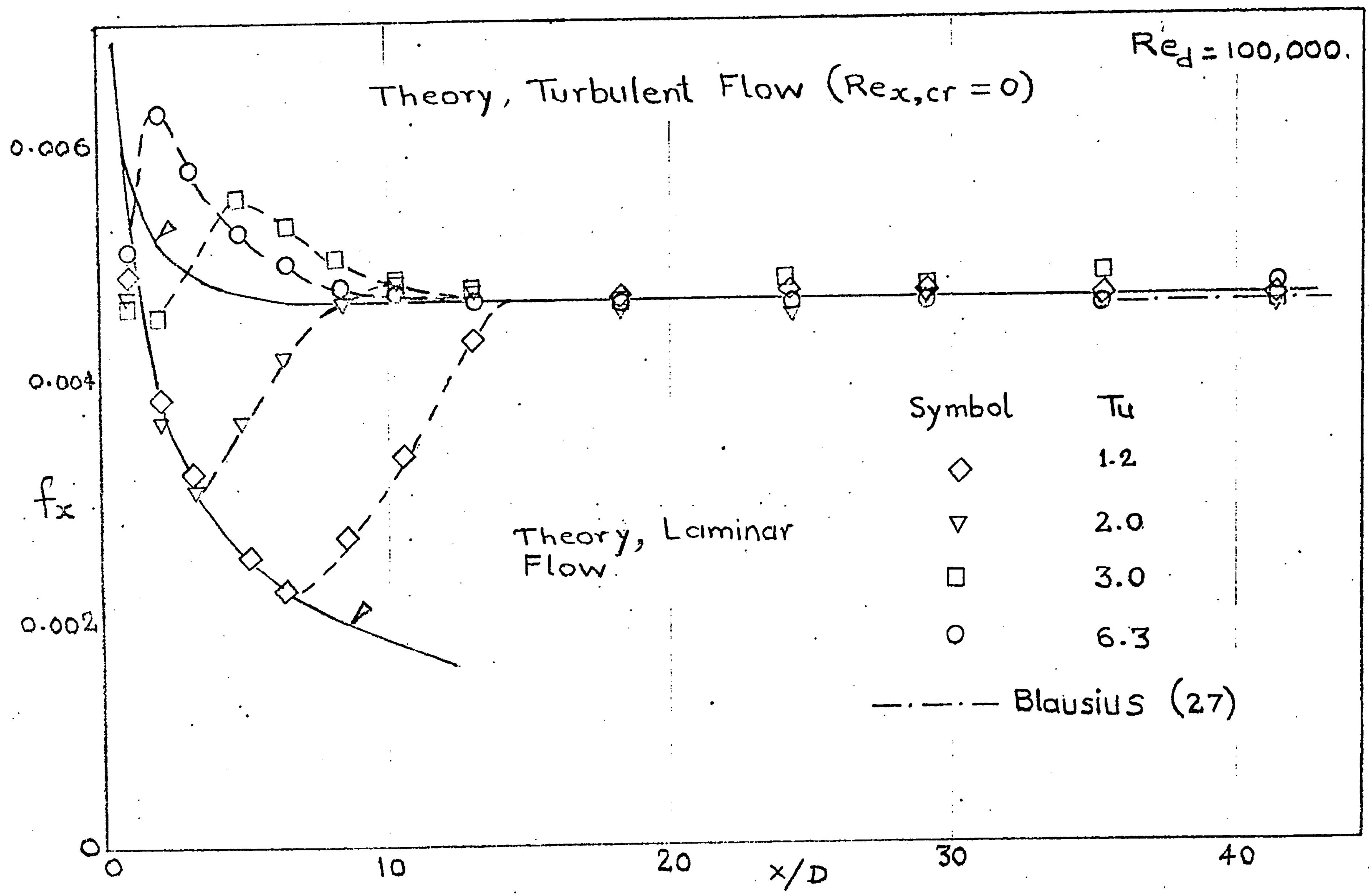

Fig. 4.9 Effect of Free Stream Turbulence on Friction Factor in the Entrance Region ($Re_d \simeq 100,000$)

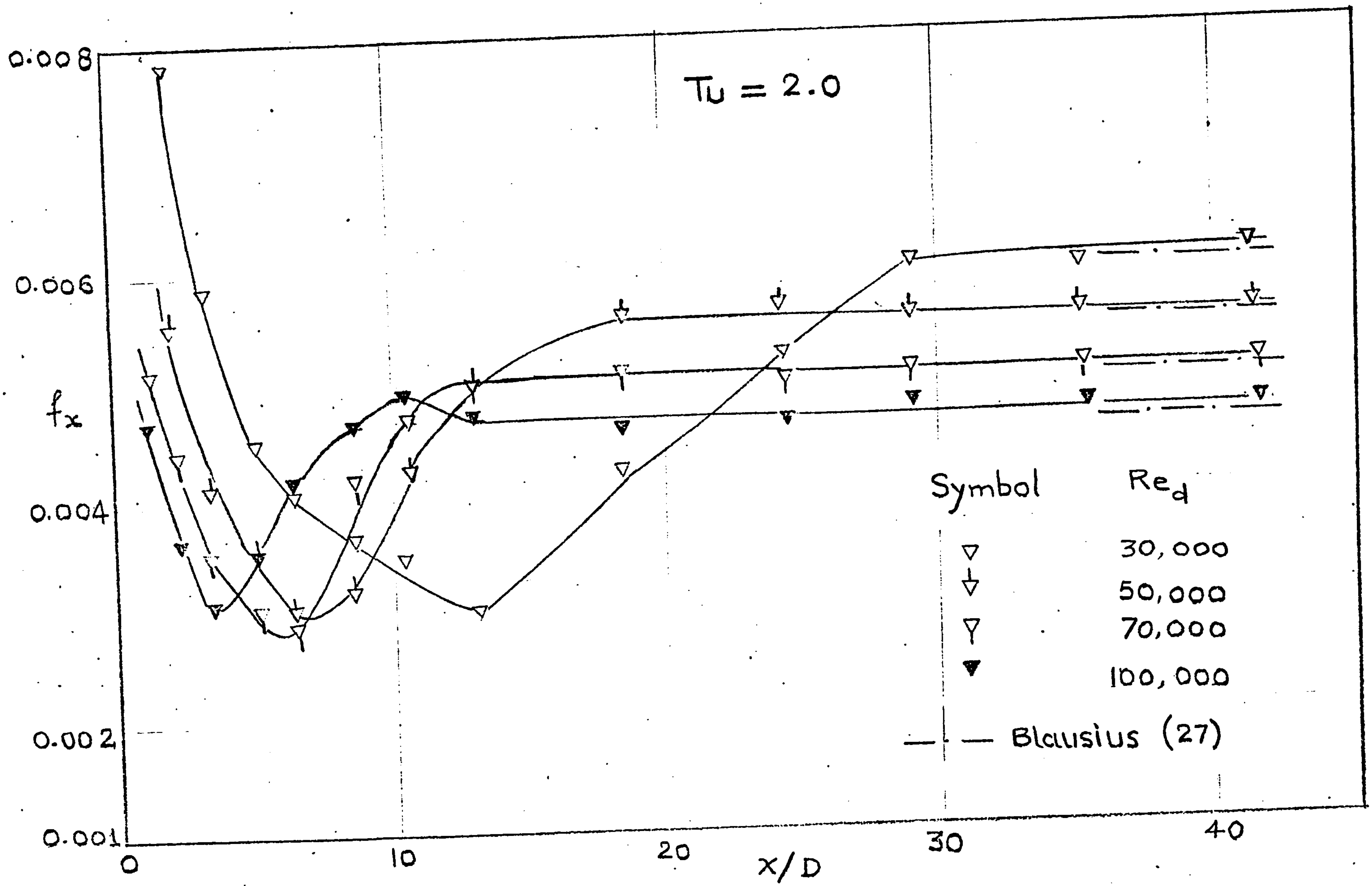

Fig. 4.10 Effect of Reynold's number on Friction Factor in the Entrance Region with Laminar Entry (Tu =2.0)

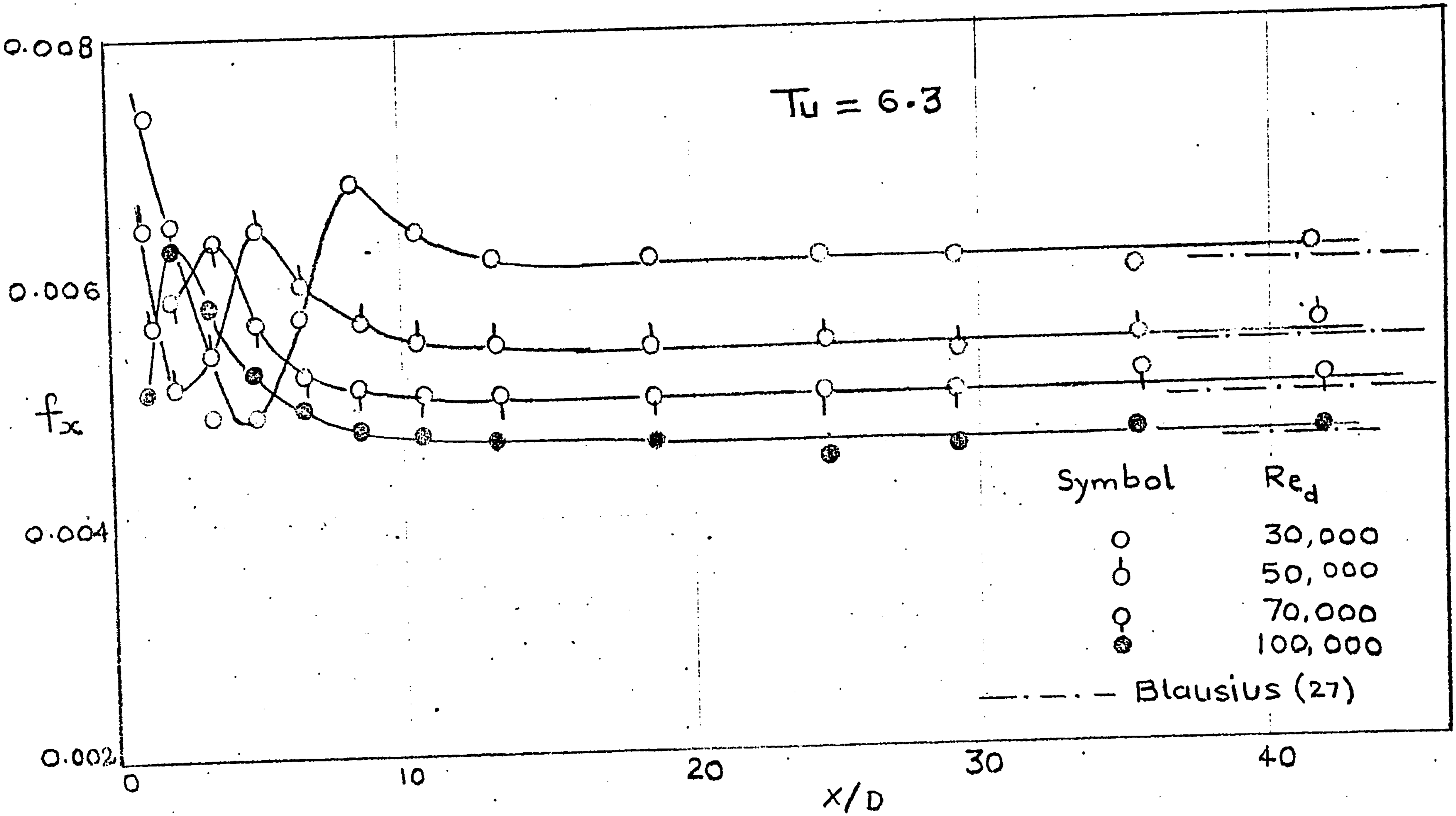

Fig. 4.11 Effect of Reynold's number on Friction Factor in the Entrance Region with Laminar Entry (Tu =6.3)

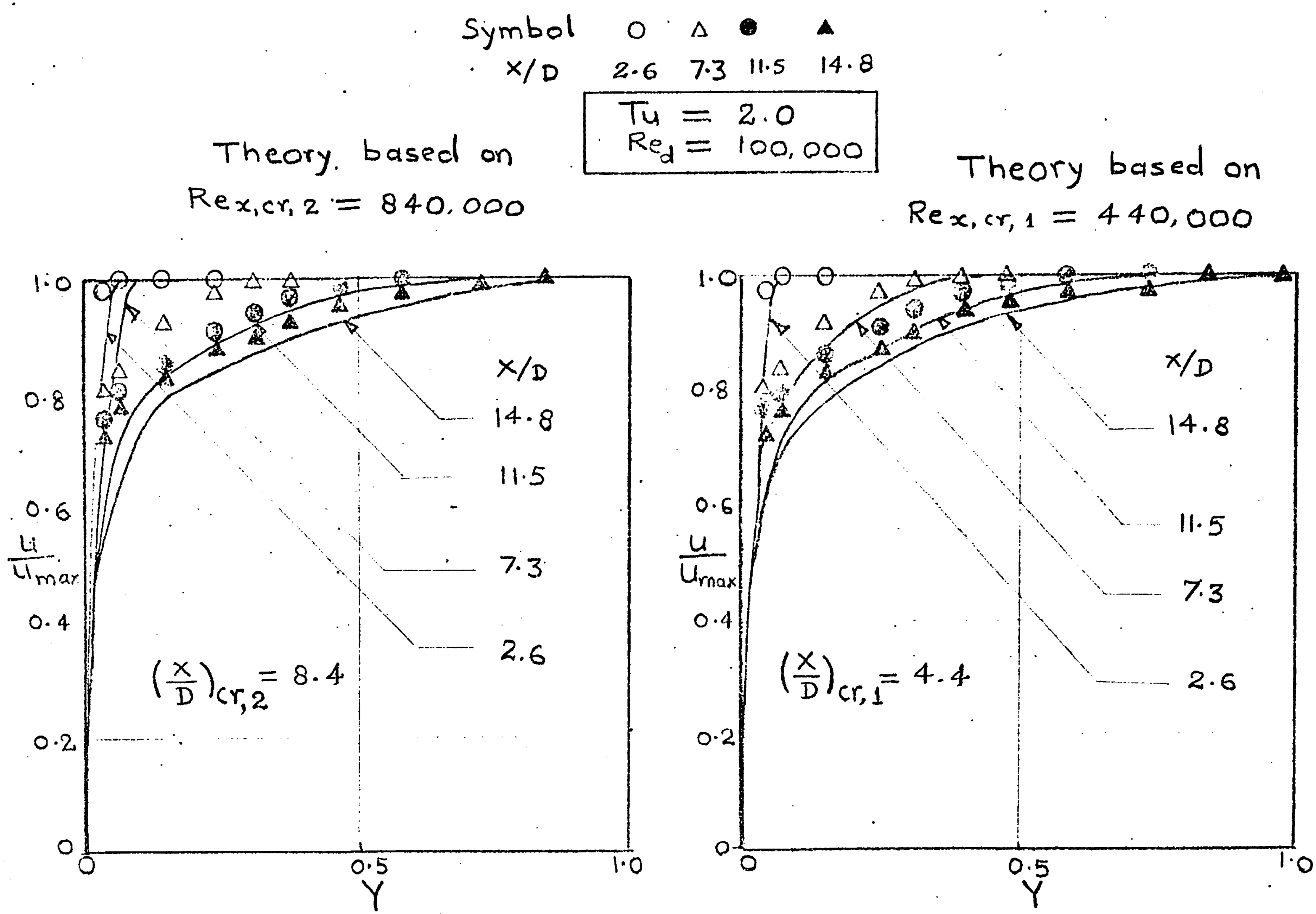

Fig. 4.12 Comparison of Experimental and Predicted Velocity Profiles in the Entrance Region

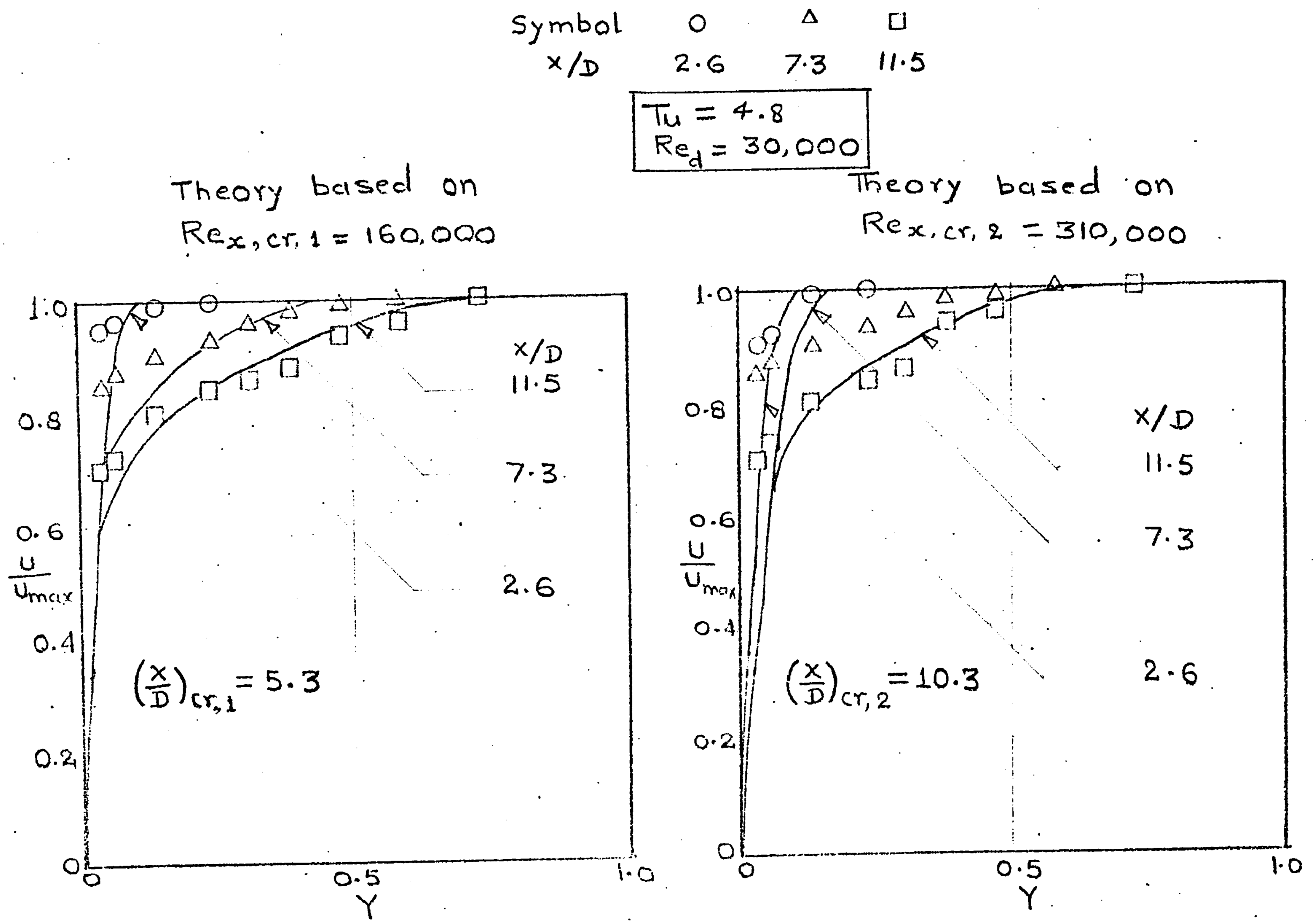

Fig. 4.13 Comparison of Experimental and Predicted Velocity Profiles in the Entrance Region

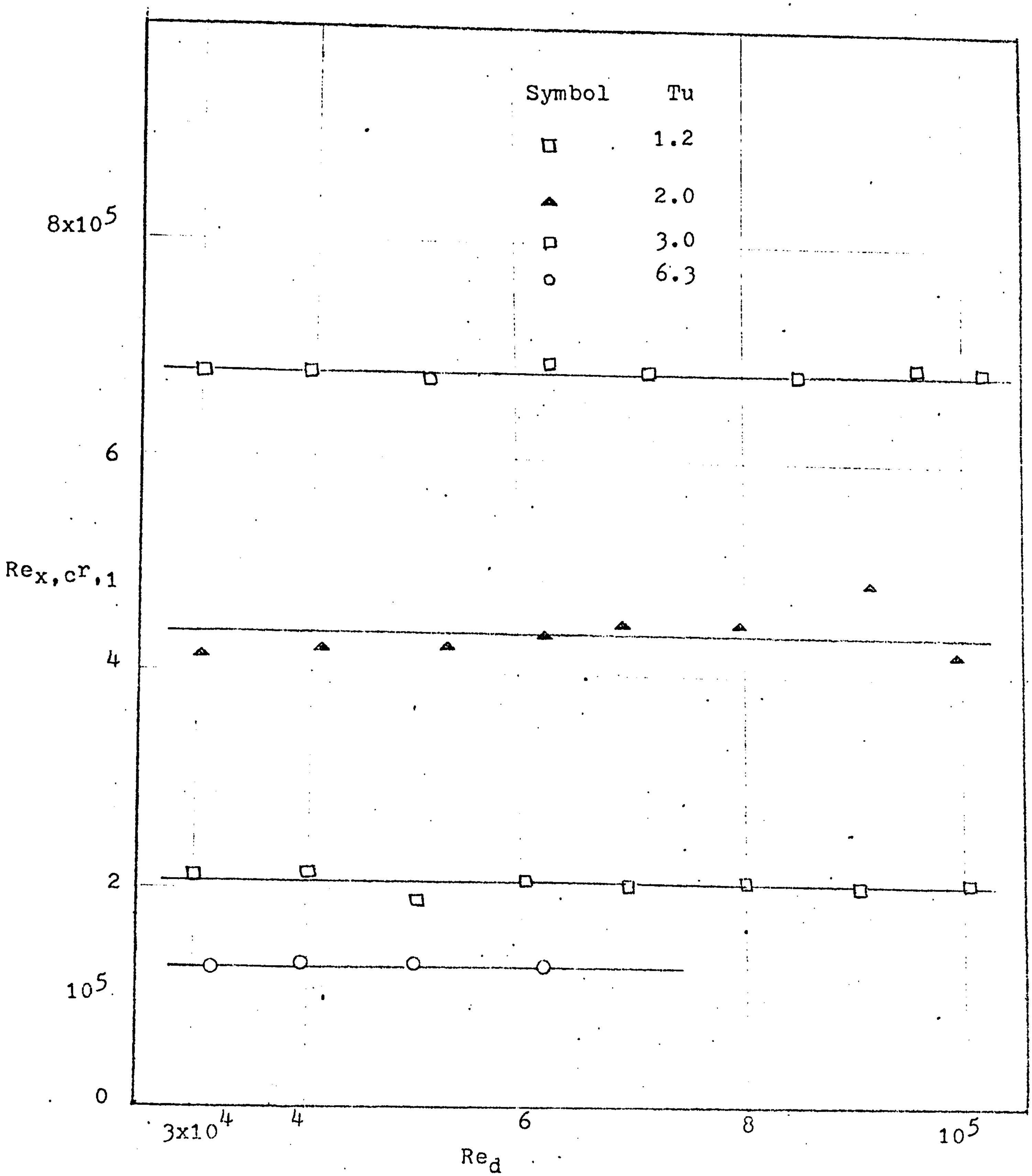

Fig. 4.14(a) Effect of Reynold's number on Transition Reynold's number ($Re_{x,cr,1}$)

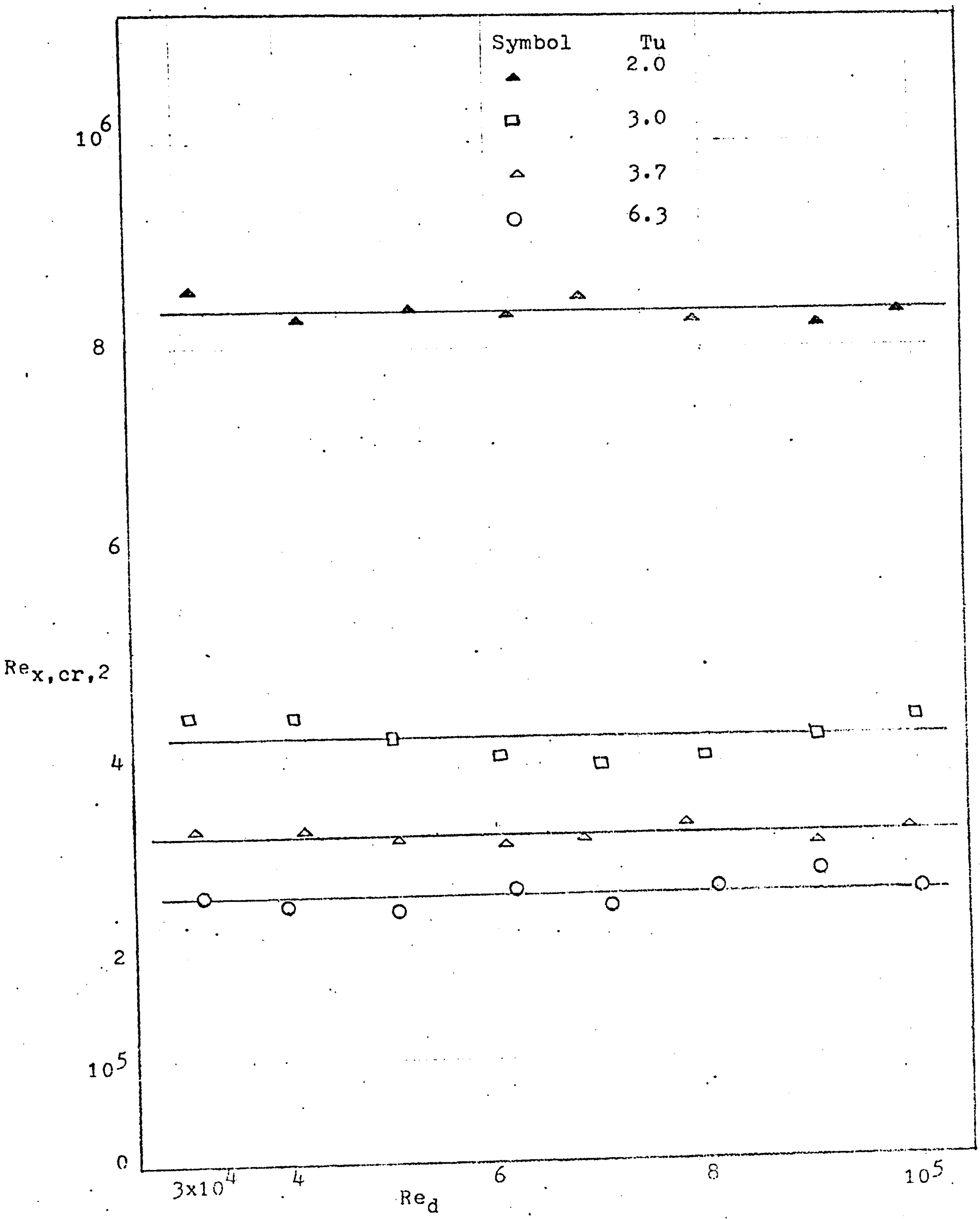

Fig. 4.14(b) Effect of Reynold's number on Transition Reynold's number ($Re_{x,cr,2}$)

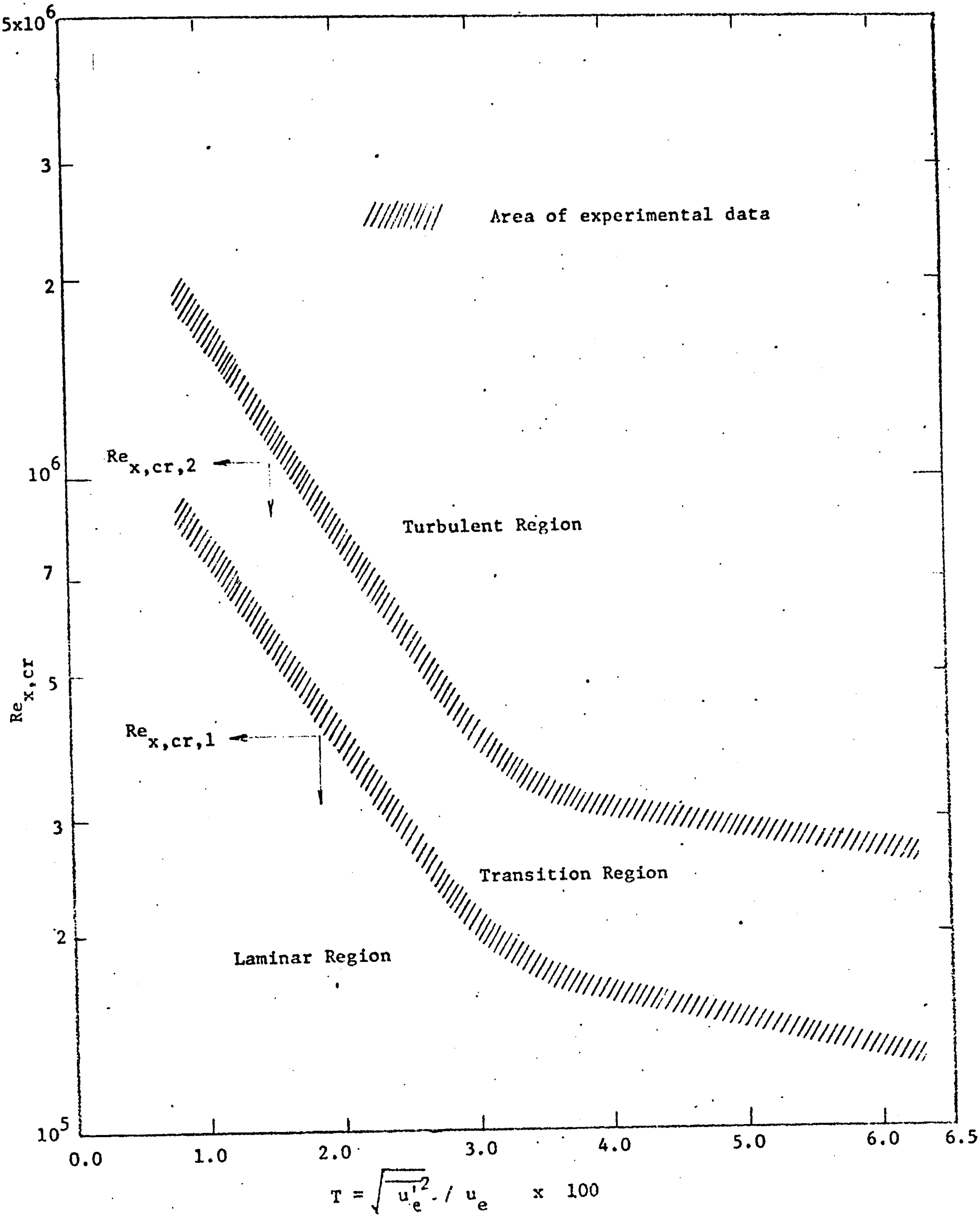

Fig. 4.15 Effect of Free-Stream Turbulence on the Transition Reynolds Number, A Circular Straigth Duct.

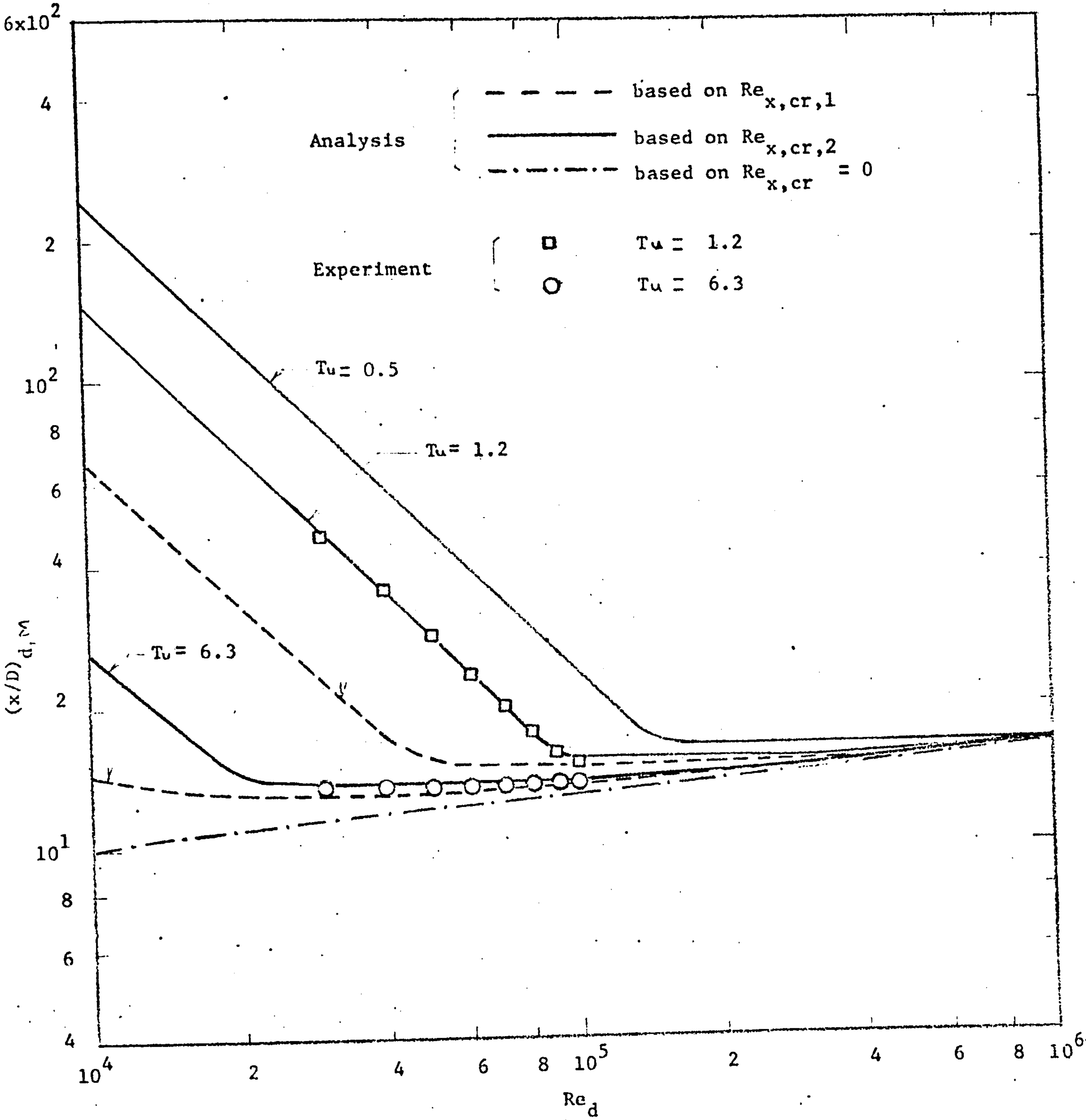

Fig. 4.16a Effect of Free-Stream Turbulence on the Entry Length, A Circular Straight Duct.

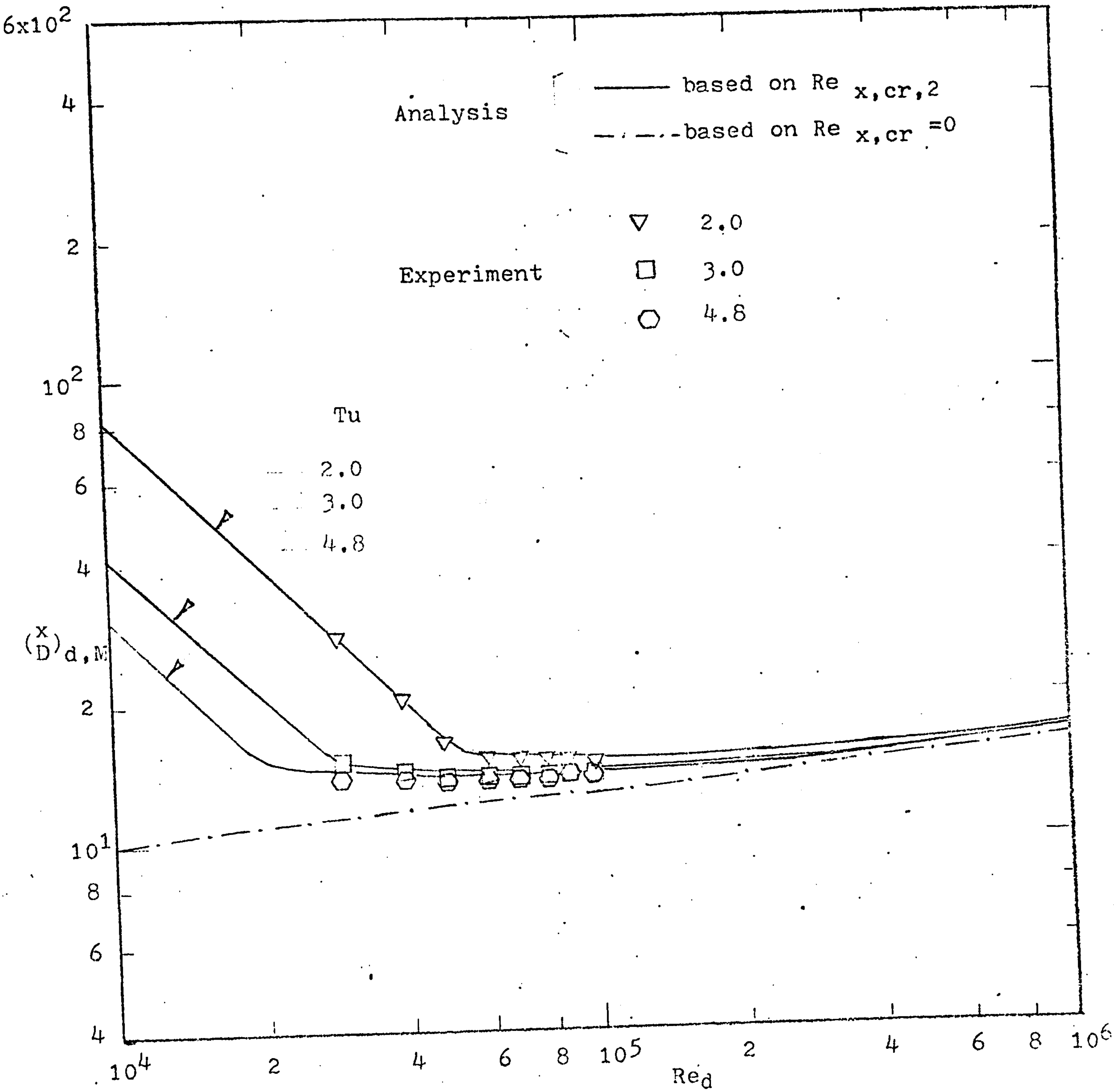

Fig. 4.16 b Effect of Free-Stream Turbulence on the Entry Length, A Circular Straight Duct.

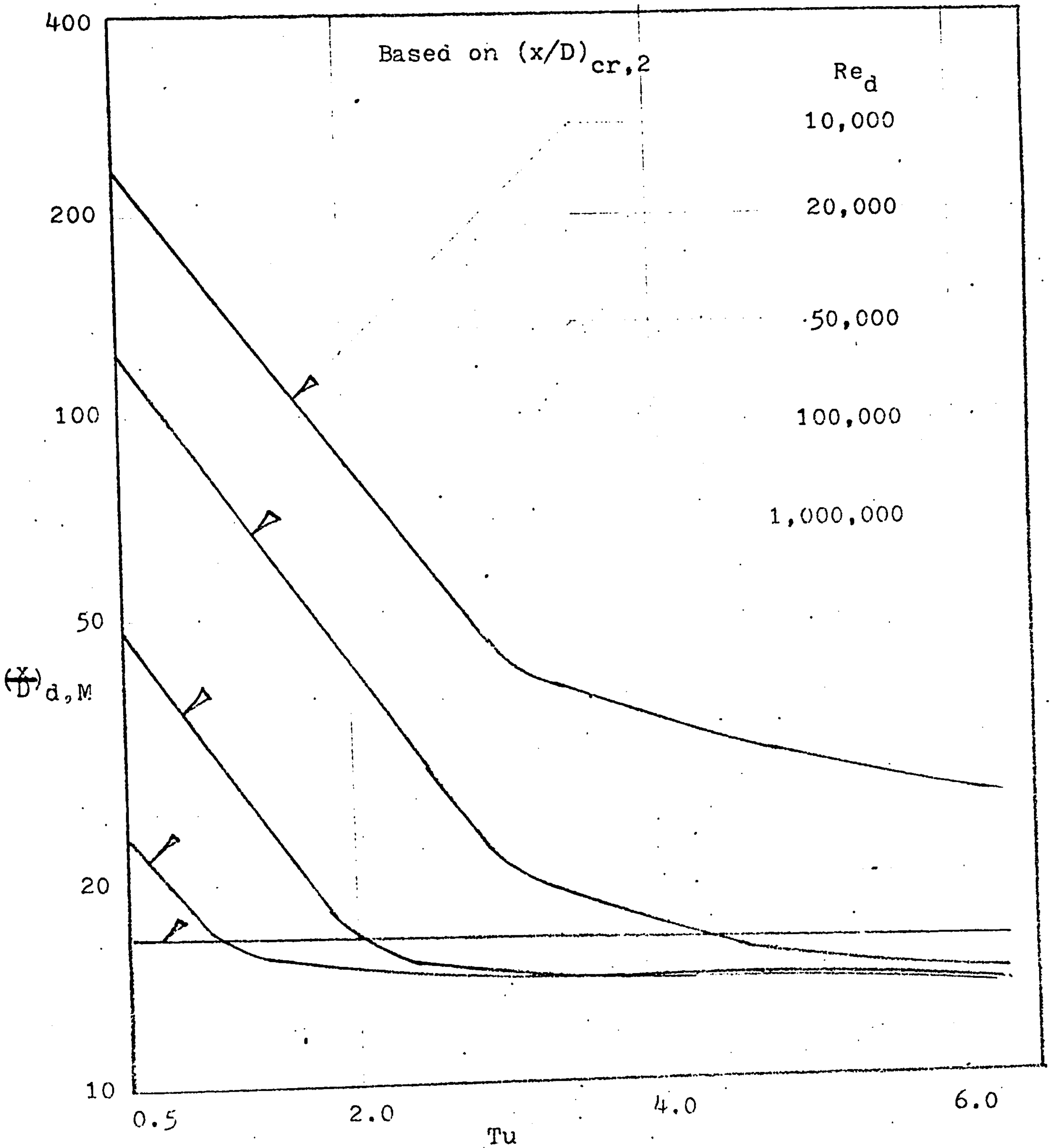

Fig. 4.17 Effect of Turbulence Intensity on Hydrodynamic Entrance Length

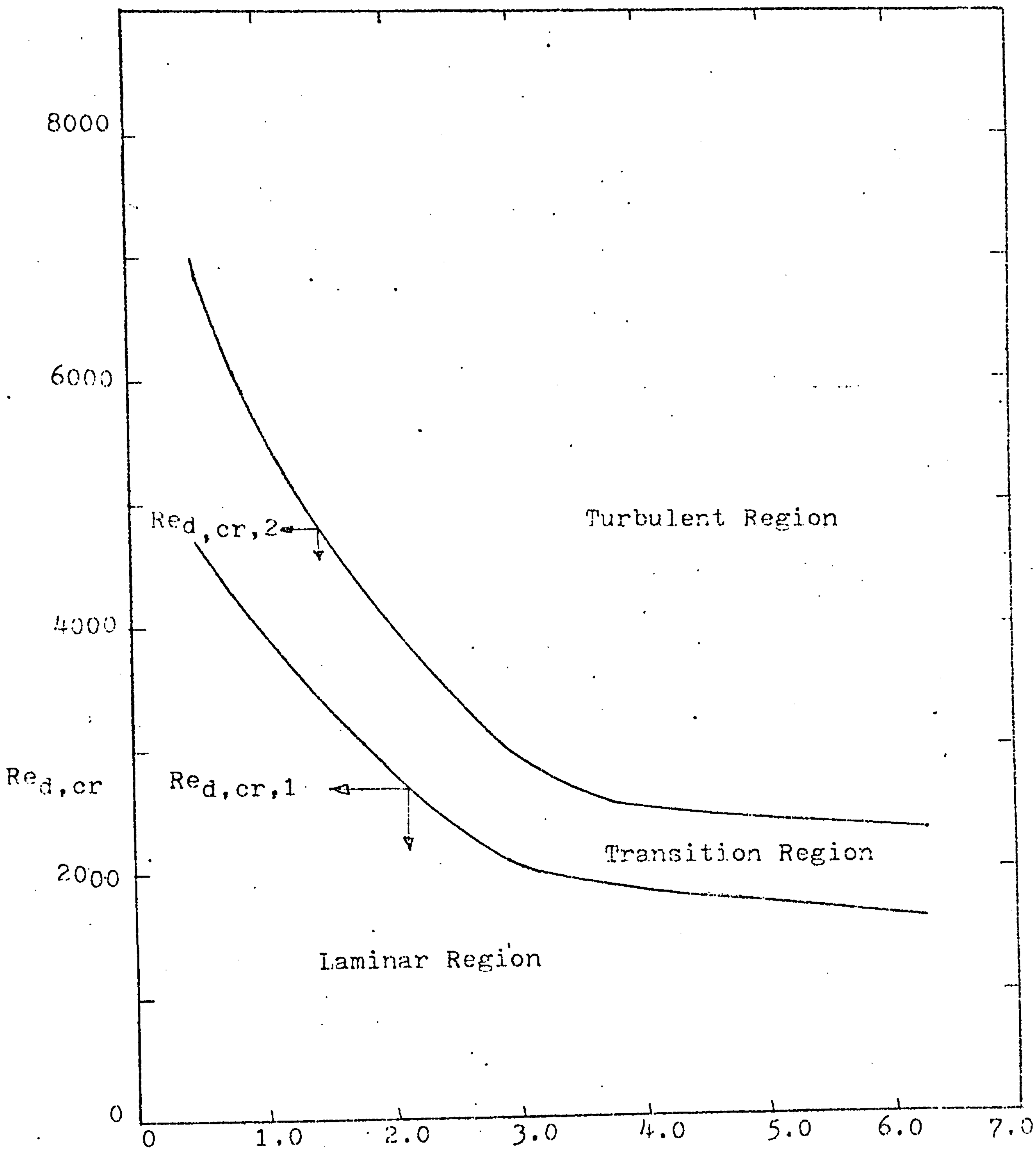

Fig. A-1 Effect of Turbulence Intensity on Transition Reynolds Number, $Re_{d,cr}$

APPENDIX

TRANSITION FROM LAMINAR TO TURBULENT

Transition in developed flow from laminar to turbulent is of fundamental importance for the whole science of fluid dynamics. For this reason, many experiments have been performed in the past to establish a definite criterion for deciding whether the developed flow is laminar or turbulent for a given set of conditions.

O. Reynolds[35] was the first to investigate in detail the circumstances of the transition from laminar to turbulent. He discovered with the help of his classical dye experiment the law of similarity which now bears his name and which states that transition from laminar to turbulent always occurs at nearly the same Reynolds Number, Re_d. The numerical value at which transition occurs was established as being approximately $Re_{d,cr}=2300$, i.e. flows for which $Re_d < Re_{d,cr}$ are supposed to be laminar and those for which $Re_d > Re_{d,cr}$ to be turbulent.

The numerical value of the critical Reynolds number depends very strongly on the conditions which prevail in the entering fluid and in the initial pipe length. Reynolds thought that $Re_{d,cr}$ increases as the disturbances in the flow before the pipe are decreased. This fact was confirmed experimentally by Barnes and Coker[36] and later by Schiller[37] who obtained the numerical value of $Re_{d,cr}$ upto 20000. Ekman[38] succeded in maintaining laminar flow upto $Re_{d,cr}$ of

40,000 by providing an inlet which was made exceptionally free from disturbances. The maximum value of $Re_{d,cr}$ which can occur in practice by taking extreme care to free the inlet from disturbances is not known at present. There exists, however, as demonstrated by numerous experiments, a lower bound for $Re_{d,cr}$ which is approximately 2000. Below this value, even the turbulent flow will become laminar; a phenomenon which is known as 'Laminarisation'.

More recent investigations of the process of transition, say for example Rotta(39), reveal that in a certain range of Reynolds number around $Re_{d,cr}$, the flow alternates in time between being laminar or turbulent. This region can be termed as the transition region in which the flow is neither laminar nor turbulent.

A quantitative analysis of the above mentioned discrepencies in the numerical value of $Re_{d,cr}$ obtained by different investigators is not available in the published literature. However, with the help of the present experimental study, the effect of turbulence intensity of the entering fluid on $Re_{d,cr}$ can be obtained by applying a simple reasoning as described below.

When the boundary layer is developing in a duct where the conditions are such that the flow changes to turbulent at an axial location downstream of the entrance where $Re_x=Re_d(x/D)$ exceeds a certain value $Re_{x,cr}$, then if the boundary layer becomes fully developed before this value of $Re_{x,cr}$ is reached, the flow in a duct will never become turbulent and it will remain laminar everywhere. This fact leads to the calculation of $Re_{d,cr}$ below which the flow will remain laminar throughout for a fixed value of $Re_{x,cr}$.

In the available literature on entrance length for laminar flow through a circular tube, the results of different investigators vary from about $0.03Re_d$ to about $0.07Re_d$ tube diameters[40]. Therefore, for the present purpose, an average of $0.05Re_d$ diameters can be used as the entrance length for laminar flow through a circular tube. Therefore,

$$\left(\frac{x}{D}\right)_d = 0.05\,Re_d \tag{A-1}$$

Also from the definition of $Re_{x,cr}$, we have:

$$\left(\frac{x}{D}\right)_{cr} = \frac{Re_{x,cr}}{Re_d} \tag{A-2}$$

For the flow to be laminar everywhere, $(x/D)_d$ should be less than or equal to $(x/D)_{cr}$; or in the limiting case:

$$\left(\frac{x}{D}\right)_d = \left(\frac{x}{D}\right)_{cr}$$

Therefore, Eqns. (A-1) and (A-2) give:

$$0.05\,Re_{d,cr} = \frac{Re_{x,cr}}{Re_{d,cr}}$$

where $Re_{d,cr}$ has been used for Re_d, because only the limiting case is being considered. From this one easily obtains:

$$Re_{d,cr} = \sqrt{20\,Re_{x,cr}} \tag{A-3}$$

Eqn. (A-3) is the governing equation which can be used to transform $Re_{x,cr}$ into $Re_{d,cr}$ and since $Re_{x,cr}$ depends on Tu (Fig. 4.15), it is obvious that $Re_{d,cr}$ will also depend on Tu.

Now in Eqn. (A-3), if $Re_{x,cr,1}$ is used for $Re_{x,cr}$, $Re_{d,cr,1}$ is obtained such that for flows with $Re_d < Re_{d,cr,1}$, the flow will always be laminar, whereas if $Re_{x,cr,2}$ is used for $Re_{x,cr}$, then $Re_{d,cr,2}$ is obtained such that the developed flow will always be turbulent for $Re_d > Re_{d,cr,2}$. For flows with $Re_{d,cr,1} < Re_d < Re_{d,cr,2}$, however, the flow is in the transition region and can be considered neither laminar nor turbulent. This is probably the range in which Rotta(39) suggested that the flow alternates in time between being laminar or turbulent.

The results are all summarised in Fig. (A-1) and it can be seen that the values of $Re_{d,cr,1}$ and $Re_{d,cr,2}$ are strongly affected by the order of Tu.

REFERENCES

1. Schlichting, H., "Boundary Layer Theory", McGraw Hill, 6th Ed., (1968).

2. Lee, Y. and Park, S.D., "Developing Turbulent Flow in Concetric Annuli; an Analytical and Experimental Study", Wärme-und Stoffübertragung, vol. 4., pp. 156-66, (1971).

3. Deissler, R.G.,"Turbulent Heat Transfer and Friction in the Entry Region of Smooth Passages", Trans. ASME, vol.77, pp. 1221-33, (1955).

4. Tollmien, W., "The Production of Turbulence", NACA TM No. 609, (1931).

5. Hinze, J.O., "Turbulence", McGraw Hill, pp. 462, (1959).

6. Schaubauer, G.B. and Skramstad, H.K., J. Aeronautical Sc., vol. 14, pp. 69, (1947).

7. Dryden, H.L., "Some Recent Contributions to the Study of Transition and Turbulent Boundary Layers", NACA TN 1168, (1947).

8. Shapiro, A.H. and Smith, R.D., "Friction Coefficients in the Laminar Inlet Length of Smooth Round Tubes", NACA TN 1785, Nov.(1922).

9. Campbell, W.D. and Slattery, J.C., "Flow in the Entrance of a Tube", Trans. ASME, J. of Basic Eng., vol. 85,

10. Schiller, L., quoted in Reference 9.

11. Latzko, H., "Heat Transmission to a Turbulent Flow of Liquid or Gas", NACA TM 1068, (1944).

12. Glauert,H., "A Theoratical Estimate of the Pressure Gradient in a Wind Tunnel", Aeronautical Research Council R & M., 1159 (1928).

13. Ross, D. and Whippany, N. J., "Turbulent Flow in the Entrance Region of a Pipe", Trans. ASME, vol. 78, pp. 915, (1956).

14. Reichardt,H., quoted in Reference 22, pp. 29.

15. Levy, S., "Turbulent Flow in an Annulus", J. of Heat Transfer, ASME, vol. 89, pp. 25-31, Feb. (1967).

16. Prandtl, L., quoted in "Introduction to the Transfer of Heat and Mass", by E.R.G. Eckert, pp. 74, McGraw Hil, 1st Ed., (1950).

17. Seigel, R. and Shapiro, A.H., "The Effect of Heating on Boundary Layer Transition for Liquid Flow in a Tube", paper No. 53-A-178, ASME, (1953).

18. Boelter, L.M., Young, G. and Iverson, H.W., "Distribution of Heat Transfer Rate in the Entrance Region of a Circular Tube", NACA TN 1451, July, 1948.

19. Manohar, R., "Analysis of Laminar Flow Heat Transfer in the Entrance Region of a Circular Tube", Int. J. Heat Mass Tr., vol. 12, pp. 15-22, (1969).

20. Ulrichson, D.L. and Schmitz, R.A., "Laminar Flow Heat Transfer in the Entrance Region of Circular Tubes", Int. J. Heat Mass Tr., vol. 8, pp. 253-58, (1965).

21. Kays, W.M., "Numerical Solutions for Laminar Flow Heat Transfer in Circular Tubes", Trans. ASME, pp. 1265-74, (1955).

22. Park, S.D., "Developing Turbulent Flow and Heat Transfer in Concetric Annulus; an Analytical and Experimental Study", Ph.D. Thesis, Mech. Eng. Dept., U. of Ottawa, Ottawa, (1971).

23. Iverson, H.W., "Variation of the Point Unit Thermal Conductance on Entrance to Tubes for a Fluid Flowing Turbulently", M.S. Thesis, Univ. of Calif., (1943).

24. Mizushina, T., Ito, R. and Ogino, F., "Eddy Diffusivity Distribution Near the Wall", 4th Int. Heat Transfer Conference, vol. 2, paper No. FC 218, (1970).

25. Zaguskin, V.L., "Solution of Algebraic and Transcendental Equations", Pergamon Press, (1961).

26. Barbin, A.R. and Jones, J.B., "Turbulent Flow in the Inlet Region of a Smooth Pipe", J. of B. Eng., Trans. ASME, pp. 29-34, March(1963).

27. Quoted in Reference 28, pp. 73.

28. Kays, W.M., "Convective Heat and Mass Transfer", McGraw Hill, (1966).

29. Barrow, H., "Semi-Theoretical Solution of Asymmetric Heat Transfer in Annular Flow", Journal Mech. Eng. Soc., vol. 2, pp. 331-36, (1960).

30. Jenkins, R., "Variation of Eddy Conductivity with Prandtl Modulus and its use in Prediction of Turbulent Heat Transfer Coefficients", Heat Transfer and Fluid Mech. Inst., 147, Stanford Univ. Press, Stanford Calif., (1951).

31. Dwyer, O.E., "Recent Development in Liquid-Metal Heat Transfer", Atomic Energy Review, vol. 4, pp. 3-92, (1966).

32. Kjellstrom, B. and Hedberg, S., "Calibration of a DISA Hot-wire Anemometer and Measurements in a Circular Channel for Confirmation of the Calibration", DISA Information No. 9, (1970).

33. DISA Electronik A/S, Herlev, Denmark, "Instruction Manual for Type 55D41/42 Calibration Equipment", (1970).

34. Eckert, E.R.G. and Drake, R.M., Jr., "Heat and Mass Transfer", McGraw Hill, Appendix of Property Values, (1959).

35. Reynolds, O., "Onthe Experimental Investigation of the Circumstances which Determine Whether the Motion of Water Shall be Sinuous, and the Law of Resistance in Parallel Channels", Phil. Trans. Royal Soc. 174, 935-982,(1883).

36. Barnes, H.T. and Coker, E.G., "The Flow of Water Through Pipes", Proc. Roy. Soc. London, vol. 74, pp. 341,(1905).

37. Schiller, L., quoted in Reference 1, pp. 432.

38. Ekman, V.W., "Onthe Change From Steady to Turbulent Motion of Liquids", Ark. f. Mat. Astron. OchFys., 6, No. 12,(1910).

39. Rotta, J., quoted in Reference 1, pp. 433.

40. Shapiro, A.H., Siegel, R., and Kline, S.J., "Friction Factor in the Laminar Entry Region of a Smooth Tube", Proceedings of the Second U.S. National Congress of Applied Mechanics, ASME, pp. 733-741, (1954).